



HAL
open science

Bâtiments éco-énergétiques : modélisation dynamique hybride pour l'analyse et le contrôle

Abhinandana Boodi

► **To cite this version:**

Abhinandana Boodi. Bâtiments éco-énergétiques : modélisation dynamique hybride pour l'analyse et le contrôle. Other. Université de Bretagne occidentale - Brest, 2021. English. NNT : 2021BRES0008 . tel-03600368

HAL Id: tel-03600368

<https://theses.hal.science/tel-03600368>

Submitted on 7 Mar 2022

HAL is a multi-disciplinary open access archive for the deposit and dissemination of scientific research documents, whether they are published or not. The documents may come from teaching and research institutions in France or abroad, or from public or private research centers.

L'archive ouverte pluridisciplinaire **HAL**, est destinée au dépôt et à la diffusion de documents scientifiques de niveau recherche, publiés ou non, émanant des établissements d'enseignement et de recherche français ou étrangers, des laboratoires publics ou privés.

Abstract

Low cost smart sensors, intelligent controllers, and IoT systems constitute key components to develop smart buildings. These smart systems produce optimal control strategies by continuous analysis of building performance. Two major parameters are controlled in the buildings: occupants' comfort and heating or cooling load consumption optimization. For such intelligent controllers applications, it is essential to have building models with high performance accuracy and computational efficiency. The existing building models range from complete analytical to fully data-driven and hybrid models. The analytical one is extremely complex to model and computationally inefficient, whereas the data-driven models require a large amount of data. However, in the case of data unavailability, application of data-driven models become impossible. This work presents, hybrid modeling for heat transfer dynamics of the building using thermal network modeling technique. An efficient building model is developed by having proper structural knowledge of low-order model and identifying its parameter values. Simplified low-order systems are developed using 2nd order thermal network models with optimal thermal resistor and capacitor values. In order to determine the low-order model parameter values, a specific approach is proposed using a stochastic particle swarm optimization. This method provides a significant approximation of the parameters when compared to the reference model whilst allowing low-order model to achieve 40% to 50% computational efficiency than the reference analytical model.

Furthermore, extensive simulations are carried out to evaluate the proposed simplified model with a more advanced complex solar gains model and identified parameters value. The developed simplified model is afterwards validated with measured data from a case study building where the achieved results clearly show a high degree of accuracy compared to the actual data.

Finally, a model-based controller is applied for the same case study building for thermal comfort optimization. Simulation results demonstrate the significance of the controller in handling the constraints, multi-objective control, and producing optimal control strategy. The energy optimization results of the controller have shown 31% of energy consumption reduction compared to a conventional controller.

Acknowledgements

There are so many people in my life without whom I would have never been able to finish writing this thesis. This journey was very special to me, indeed it was challenging yet exciting. Finally I am here at the end of the journey. I would like to express my sincere appreciation to many people whom have helped me directly or indirectly to complete this journey.

I would like to first thank my supervisors. I thank my PhD director, Prof. Mohamed Benbouzid, who guided me, helped me, and encouraged me during the PhD tenure. I truly admire his patience, positive attitude, and readiness to help at any time. I would like to thank him for the coffee meetings that really helped me to understand my colleagues and work culture. I was always impressed by his logical ideas, discipline, and dedication. I also thank Dr. Karim Beddiar, head of research, CESI west, France for his supervision during my PhD. I could never forget his enthusiasm, continued guidance, and endless support. Discussions with him were insightful and interesting. I would like to thank Associate Prof. Dr-HDR Yassine Amirat, ISEN Brest, France my other supervisor for his valuable guidance, encouragements, and support. I liked very much his questions during the discussion and giving solutions whenever I was blocked in the work. Particularly, I appreciate his abilities of making analogy between thermal and electrical systems, and for providing good ideas. I would also like to thank Dr. Malek Benamour for the valuable guidance during my initial stage of the PhD. I thank again all these wonderful supervisors.

I would like to thank the members of jury board. I thank Prof. Stéphane Ploix and Prof. François Auger for their willingness to be reviewers of this thesis and for their critical comments. I appreciate their valuable suggestions and comments. Indeed, these suggestions helped to improve the quality of the manuscript. I would also like to thank Prof. Seddik Bacha, Prof. Bélahcène Mazari, and Dr. Laurence Miegerville for agreeing to participate in the jury and for their insightful discussions, suggestions, and comments. I also thank Dr. Yves Jaboin, Directeur Technique, Groupe ESSOR, an invited member of the jury and his industry perspective discussion and suggestions.

I would like to thank my colleagues and also my friends Dr. Muhammad Fahad Zia, Dr. Khalil Touimi, and Mohamed Nadir Boukoberine for their constant encouragements. I truly loved off-topic discussions with them. Special thank to Dr. Zakarya Oubrahim for your help during my initial days at Brest.

I would also like to thank Dr. Tony El Tawil, Dr-HDR Elhoussin Elbouchikhi, Dr. Henrique Fagundes Gasparoto, and Jorel Flambard.

I would also like to thank my colleagues at CESI Campus Brest, Firstly, Alexandre Dalla Riva, Director, CESI, Brest for all his support. He was supportive and always encouraging. A very special thanks to my friend Pauline Walczak for her support at CESI. I really appreciate your efforts in teaching French and for the short trips around Brest. I would also like to thank Pauline Cottin, Valerie Dhautel, Dorine Guinvarch, Pierre Hymery, Sam-ang Keo, Claire Kerandel, Fanelie Kergil, Elodie Keriell, Elise Le Gall, Cindy Le Meur, Lise Le Meur, Marie Lollier, Nicolas Masson, Francoise Nadal, Laetitia Jezequel, and Montacer Dridi for the amazing experience during my PhD.

Finally, my heartfelt thanks to my wife and friend Chinmayi Kanthila for her constant support during my difficult times. I also thank her for believing in me and being there by side always. Finally yet importantly, I would like to thank my parents and family for their continuous encouragements, patience, and support until my completion of PhD.

List of Publications

Journal publications:

- A. Boodi, K. Beddiar, M. Benamour, Y. Amirat, and M. Benbouzid, "Intelligent systems for building energy and occupant comfort optimization: A state of the art review and recommendations," *Energies*, vol. 11, no. 10, 2018, doi: 10.3390/en11102604.
- A. Boodi, K. Beddiar, Y. Amirat, and M. Benbouzid, "Simplified Building Thermal Model Development and Parameters Evaluation Using a Stochastic Approach," *Energies*, vol. 13, no. 11, p. 2899, Jun. 2020, doi: 10.3390/en13112899.

Conference Publications:

- A. Boodi, K. Beddiar, Y. Amirat, and M. Benbouzid, "A Numerical Approach for Buildings Reduced Thermal Model Parameters Evaluation," in *IOP Conference Series: Earth and Environmental Science*, 2019, vol. 322, p. 012015.
- A. Boodi, K. Beddiar, Y. Amirat, and M. Benbouzid, "Model Predictive Control-based Thermal Comfort and Energy Optimization," in *IECON 2019-45th Annual Conference of the IEEE Industrial Electronics Society*, 2019, vol. 1, pp. 5801–5806.

Contents

Abstract	3
Acknowledgements	5
List of Publications	8
1 Introduction	21
1.1 Background	22
1.2 Thesis Contributions	26
1.3 Thesis outline	28
2 State of the art review	31
2.1 Introduction	32
2.2 Background	32
2.2.1 Heat and mass transfer in buildings	34
Heat Transfer	34
Conduction	35
Convection	36
Radiation	37
2.2.2 Thermal – Electrical System Analogy	40
Thermal Resistance	40
Thermal Capacitance	41
2.3 Building Thermal Modelling Approach	42
2.3.1 Indoor Comfort Parameters	45
2.4 Building Energy Management Systems—BEMS	45
2.4.1 White Box Models	45
2.4.2 Black Box Models	48
2.4.3 Gray Box Models	53
2.4.4 Building Models Comparative Analysis	57
2.5 Model Predictive Control	61
2.5.1 Introduction	61
MPC General Form	62

2.5.2	HVAC Systems	64
	Air-Conditioning System	64
	Heating System - Air Source Heat Pump - Variable Re-	
	frigerant Flow Systems	65
2.6	Conclusions	67
3	Lumped Parameter Thermal Network Modeling	69
3.1	Introduction	70
3.2	Lumped Parameter Thermal Network Model (LPTNM) . . .	72
3.3	Building Envelope Modeling	78
	3.3.1 Numerical Modeling	80
	3.3.2 Finite Difference Method	81
3.4	Optimization Techniques	84
	3.4.1 Particle Swarm Optimization	85
3.5	Building Envelope Model Development and Parameters Iden-	
	tification	88
	3.5.1 Thermal Network Model Comparison	88
	First Order Model - 2R1C	89
	Second Order Model - 3R2C	89
	RC Models Comparison Analysis	90
	3.5.2 Simulation Model	91
	3.5.3 Simulation Results of Parametric Identification	96
	Low Thermal Mass Wall	98
	Medium Thermal Mass Wall	102
	Heavy Thermal Mass Wall	105
	3.5.4 Comparison with Conduction Transfer Function (CTF)	
	Model	110
3.6	Conclusion	112
4	Case Study Building	115
4.1	Introduction	116
4.2	Case Study Building Description	116
	4.2.1 Data Collection	119
	Temperature Data Collection	119
	Weather Station	119
	HVAC Systems	120
4.3	Air Source Heat Pump - Variable Refrigerant Flow Heating	
	System Model	123
	4.3.1 VRF System Model - Results	127

4.4	Conclusion	130
5	Thermal Network Model for Whole Building and Simulation	
	Results	133
5.1	Introduction	134
5.2	Thermal Network Model—CESI Smart Building	134
5.2.1	Model Inputs	140
	Solar Heat Gains Model	141
	Internal Heat Gains	144
5.3	Simulation Results - Whole Building Model	146
5.4	Conclusion	149
6	Model Predictive Control (MPC)	151
6.1	Model Predictive Controller	152
6.1.1	Linearization of Thermal Network Model	154
6.1.2	Simulation Results	156
6.2	Conclusion	160
7	Conclusions and perspectives	161
	References	165
	Appendices	
A.1	Control System HMI	181
A.2	Jacobian Linearization	182
A.3	Sensor Data Collection System	185
A.4	Heat Pump Outdoor Unit	196
A.5	Heat Exchanger Indoor Unit	197

List of Figures

1.1	Total final consumption per sector by European Union - 28 countries.	22
1.2	Final energy consumption in the residential sector by use, 2018.	23
1.3	Part of the main energy products in the final energy consumption in the residential sector for each type of end-use, 2018. . .	24
2.1	Heat and mass transfer processes involved in buildings.	36
2.2	Heat transfer through a plane wall. Temperature distribution and equivalent thermal circuit.	41
2.3	Building thermal modeling approaches.	43
2.4	behavior of white box, black box, and gray box approaches. . .	44
2.5	Process of generating a weather data file based on the forecasted weather.	48
2.6	Artificial neural network implementation.	50
2.7	Basic principle of model predictive control for buildings. . . .	54
2.8	RC thermal network for single zone building.	55
2.9	Resistor capacitance thermal network for multi-zone building.	55
2.10	Building thermal structures—1R1C and 3R2C.	56
2.11	Building thermal structures—4R2C and 8R3C.	57
2.12	Research conducted on type of building.	58
2.13	Controller application on both type of buildings.	59
2.14	Controller application on comfort parameters.	59
2.15	Renewable energy sources integration in both type of buildings.	60
2.16	Controller used for demand response application in non-residential and residential buildings.	60
2.17	Controller used for renewable energy sources integration in non-residential and residential buildings.	60
2.18	ASHP-VRF system with multiple indoor units.	66
3.1	Thermal network model for whole building.	72
3.2	Simplified thermal network model - 2R1C.	73
3.3	Simplified thermal network model - 3R2C.	74

3.4	Building thermal structures—1R1C and 3R2C.	75
3.5	Building thermal structures—4R2C and 8R3C.	75
3.6	Thermal Network for Overall Building Model.	76
3.7	Heat flow through wall.	79
3.8	Multi-particle gbest PSO Illustration.	88
3.9	First order lumped parameter model - 2R1C	89
3.10	Simplified thermal network model - 3R2C.	89
3.11	Comparison of simulated heat load from RC models and reference model.	90
3.12	Minimized value of objective function for medium weight wall.	97
3.13	Optimized values of R_1 , R_2 , and C_1 coefficients (x_1 , x_2 , and x_4) with PSO algorithm.	98
3.14	Temperature dynamics of reference, optimized and comparison models for light weight wall.	100
3.15	Evolution of APE of the low thermal mass wall.	101
3.16	Temperature dynamics of reference, optimized and comparison models for medium weight wall.	103
3.17	Evolution of APE of the medium thermal mass wall.	104
3.18	Temperature dynamics of reference, optimized and comparison models for heavy weight wall.	106
3.19	Evolution of APE of the heavy thermal mass wall.	107
3.20	Comparison between CTF and simplified thermal network model.	111
4.1	Building site top view.	117
4.2	CESI smart building.	117
4.3	CESI smart building and the case study room.	118
4.4	Wall mount temperature installed in the building.	119
4.5	Measured solar radiation incident on wall surfaces.	120
4.6	Installed weather station and VRF system heat pump setup on the building.	121
4.7	HMI installed in each room of the building.	122
4.8	Power consumed by the ventilation system.	122
4.9	Heat gains from the occupants.	123
4.10	Thermodynamic process $\log(p, h)$ diagram.	125
4.11	VRF system installed in the case study building.	128
4.12	Cooling load output and electricity consumption of the VRF system.	129
4.13	Comparison of room temperatures from VRF system with measured values.	129

5.1	Equivalent thermal network model of the case study building.	136
5.2	Solar sky models and solar angles diagram.	142
5.3	Hourly solar irradiation sums on south facade of the building.	144
5.4	Validation of simplified thermal network model with measured zone temperature data (winter).	147
5.5	Validation of simplified thermal network model with measured zone temperature data (summer).	147
5.6	Measured inputs of the model: ambient and adjacent zones temperatures, solar irradiation, and occupant numbers (winter).	148
5.7	Measured inputs of the model: ambient and adjacent zones temperatures, and solar irradiation (summer).	149
6.1	Validation of developed model against the measured room temperature.	157
6.2	Comparison of results of the MPC and conventional controller.	158
6.3	Measurable disturbances of the system: solar radiation, adjacent rooms temperature, and ambient temperature.	159

List of Tables

2.1	Examples of different equation types of white-box model. . . .	46
2.2	Overview on black-box models.	51
2.3	Thermal sensation scale of PMV.	52
2.4	Comfort classification based on ISO-7730.	52
3.1	Thermal to Electrical system analogy.	71
3.2	Thermo-physical properties of the wall.	89
3.3	Symmetric mean absolute percentage error (sMAPE) between reference and RC models.	91
3.4	Low thermal mass wall performance evaluation results.	102
3.5	Medium thermal mass wall performance evaluation results.	105
3.6	Heavy thermal mass wall performance evaluation results.	108
3.7	Multilayer wall classification, thermal properties, and optimized <i>R</i> and <i>C</i> values.	109
3.8	Root mean square error (RMSE) between reference and simpli- fied thermal network model.	110
3.9	Sensitivity analysis results of the 3R2C model parameters.	110
4.1	Building wall and windows physical dimensions.	119
4.2	Measurement and associated error ranges of sensors.	120
5.1	Standard data of average body surface area of occupants in different types of building.	145
5.2	Heat loss from the occupants during summer.	145
5.3	Heat loss from the occupants during winter.	145
5.4	Model performance evaluation for summer and winter simu- lations.	148

List of Abbreviations

ABC	Artificial Bee Colony
ABM	Agent-Based Modelling
AFLC	Adaptable Fuzzy Logic Model
ANFIS	Adaptive Neuro-Fuzzy Interference System
ANNs	Artificial Neural Networks
ASHRAE	American Society of Heating, Refrigerating and Air-Conditioning Engineers
BAS	Building Automation System
BACS	Building Automation Control System
BBC	Bâtiment à Basse Consommation
BCHPs	Building Heating Cooling Power Systems
BCVTB	Building Controls Virtual Test Bed
BEMS	Building Energy Management System
BMS	Building Management System
BNs	Bayesian Networks
BPA	Back Propagation Algorithm
BRL	Batch Reinforcement Learning Model
BTO	Building Technologies Office
CEBEMS	Cyber Physical System Enabled BEMS
CEMS	Centralised Energy Management System Framework
CEMS	Centralized Energy Management System
CNFDM	Crank-Nicolson Finite Difference Method
CPS	Cyber Physical Systems
DER	Distributed Energy Resources
DOE	Department of Energy
DR	Demand Response
DSM	Demand-Side Management
DTS	Dynamic Thermal Sensation
EEEC	European Energy Efficiency Commission
EKF	Extended Kalman Filter

EML	Extreme Machine Learning
EU	European Union
FDM	Finite Difference Method
FFNNs	Feed Forward Back-propagation Neural Networks
FLC	Fuzzy Logic Controller
FRSC	Fuzzy Rough Set Controller
GAs	Genetic Algorithms
GMBA	Global Model Based Anticipative
GMM	Gaussian Mixture Regression Model
GPM	Gaussian Process Regression Model
GRNN	General Regression Neural Network
GUM	Guide to the expression of Uncertainty in Measurement
HDKR	Hay–Davies–Klucher–Reindl
HMI	Human Machine Interface
HVAC	Heating, Ventilation and Air-Conditioning
ICA	Incremental Conductance Algorithm
IEA	International Energy Agency
IoT	Internet of Things
LINEACT	Laboratoire d’Innovation Numérique pour les Entreprises et les Apprentissages au service de la Compétitivité des Territoires.
LMA	Levenberg-Marquardt Algorithm
LQT	Linear Quadratic Tracking
MAC	Multi-Agent Controller
MAS	Multi-Agent System
MBPC	Model-Based Predictive Control
MBPETM	Model Based Periodic Event-Triggered Mechanism
MCA	Monte Carlo Analysis
MIMO	Multi Input Multi Output
MLP	Multi-Layer Perceptron
MOEA-GA	Multi-Objective Evolutionary Algorithms
MOGA	Multi-Objective Genetic Algorithm
MPC	Model Predictive Controller
NNARX	Artificial Neural Network with External Output

NREL	National Renewable Energy Laboratory
NSGA	Non-dominated Sorting Genetic Algorithm
NSGA-II	Non-dominated Sorting Genetic Algorithm
NZEB	Nearly Zero-Energy Building
PAB	Parameter Adaptive Building
PDE	Partial Differential Equations
PI	Proportional Controller
PIA	Programme d'Investissements d'Avenir
PID	Proportional Integral Derivative
PMV	Predictive Mean Vote
PPD	Predicted Percentage of Dissatisfied
PSO	Particle Swarm Optimization
RBFNs	Radial Basis Function Networks
RBM	Rule-Based Modelling
RC	Resistor Capacitor
RES	Renewable Energy Sources
RL	Reinforcement Learning
SA	Sensitivity Analysis
SVM	Support Vector Machine

Chapter 1

Introduction

1.1 Background

Currently, buildings are responsible for preeminent amount of world's energy consumption and CO₂ emission. There are major four sectors of primary energy consumption: Industry, Transportation, Buildings, and Others. Although the industry sector alone represents major part of energy consumption, buildings along with services constitute for the larger portion of energy consumption as show in Figure 1.1. It indicates that buildings sector becomes the largest consumer of primary energy consumption. According to the European Energy Efficiency Commission (EEEC), buildings in EU represent 40% of total primary energy consumption [1] and nearly 36% of CO₂ emission [2]. The energy generated from fossil fuels contributes considerable CO₂ emission and causes global warming. Consequently, the government authorities, regulators and policy makers have been influencing people in the direction of sustainable buildings by introducing energy efficiency policies.

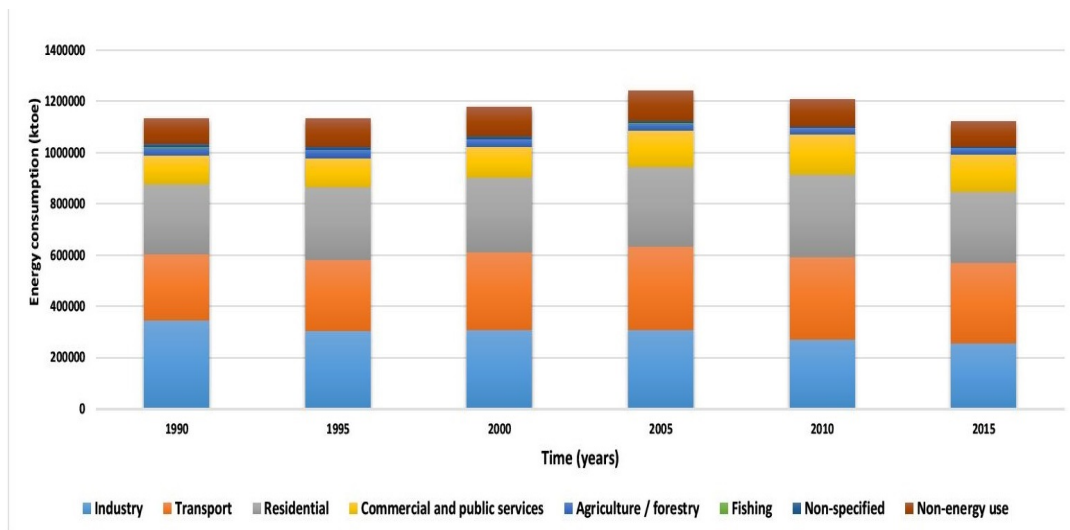


FIGURE 1.1: Total final consumption per sector by European Union - 28 countries [3].

The International Energy Agency (IEA) specifies: "Globally, the wide deployment of best available technologies and energy efficiency policies could yield annual savings in buildings final energy use of roughly 53 exajoules (EJ) by 2050" [4]. This amount is equivalent to cumulative energy consumption by buildings in China, France, Germany, Russia, the United Kingdom and the United States in 2012 [5]. Capturing this energy savings potential will offer a variety of benefits:

- much lesser energy and fuel prices for industries and residential,

1.1. Background

- better reliability in meeting energy demand without expensive infrastructure,
- high efficient systems with low energy consumption,
- lower emissions of heat-absorbing greenhouse gases and other contaminants that cause damage to human health.

Therefore, optimization of energy consumption is crucial for healthy environment and sustainable development. Integration of renewable energies [6] and intelligent systems [7] to the buildings could achieve the estimated savings in energy consumption.

In the residential buildings of EU, the end-energy is used for lighting, water heating, space heating/cooling, cooking, and others. Figure 1.2 shows that the main use of energy is for space heating/cooling around 64 %, the next major portion is used for domestic water heating, representing 14.8 %. For cooking devices, the energy required is 6.1 % of total energy, while lighting and electrical/electronic appliances represents 14.1 %.

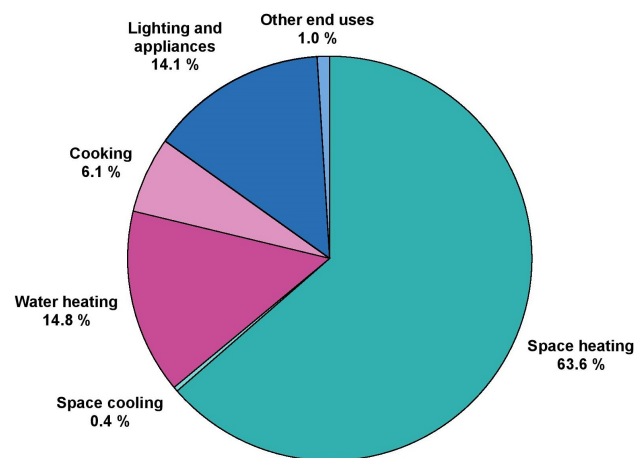


FIGURE 1.2: Final energy consumption in the residential sector by use, 2018 [3].

Electricity meets 100 % of the energy requirements for space cooling and lighting in the residential buildings of EU. Gas plays a vital role in terms of room and water heating and cooking. All available energies from renewable have been used for space heating and water heating, it indicates that the necessity of adapting to renewable energies for others as well. While for space heating apart from gas and renewable energies, considerable part of electricity is also used (Figure 1.3).

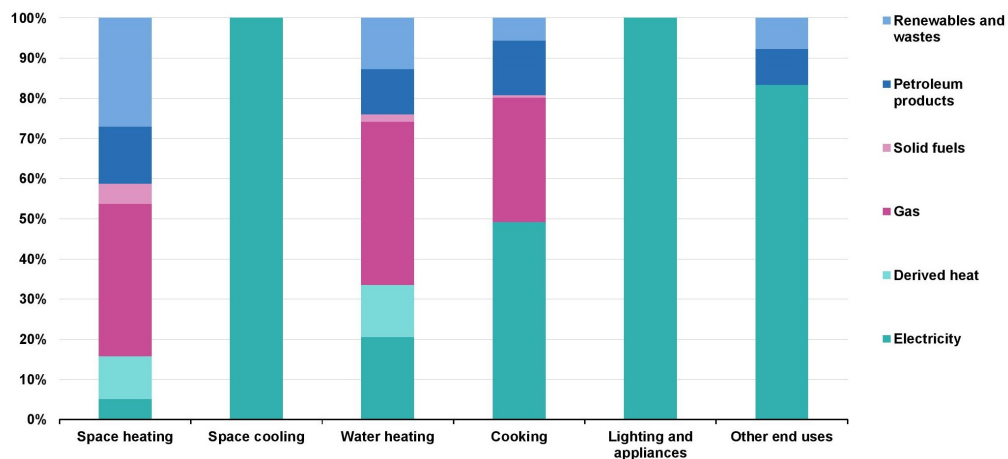


FIGURE 1.3: Part of the main energy products in the final energy consumption in the residential sector for each type of end-use, 2018 [3].

Considering the above statistics, it is certain that there is a need to reduce energy consumption from the buildings, mainly the space heating/cooling requirements. These energy demands are low in energy efficient buildings that have very high thermal insulation. The properly insulated buildings require less energy for space heating in winter as the thermal loss is low and in summer, it prevents from overheating of the indoor environment thus reducing the space-cooling requirement. Nevertheless, rapid increase in the need of new buildings due to the population growth and mass migration to the urban areas accounts for increased energy demand in the buildings. Making all new buildings as nearly zero-energy buildings (nZEB), and retrofitting the conventional buildings structurally and operationally will have a greater impact on the reduction of primary energy consumption [8–10].

There are two key factors influencing space heating energy demand in residential buildings: the energy performance of the building envelope, and the occupants number and behavior. Improvements in the energy performance of the building can be made by taking effective retrofit steps and constructing all new buildings as nearly zero-energy buildings (nZEB). This include high thermal insulations, air tightness and ventilation maintenance, the replacement of current mechanical systems with advanced technology, and the introduction of renewable energy sources to fulfil the energy demands. On the other hand, occupants behavior is complex, and has significant impact on the indoor conditions. To improve overall performance of buildings there

is a need of systems that can be used to control multi-objectives of the buildings [11–13]. A Building Automation System (BAS), or a Building Automation Control System (BACS), is an intelligent controller installed in building to provide better understanding of required comfort conditions and occupants behaviors and controlling the HVAC systems optimally to avoid unwanted heating/cooling or any other operation based on the habits and behavior. Indoor comforts and energy consumption are affected by various parameters, particularly occupants behavior [14], construction type [15], and weather conditions [16]. The occupants behavior and environmental conditions are volatile in nature. They cause unexpected changes in indoor comfort and could result in excessive energy consumption [17, 18]. Hence, an intelligent controller should be able to consider occupancy behavior along with weather conditions to predict and control indoor comfort while optimizing energy consumption. A promising controller for BACS is Model Predictive Control (MPC). MPC applied to Heating, Ventilation, and Air-Conditioning (HVAC) has shown excellent performance abilities to achieve comfort and energy optimization in buildings. MPC has the ability to make a better trade-off between indoor comfort and energy consumption of buildings [19] while considering constraints (occupants behavior and weather conditions).

The performance efficiency of model-based controllers, such as MPC applied for HVAC control mainly depends on accuracy and computational efficiency of the building model [20–22]. The building model (zone model) should replicate dynamics of the heat transfer dynamics in building, able to predict zone heat loads/air temperatures as a function of controllable (HVAC systems) and uncontrollable measurable inputs (weather, internal heat gains, solar gains, etc.), and simplified enough to implement optimization techniques.

These building models can be are of two types: direct (forward) modeling and inverse modeling [23]. Generally, direct models are analytical models that begins with complete physical description of the building, materials, and HVAC systems. Significant amount of buildings data is required to develop such models. Whereas, inverse models are developed from empirical methods using data collected from the buildings. Furthermore, building model performance accuracy is greatly influenced by its system and parameters. Generally, system parameters are identified using inverse methodology as it is relatively simple to model and simulate. Typically, a building model is developed with resistor-capacitor (RC) thermal network model, and values of these resistors and capacitors are identified using an optimization method by

minimizing the error between RC thermal network model temperature and measured temperature data. However, such inverse model methodologies require measured data from building, data about building geometry, and HVAC system data. Consequently, developing a model for buildings that lack of measured data become very difficult, and affects the model performance and poor control strategies.

In this regard, this study focuses on proposing a new hybrid methodology, combination of direct and inverse models to develop building model. For this model, we need building geometry, materials thermo-physical properties data. The developed model is used to predict zone temperature or heating/cooling loads and implemented for controller application for validation. This thesis looks for new ways of modeling techniques that can be used to improve performance.

1.2 Thesis Contributions

This thesis presents the buildings different modeling techniques, controlling methodology, parameters identification methods, HVAC system design and implementation of these models to predict zone temperature or heating/cooling loads to have better supervisory control. The main objective is to develop simplified building models for retrofit or new buildings that do not have any measured data, and to improve indoor thermal comfort condition while optimally consuming the energy through intelligent controllers and HVAC systems. In addition, this work presents design and development of air source heat pump-variable refrigerant flow (ASHP-VRF) system that installed in the case study building to provide thermal comfort.

There have been many works on the development of simplified building models using hybrid methods. However, these works use complex analytical model for reference model development and parameters are identified only by giving step excitation, but the ambient temperature is periodic in nature, it is important to identify parameters by using periodic input. Similarly, for ASHP-VRF systems there is no standard or generic models for its modeling, hence this study focuses brief introduction on generic modeling technique. The developed parameters identification methodology is extensively analyzed by applying it to different wall configurations, validating against

literature model, and finally implementing on case-study building and validate against the measured values. The major contributions of this thesis are detailed below:

- A state of the art review in building modeling and controller techniques for energy and comfort optimization. A critical review was carried out to investigate recent developments in controller and modeling techniques. A detailed analysis provided on white box models, data driven black box models, and hybrid gray box models. These models are been compared and critically reviewed on many different criteria.
- Analysis of the recent developments in lumped parameter thermal model techniques. Lumped parameter thermal network model development, different configurations, and its parameters identification techniques are thoroughly reviewed. Through these review studies, we found that there is a need of proper investigation of different configurations of lumped parameter thermal network model and its parameters identification. The parametric identification techniques in literature have used either inverse method by using data collected from buildings or forward method with reference complex analytical model and the parameters values obtained by step response but ambient temperature is periodic in nature. These investigations show that there is a need of simplified model development with its parameters identification methods.
- Identification of the best performance lumped parameter thermal network model. Various most utilized configurations of thermal network models are developed, simulated, and compared for their performance accuracy and computational cost. We found that the 3R2C configuration has shown acceptable accuracy and computational cost. The same 3R2C model for multilayer wall with different values for parameters has shown different result, it shows that the parameter values have high influence on the performance of models
- Development of parameters identification approach using stochastic optimization technique. We proposed a new parametric identification method using particle swarm optimization (PSO) and a reference Crank-Nicolson finite difference method (CNFDM). We choose CNFDM because it is an unconditionally stable method and PSO selected for its better convergence behavior and robustness. Both reference model and PSO algorithm are developed using Python programming language.

The simulations were carried out on three different thermal mass multilayer walls (ASHRAE standards) for both step and periodic response, and results are compared with two other models. The comparison showed 3R2C model with parameters optimal value has shown better performance accuracy over two other models with different parameter values.

- Development and validation of a lumped parameter model with identified parameter value for a case study building. A lumped parameter thermal network model is developed (using Python programming language) to describe the dynamics of building heat transfer under dynamic conditions. The model input, construction, thermos-physical properties data were collected from case study building. The solar irradiance data obtained from the building is of global horizontal irradiance, hence we introduced advanced complex Hay Davies Klucher Reindl (HDKR) using anisotropic sky model. The model is validated using the operational data collected from the case study building and is validated for two seasons: winter and summer.
- Development and validation of model predictive controller. A simple model predictive controller developed for energy and comfort optimization in the case study building. The controller is simulated for one week and the results are compared to the operational data of case study building. The MPC based on the developed simplified model has shown greater efficiency compare conventional on/off controller. We used the Python programming language with CVXOPT solvers for minimizing the cost function.
- Analysis of air source heat pump variable refrigerant flow (ASHP-VRF) systems and development of a simulation model. A brief introduction is given on generic simulation modeling on the ASHP-VRF systems and presented simulation results for two rooms.

1.3 Thesis outline

This thesis is organized as follows:

- The [chapter 1](#) presents an introduction to the thesis background, motivations, objective, and contributions. A detailed background information is given on energy consumptions by different sectors, different energy usage in residential buildings in EU. Furthermore, how the buildings are impacting environment is detailed. A solution perspective is provided for improving both energy performance of building envelope and controllers for building operation and control. In addition, a brief introduction is given to the lumped parameter thermal network model and its importance in controller applications.
- In [chapter 2](#), a state of the art review of different controllers and modeling techniques is presented. A comparison is provided for the three different modeling techniques. Furthermore, suggestions and recommendations are provided in terms of controller selection for different scenarios and advantages and disadvantages of each controller is detailed. This chapter aims to provide description on thermal behavior of the building systems and importance of building physical and thermal properties, occupancy number and behavior, building type, and environmental conditions.
- The [chapter 3](#) presents an approach to design and develop building dynamic thermal models that are of paramount importance for controller application. An efficient building model is developed by having proper structural knowledge of low-order model and identifying its parameter values. Simplified low-order systems can be developed using thermal network models using thermal resistances and capacitances. In order to determine the low-order model parameter values, a specific approach is proposed using a stochastic particle swarm optimization. This method provides a significant approximation of the parameters when compared to the reference model whilst allowing low-order model to achieve 40% to 50% computational efficiency than the reference one. Additionally, extensive simulations are carried to evaluate the proposed simplified model with solar radiation and identified model parameters.
- The [chapter 4](#) presents chosen case-study buildings along with the IoT system installed in it. Different sensors installed in the building are presented. Furthermore, HVAC systems are detailed and a brief introduction is presented on ASHP-VRF systems and modeling techniques.

An attempt is made on developing a generic model for ASHP-VRF systems simulations, and results are presented in this chapter. The model is implemented for two rooms and in future it will be extended to all rooms of the building.

- In [chapter 5](#), the developed whole zone model is validated against the measure data from the case study building (container building). An analysis is done on the different input models of the building. A complex solar heat gains model presented in this chapter. The model is developed on the basis of HDKR approach, the results show that HDKR approach based model has better estimation of the solar heat gains as compared to the simple conventional models and measured global horizontal radiation. Furthermore, a detailed analysis of importance of occupants number and behavior is provided in this chapter. The thermal network model results show that using proposed parametric identification method the accuracy of the model can be increased.
- The [chapter 6](#) presents the simple MPC controller applied on the case-study building to control thermal comfort while reducing the energy consumption. MPC model implemented in the building for one week has shown promising results of almost 31% energy savings as compared to the conventional control system installed in the building. Some discussion is provided on the results.
- Conclusion [chapter 7](#) summarizes the main contributions of this thesis and makes some recommendations for future research.

Chapter 2

State of the art review

2.1 Introduction

This chapter reviews the literature papers related to this thesis work. The first part of this chapter deals with a state of the art review on recent developments in building energy management system (BEMS) and occupants comfort, focusing on three model types: white box, black box, and gray box models. This literature review was done to define the research methodology and to identify the better suited modeling technique for the thesis work considering various parameters such as: availability of data, efficiency, adaptability and reliability. In the second part, some observations and discussions are provided by comparing each modeling technique via literature review. Third part presents the model predictive control of building heating/cooling systems. In the fourth and final part details on air source heat pump - variable refrigerant flow systems (ASHP-VRF) and conclusions with some recommendations are given, respectively.

2.2 Background

In the previous chapter, it was noticed that buildings consume more than 40% of primary energy and produces more than 36% of CO₂. An intelligent controller applied to the buildings for energy and comfort management could achieve significant reduction in energy consumption while improving occupant's comfort. Conventional on/off controllers were only able to automate the tasks in building and not enough suited for energy optimization tasks. Therefore, building energy management has become a focal point in recent years, promising the development of various technologies for various scenarios.

Integration of renewable energies [6] and intelligent systems [7] to the buildings along with intelligent controllers could achieve the greater savings in energy consumption. However, efficient building energy consumption optimization is still a challenging task because of various parameters affecting the building energy consumption. These influential factors can be divided into major five types:

1. Building physical and thermal properties (thermal conductivity, specific heat, thickness, density, etc.) [24].
2. Occupancy behavior (occupancy activities, interaction with the building, etc.) [25].

2.2. Background

3. Building sector type and building energy policies (type of building, location, regional policies, etc.) [26].
4. Population size (number of occupants present, indoor activities) [27].
5. Climatic conditions (outdoor dry bulb temperature, wind speed, outdoor relative humidity, solar radiation, etc.) [4].

Among these five influential factors, building physical properties, climatic conditions and occupancy behavior have a direct impact on energy consumption. At the same time, other parameters represent slightly minimal effect on the energy consumption. A study conducted on university buildings to evaluate the relationship between energy consumption and population size, user activities, and demand profiles reveals population size have a minimal impact on electrical energy consumption as compared to other parameters [27]. Generally, people spend 90% of their life in buildings [28], hence the maintenance of comfortable environment is important to assure occupants' health and productivity. The quality of occupants' living is determined by three comfort parameters: thermal comfort, indoor air quality and visual comfort. These three comforts are achievable by exploiting Heating, Ventilation and Air-Conditioning (HVAC) controller and lighting systems with natural resources (day lighting, outside temperature, etc.).

A Building Energy Management System (BEMS) is required to improve energy performance meanwhile ensuring improved occupants' comfort. Conversely, realization of indoor comfort environments draws more energy to achieve and maintain the optimal comfort. Therefore, a proper trade-off is required between energy and indoor comfort [29]. In this context, recent developments in the BEMS are focusing on smart technologies to address the gap between energy consumption and occupants' comfort [30].

Thermal modeling of the building allows to replicate the actual dynamics of the real building and to predict its thermal behavior. This prediction can be well used for scheduling of energy systems, optimizing comfort conditions, and energy savings. Dynamics of the heat flux has significant impact on performance of the building. Hence, accurate modeling of heat flux dynamics is essential.

2.2.1 Heat and mass transfer in buildings

The fundamental thermal properties of building elements are heat storage capacity and transmissibility. Building components that can store heat include envelopes, ceilings, floors, multi-glazing windows, and the zone air. The two factors mainly influence the heat storage in building elements: thermal mass and specific heat capacity. The stored heat is further transmitted to low temperature sides (outside or inside). These thermal properties of the building envelope determines the time lag and decrement factor [31]. Such thermal dynamics can be represented by thermal networks by means of electrical circuit based on the thermal-electrical analogy. Electrical resistors represent thermal transmittance, while electrical capacitors represent heat storage. We use the lumped capacitance method to represent a whole building model's thermal dynamics as an electrical circuit based on the analogy. The main advantage of using electrical circuits is to use effective methods for solving and simulation. Furthermore, because of their simplicity, computational efficiency, and acceptable accuracy, the models can be used for control purposes. Despite the fact that such thermal networks fail to consider all heat dynamics of the building due to the lumped parameter, the results show good accuracy with real dynamics.

Heat Transfer

The different modes of heat and mass transfer dynamics that occurs in buildings is shown in Figure 2.1. There are three types of heat transfer processes [32]:

- Conduction heat transfer: occur in solids and fluids in which the vibrating molecules are unable to break free from another molecule due to the presence of boundary surfaces with a small temperature differential.
- Convection heat transfer: occur in fluids when its molecules are able to move freely and independently. This occurs due to the phenomenon of expansion or contraction of the fluids when it is heated or cooled causing changes in its density.
- Radiation heat transfer: occurs due to the interchange of electromagnetic waves between surfaces having differing temperatures that are facing each other.

Figure 2.1 shows the heat transfer dynamics that occur in buildings. The room is isolated from the outside environment by an exterior wall and a window. The room is equipped with an HVAC system which would supply the room with heating or cooling energy by circulating air. The environmental conditions, such as the external air temperature and the solar radiance are some of the most influential parameters of heat transfer processes in buildings.

Conduction heat transfer occurs through the building envelope, such as external walls, floor slabs, ceilings, roofs, and internal partitions. Solar radiation transfers through windows and doors, this is an example for radiation heat transfer. Air movement (infiltration) from outside/adjoining rooms to inside due to temperature difference. Heat and moisture dissipation from electrical appliances, inhabitants and furniture's within the room, and heating or cooling and humidification or dehumidification provided by the HVAC system [33].

Conduction

Heat conduction is a type of heat transfer, where heat is transferred through a solid from higher temperature to the lower temperature region. Conduction occurs through the transfer energy between the particles of the medium and this transfer is continuous process until the system reached thermal equilibrium [32]. This type of heat transfer in buildings mostly occurs through the walls, ceilings, floors, and windows.

The rate of heat transfer is mainly dependent on the thermal properties of the material. Thermal conductivity is one of the properties that influence heat transfer rate. The conduction heat transfer equation is also known as Fourier's conduction law. Fourier's law for one-dimensional heat flow through a single slab of homogeneous material is shown in Figure 2.1. The heat rate equation of conduction transfer is given by:

$$q_x = -kA \frac{dT}{dx} \quad (2.1)$$

where, q_x (W) is the heat transfer rate in the x direction and is proportional to the temperature gradient, $\frac{dT}{dx}$,

k is the thermal conductivity (W/mK) of the material, and

the minus sign in the right hand side of the equation 2.1 indicates that heat is always transferred in the direction of lower temperature. Thus, the loss of energy from the higher temperature side.

The steady-state heat conduction through a homogeneous wall is given by:

$$\frac{dT}{dx} = \frac{T_{high} - T_{low}}{L} \quad (2.2)$$

$$q_x = kA \frac{T_{high} - T_{low}}{L} \quad (2.3)$$

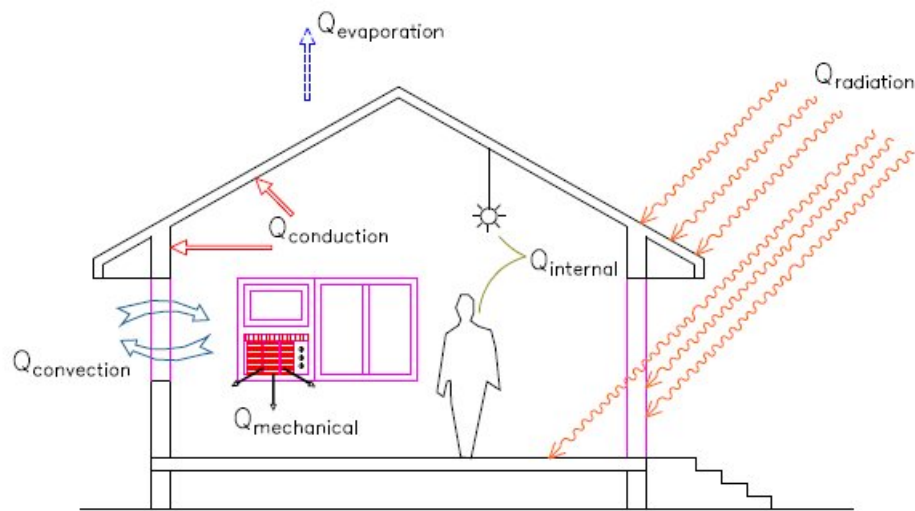


FIGURE 2.1: Heat and mass transfer processes involved in buildings [34]

Convection

Convection occurs in liquids and gases, in which the molecules have free and independent motion. There two types of convection: natural and forced. In natural convection, warmer molecules rise and cooler molecules drop, due to the effects of gravity [32]. In general, HVAC systems use forced convection to heat/cool the zone space. The heat transfer rate of convection process is given by:

$$q = hA(T_{surface} - T_{fluid}) \quad (2.4)$$

Where q , the convective heat transfer (W),

2.2. Background

$T_{surface}$ is the surface temperature,

T_{fluid} is the temperature of the fluid in contact with the surface,

h is the convective heat transfer coefficient ($W/m^2.K$),

The equation 2.4, is also known as Newton's cooling law. The rate of convective heat transfer mainly depend on the temperature gradient and the convective heat transfer coefficient. In buildings, the convection heat transfer occurs near the surface of walls, floors, windows, roofs, partitions, furnitures, HVAC systems, and occupants.

Radiation

Radiation heat transfer is the electromagnetic waves emitted by a surface that is at a finite temperature. All surfaces that are above absolute zero degree Kelvin ($> 0.0K$) emit, absorb, reflect, and transmit the thermal radiation [32]. Furthermore, for radiation, a transfer medium is not required unlike other heat transfers that need a medium to transfer the heat. In fact radiation transfer occurs most efficiently in a vacuum.

The effectiveness of radiation exchange is dependent upon the texture of the radiating and receiving surfaces. Surface characteristics include: reflectivity (r), transmissivity (t), absorptivity (α) and emissivity (ϵ).

A perfect radiator will emit 100% radiation, this is know as black body radiation. The expression for radiation heat transfer between two surfaces is given by:

$$q_{rad}'' = \epsilon\sigma(T_s^4 - T_{sur}^4) \quad (2.5)$$

In the buildings, the radiation heat transfer between internal surfaces is minimal as the difference between surface temperatures is very low. Furthermore, radiation between internal surfaces introduces non-linearity in the system, we have shown radiation heat transfer linearization in the next section.

The conductive heat transfer occurs through building envelope, mainly through external walls. This heat transfer is the result of the convective heat transmitted by the surface on either side of the wall due to the temperature difference between wall surface and ambient air, and the radiative heat transfer with other wall surfaces that are facing towards each other and on the external side the wall is exposed to direct/diffused solar radiation.

Similarly, the solar radiation heat is transferred inside via the window glasses. A part of incident solar radiation is transmitted directly to the inside, some part is reflected back to environment, and remaining part is absorbed by the glass, thus increasing the glass temperature leading to heat transfer to both indoor and outdoor through conduction within the glass and convection and radiation at both the surfaces. The outside surface temperature of the external wall varies due to the effect of absorbed solar gains and outdoor temperature, these two parameters are regularly addressed together as 'sol-air temperature'. The sol-air temperature is defined as the outside air temperature which, in the absence of solar radiation, would give the same temperature distribution and rate of heat transfer through a wall (or roof) as exists due to the combined effects of the actual outdoor temperature distribution plus the incident solar radiation [35,36].

The solar radiation transmitted through the windows to the indoor, will become a cooling load only after the indoor surfaces absorbing the incident solar radiation. As a consequence, surface temperatures will increase, resulting into convective heat transfer from wall surfaces to indoor air. This phenomenon influences the indoor air temperature and becomes a part of space cooling load. The magnitude and occurrence of the peak of cooling load differs from those of the radiant heat gain from the building envelope. This difference occurs due to the presence of thermal capacitance of the building envelope.

The conduction heat transfer responsible for higher percentage of heat transfer compare to the other two processes. The building envelopes plays major role in conduction heat transfer and the most significant thermal properties of building envelope are thermal capacitance and thermal resistance of the materials. Thermal capacity (C) is the property of a material to absorb heat when it is heated and to release heat when it is cooled [37]. It is defined by:

$$Q = C_{th} (T_H - T_C) \quad (2.6)$$

where Q - the heat absorbed or released by a material (J)

$C_{th} = m \times C$ - the thermal mass of the material

m - mass of the material (kg)

C - specific heat capacity of the material ($J/(kg.K)$)

$T_H - T_C$ - the temperature difference (K)

2.2. Background

Thermal resistance is a building envelope's material property and refers to that material's ability to resist the flow of heat. It is inverse of thermal conductance. It is defined by:

$$R = l/k \quad (2.7)$$

where R - the thermal resistance per unit area of the piece of a material (m^2K/W)

l - the thickness of the material (m)

k - the conductivity of the material (W/mK)

The heat transfer through building envelope under steady state conditions is only affected by the temperature difference between indoor and outdoor, and the thermal resistance of the building envelope. However, under dynamic conditions, the thermal capacitance plays an important role, its ability to store heat and transfer it later significantly affects the phenomenon of the heat transfer. The ability of storing heat by the building envelope is called as thermal mass. Thermal mass depends on the specific heat capacity and the density of the material.

When air moves into and out of the indoor space, heat and moisture will be taken into or out of the room if the air entering the space is thermodynamically different from the indoor air. Air movements can be measured by the difference in pressure between the space and the adjacent rooms and the outdoor, due to the influence of wind or stack, or the imbalance in the flow rate of supply and extraction air maintained by the ventilation system. The thermodynamic state of the air inside the room will vary from the net heat and moisture gain encountered by the room air resulting from the heat and moisture exchange with the enclosure surfaces, the transfer of air into or out of the room, taking with it heat and moisture, heat and moisture from the room's sources, and supplying heat, cooling, humidification or dehumidification. These heat and moisture transfer processes will have to be modeled in order to predict the indoor air condition or the rate of heating or cooling, and the humidification or dehumidification needed to sustain the indoor air condition at the specified state.

2.2.2 Thermal – Electrical System Analogy

Thermal Resistance

As we have seen in above section 2.2.1, the analogy between thermal to electrical system is significant in the building modelling. In electrical system, the resistance is the measure of opposition to electricity conduction, likewise thermal resistance is the measure of opposition to heat conduction in thermal systems. The electrical resistance is given Ohm's law:

$$R_e = \frac{V_1 - V_2}{I} = \frac{L}{\sigma A} \quad (2.8)$$

Likewise, the thermal resistance from the above section 2.2.1 for a conduction heat transfer in plane wall is given as:

$$R_{t,cond} = \frac{T_{high} - T_{low}}{q_x} = \frac{L}{kA} \quad (2.9)$$

Similarly, the analogy between the convection thermal resistance ($1/hA$) and electrical resistance can be made. The convection heat transfer equation is given by:

$$q = hA(T_s - T_\infty) \quad (2.10)$$

the thermal resistance for convection that is inverse of the convective heat transfer coefficient and surface area is then,

$$R_{t,conv} = \frac{T_{surface} - T_{air}}{q} = \frac{1}{hA} \quad (2.11)$$

An example can be seen below representing a simple plane wall with single layer. The two modes of heat transfers, conduction and convection are considered here. The equivalent thermal network for the wall is shown in Figure 2.2. The corresponding heat transfer dynamics are derived as follows:

$$q_x = \frac{T_{air,out} - T_{s,out}}{\frac{1}{h_1 A}} = \frac{T_{s,out} - T_{s,in}}{\frac{L}{kA}} = \frac{T_{s,in} - T_{air,in}}{\frac{1}{h_2 A}} \quad (2.12)$$

The overall heat transfer rate can be also expressed as:

2.2. Background

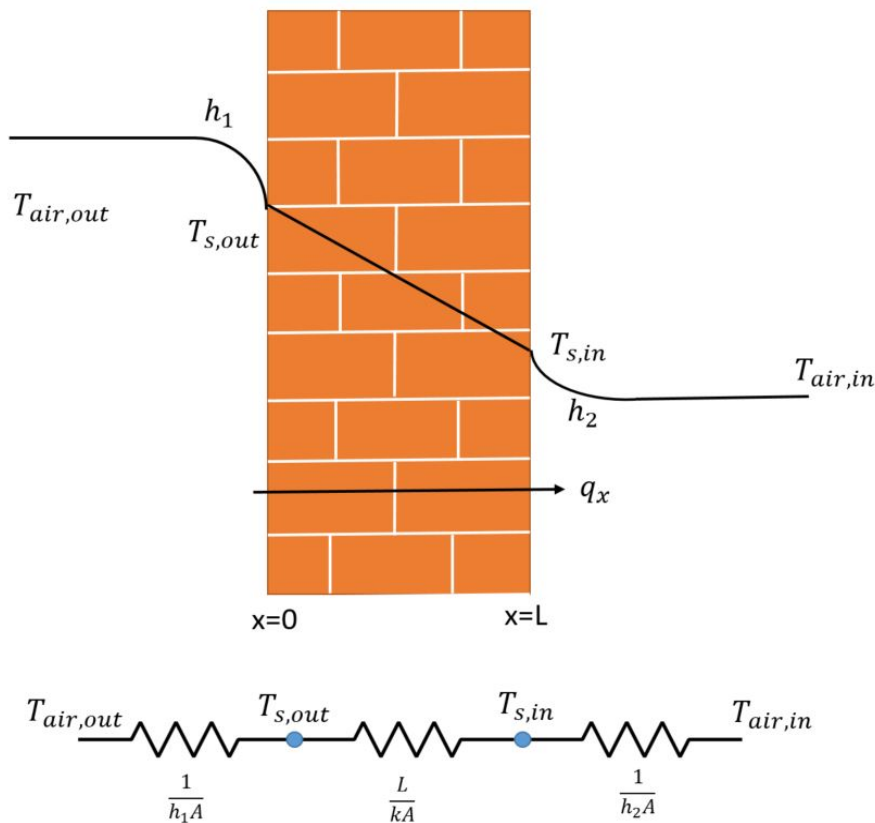


FIGURE 2.2: Heat transfer through a plane wall. Temperature distribution and equivalent thermal circuit.

$$q_x = \frac{T_{air,out} - T_{air,in}}{R_{eq}} \quad (2.13)$$

Just like electrical resistances in series are summed, similarly, in thermal network the conduction and convection resistances are in series, hence they can be summed.

$$R_{eq} = \frac{1}{h_1 A} + \frac{L}{k A} + \frac{1}{h_2 A} \quad (2.14)$$

Thermal Capacitance

The thermal dynamics that are derived above are suitable for the steady-state system. However, we are interested in transient heat transfer in the buildings. The internal energy of the materials is temperature and time dependent during transient conditions. Thermal capacitance or heat capacity is

the capacity of a body to store heat. It is typically measured in units of $(J/^\circ C)$ or (J/K) (which are equivalent).

In the buildings, envelopes thermal mass opposes the temperature fluctuations by thermal inertia, it is also known as thermal flywheel effect. During the daytime, thermal mass flatten out the temperature fluctuation effect on indoor conditions. During this process, it stores the heat and releases it later to the cooler environment. The time taken to release the heat is called as time-lag and the ratio between the fluctuation on outer and inner temperature is known as decrement factor. The thermal mass can be used for passive heating to reduce active heating energy consumption.

For a single layer wall, the thermal mass is simply the mass of the materials times the specific heat capacity of the material. However, for multilayer walls, the cumulative of heat capacities can be considered for the thermal mass calculation. In the multilayer, each layer has different thermal capacitance, hence it is essential to consider the effect of each layer on the transient heat transfer. However, this may increase complexity of the whole model and results in poor computational efficiency.

2.3 Building Thermal Modelling Approach

There are several approaches and models for energy performance analysis in buildings. No single approach is universally suitable for all buildings. Rather, the choice of best model selection decision depends on what you choose to quantify and what data is available. However, these various models can be broadly categorized into two types:

1. Steady state models
2. Dynamic/Transient models

Steady state approaches appeal to simplicity, and lack of data prevents more detailed and precise transient analysis. Steady state analysis simplifies the calculations by neglecting thermal capacitance, dynamic temperature changes, occupants influence on the system, and heat sources. Steady state modeling is useful when there is not much data available and for long duration energy analysis. There are various steady state analysis methods [38]:

- Degree-day method,
- Modified degree-day method,

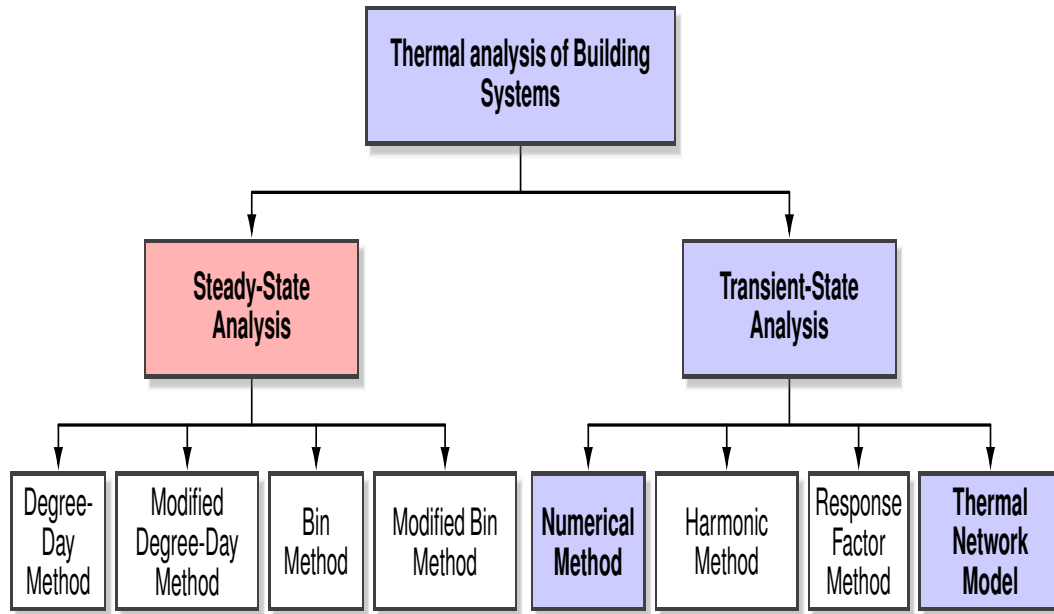


FIGURE 2.3: Building thermal modeling approaches.

- Variable-base degree-day method,
- Bin method,
- Modified bin method

However, in this thesis only transient state models are considered and reviewed as it's quite obvious that the heat transfer process in building is transient (dynamic). Hence, in this thesis building energy modeling indicates only dynamic modeling. Three main approaches have been used for building energy management systems (see Figure 2.4): white box models, black box models and gray box models.

- White box models [40, 41] are a physical modelling approach relying on thermodynamic and/or mathematical equations and engineering methods for energy modelling, analysis and control. White box-based modelling approach examples are the building energy analysis simulation software such as: EnergyPlus [42], Transient System Simulation Tool (TRNSYS) [43], eQuest [44], etc. These software tools basically are used during building planning and designing phases, prior to the building construction. They calculate overall energy consumption [45], HVAC design [46], operation scheduling, lighting information [47], etc., based on the detailed building physical properties [48], occupancy schedule, geographical conditions, and type of building and climatic parameters. However, availability of such precise data for the

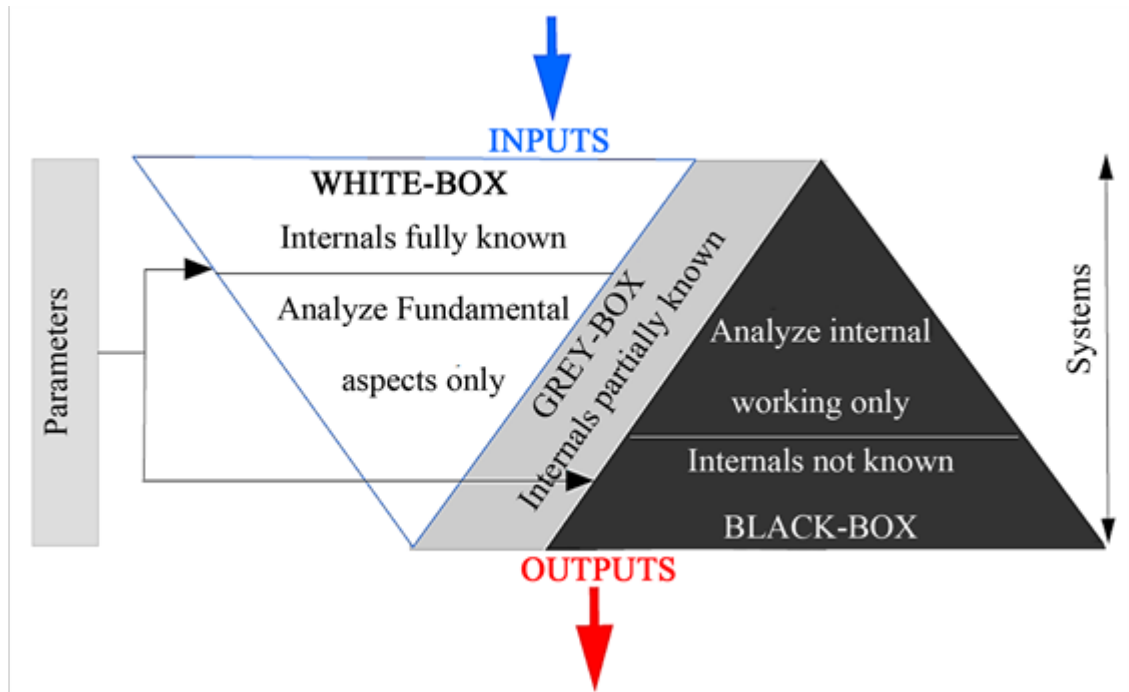


FIGURE 2.4: behavior of white box, black box, and gray box approaches [39].

simulation is troublesome and in some cases impossible to obtain. In addition, due to the non-linear behavior of building parameters, white box models are suitable for simple models and as when applied to complex buildings, the model tends to be thermodynamically complex.

- Black box models are data driven building energy models, which are built on data basis [49–52] often considered as easy to model over physics-based white box models. Generally, black box models are applied for prediction of energy consumption [51], HVAC operation scheduling [53], and adaptive control systems [54]. Black box models methods examples are Artificial Neural Networks (ANNs), Support Vector Machine (SVM), Genetic Algorithms (GAs), Reinforcement Learning (RL), deep machine learning [55], etc. Aside from the ease to apply, black box models require large input data to train the model [56]. This data may not be available in buildings in which sensors are not installed, thereby limiting their application to the few buildings with installed sensors.
- To overcome white box and black box models drawbacks, hybrid models were introduced [57]. Hybrid models (gray box models) are combination of physics-based models (white box models) and statistical

methods (black box models). Gray box modelling is found out as robust and accurate for building systems modelling and in building performance improvement [57].

2.3.1 Indoor Comfort Parameters

People spend most of their time in buildings. Maintenance of indoor comfort parameters is therefore significant to improve occupant's productivity, health, and comfort feeling [58]. Thermal comfort in indoor environment is the principal component for ensuring indoor environment quality. Thermal comfort is generally expressed as the satisfaction of thermal environment, usually referred as psychological sensation of thermal environment [59]. Visual comfort is another parameter affecting the indoor environment quality. Proper illumination level is essential for commercial, institutional, and industrial buildings to preserve inhabitants working efficiency.

2.4 Building Energy Management Systems—BEMS

BEMS are generally installed in buildings to monitor and control indoor comfort conditions and energy consumption [45]. These systems are mainly based on sensors, actuators, software, and hardware networks [7, 60]. Normally, buildings with few occupants (residential, and office buildings) may permit to interact with BEMS technologies via a human machine interface (HMI) [61] to control electrical appliances and HVAC system operation [62]. These interactions could be restricted in institutional, commercial, and industrial buildings because of the large number of occupants, where each may possess a unique set point, resulting in higher energy consumption. Hence, HVAC system operating values are set to a standard range to maintain indoor comfort in such buildings. However, heterogeneous parameters affecting building energy and comfort hinder the performance of BEMS models.

2.4.1 White Box Models

White box models are thermal dynamics modelling, which are based on fundamental laws of physics, thermodynamics, and heat transfer, which require a greater amount of data about building [48]. Various types of white-box models can be found in both steady state and dynamic models, such as: linear, non-linear models, differentiable, continuous, non-continuous models (see Table 2.1). The performance of white-box method does not depend

on time in static models. While in dynamic models, the performance varies based on the dynamic thermal balance of time evolution. Usually, these complex white-box models are represented by differential equations. However, their mathematical representation also relies on the relationship between the parameters. These relationships may be ordinary, partial, linear and non-linear differential equations [39].

TABLE 2.1: Examples of different equation types of white-box model [39]

Type	Example	Application
Static linear equations	$q = R(T - T_a) - A_s I + \varepsilon$ $\dot{q} = hA(T_2 - T_1)$	Transmission through component
Static non-linear equations	$\dot{q} = \varepsilon\sigma A(T_2^4 - T_1^4)$	Building simulation radiation exchange (walls and ceilings)
Dynamic linear equation Ordinary differential equation	$C \frac{dT}{dt} = U(T - T_a)$	Passive/active Energy storage
Dynamic linear equation Partial linear	$\frac{\partial u(x,t)}{\partial t} = k \frac{\partial^2 u(x,t)}{\partial t^2}$	Dynamic heat flux

Due to the diversified and heterogeneous behavior of building parameters, complexity of hardware network (sensors, and actuators), and occupants interaction with buildings, it is difficult to carry out full-scale experiments. Hence, software tools are affordable and ease-to-use platforms that can be used for building dynamics evaluation and analysis. Numerous software tools have been developed over the last few decades for the analysis of energy consumption, HVAC design, operation scheduling, lighting information, renewable energies, etc., Regular up-gradation is performed on these simulation tools to improve the performance efficiency and decreasing computational cost. The list of US Department of Energy (DOE) organization approved building simulation tools is available in [63].

EnergyPlus is a building energy performance analysis simulation software and console-based program that reads inputs and writes outputs in text files, developed based on DOE-2 [64] and the Building Loads Analysis and System Thermodynamics (BLAST) by National Renewable Energy Laboratory (NREL) and U.S. DOE Building Technologies Office (BTO) [42]. Zhao et al. [65] used EnergyPlus to procure raw data for commercial building to perform overall energy performance and dynamic pricing by using Cyber Physical Systems (CPS)—enabled BEMS [66]. Furthermore, a fuzzy logic controller (FLC) is initially designed based on the data probation from EnergyPlus and

a GA method applied to FLC for evolution of improved member functions population for improved comfort control energy optimization of a food service center. The results were compared with stand-alone EnergyPlus output and investigated that the GA-FLC-based method resulted notable decrease in energy consumption during both cooling and heating [67]. This shows that EnergyPlus lacks interactive control optimization techniques and would be coupled with other dynamic computational software (Matlab, Modelica [68]) via co-simulation software building controls virtual test bed (BCVTB). Kim et al. [46] used EnergyPlus for training ANNs and coupled GA for optimization of integrated daylighting and HVAC systems. This was performed to ensure large database available for training ANNs in less time, otherwise 3 months would have been needed to procure data from sensors. A multi-objective optimization strategy is validated using non-dominated sorting genetic algorithm (NSGA), implemented in the GenOpt [69] optimization engine through the Java genetic algorithms package, to instruct the EnergyPlus simulation tool [29]. Meanwhile, Huh et al. [70] developed a system to generate predicted real-time weather data for 24 h duration using EnergyPlus coupled with GenOpt through BCVTB [71]. This approach improves the building energy control optimization based on real time prediction control.

TRNSYS (Transient systems simulation program) is a dynamic computational software for building energy performance analysis [43]. It is incorporated with Matlab for database generation to train 2 ANNs used for predictive and adaptive approach applied to hotel building. The developed model efficiently improved thermal comfort and building energy optimization during summer season resulting in 18–38% energy savings over the simulation period [54]. TRNSYS was used for determining building cooling load needed from the chiller plant, Later, these data were fed to Matlab for performing optimization analysis [72].

BCVTB is used for coupling various simulation tools for co-simulation and co-simulation to hardware. Refs. [40, 67, 73] used BCVTB to ease the simulation process by coupling EnergyPlus, Matlab in their model for building energy performance analysis. Meanwhile, BCVTB was coupled with EnergyPlus to generate real-time weather data file for energy consumption prediction in one day [70]. Figure 2.5 shows the process of generating a weather data file based on the forecasted weather using BCVTB as a coupling platform between EnergyPlus and other tools. The weather elements

from weather forecast by national weather station, calculated weather parameters, measured weather elements, and default parameters are coupled in BCVTB platform for generating weather forecast.

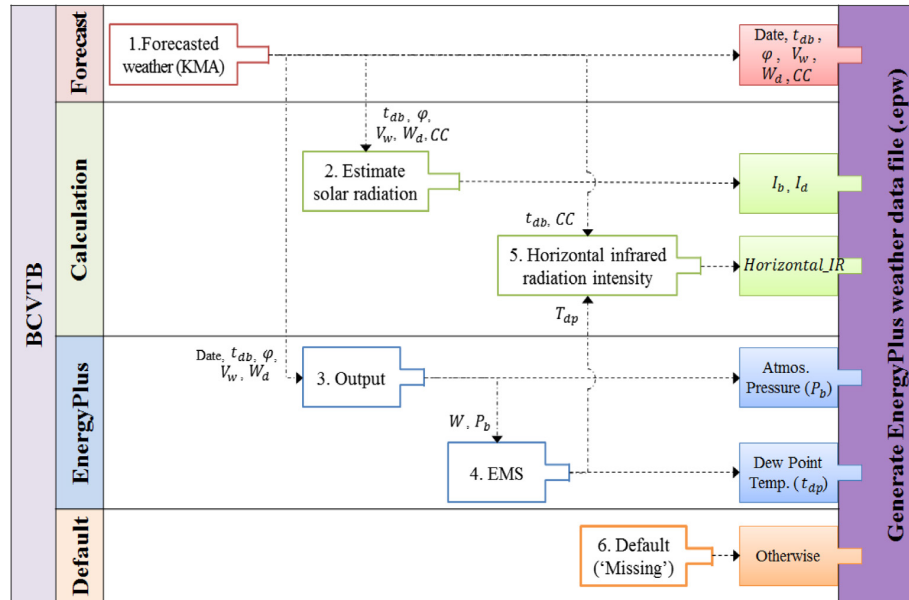


FIGURE 2.5: Process of generating a weather data file based on the forecasted weather [70].

Although simulation tools are the first choice for building energy performance analysis because of accuracy and effectiveness, they require proper data of building, weather parameters, and physical properties. However, collecting appropriate data is always difficult and in some cases these data are not available. This is the major challenge in retrofitting existing buildings. In addition, these tools lack controller development flexibility and absence of high performance controller systems in their libraries yields difficulty to develop and integrate in practical application/implementation [74].

2.4.2 Black Box Models

These are also known as data-driven models and are developed based on statistical models by quantifying historical data parameters and correlating between building performance and data to find optimal pattern. Data-driven model approach is often considered as less complex with high accuracy and low computational cost. However, the inner process is mostly unknown, leading to reduced control flexibility of the overall process. The primary requirement of black box models are pre-collected data. These can be obtained from following sources:

- Real data collected from existing building through sensors, smart meters, and other smart systems [75].
- Simulated data collected from the simulation tools such as EnergyPlus, BCVTB, etc., [56].
- Standard data available in public benchmark datasets such as ASHRAE's data [50].

Black box models are known for prediction techniques and gained huge consideration over last decade. Commonly, these models are used in prediction of building energy consumption [50,51,76], indoor temperature [75,77], heating/cooling load demand, HVAC parameters, occupancy [78,79], and energy generation from RES. Some major algorithms of these models are ANNs [80], SVM [81], GAs [82], decision trees [83], and other statistical machine learning methods.

Indoor comforts are influenced by various parameters, especially weather conditions (e.g., wind speed, air temperature, and humidity) that are volatile in nature. In such conditions, indoor thermal comfort can be rapidly affected and could cause excessive energy consumption to maintain temperature range. To maintain indoor thermal comfort under a given range despite of rapid changes in influential parameters, a prediction model and temperature controller is introduced by Marvuglia et al. [75]. In this framework, outdoor temperature, air relative humidity, wind speed, and indoor temperature data are used to train artificial neural network with external inputs (NNARX) model and predicted values fed to fuzzy logic controller to maintain indoor temperature in a given range. Results show good efficiency of predictions and temperature controller. Mararulla et al. [53] implemented ANN-based predictive controller to a commercial building energy management system for operation of boilers in buildings, shown in Figure 2.6. This method resulted in around 20% reduction in energy required to heat the building. The ANN implementation is illustrated in Figure 2.6, where data obtained from the simulation tool are fed to the ANN with 10 neurons in each hidden layer and predicted results are given to BEMS for optimal operation.

In 2016, Ascione et al. [49] used feed-forward multilayer perceptron (MLP) ANN structure to predict building energy and thermal behavior in retrofit scenarios, which produced significant prediction values. Furthermore, the authors indicated that the number of hidden layers highly influences the

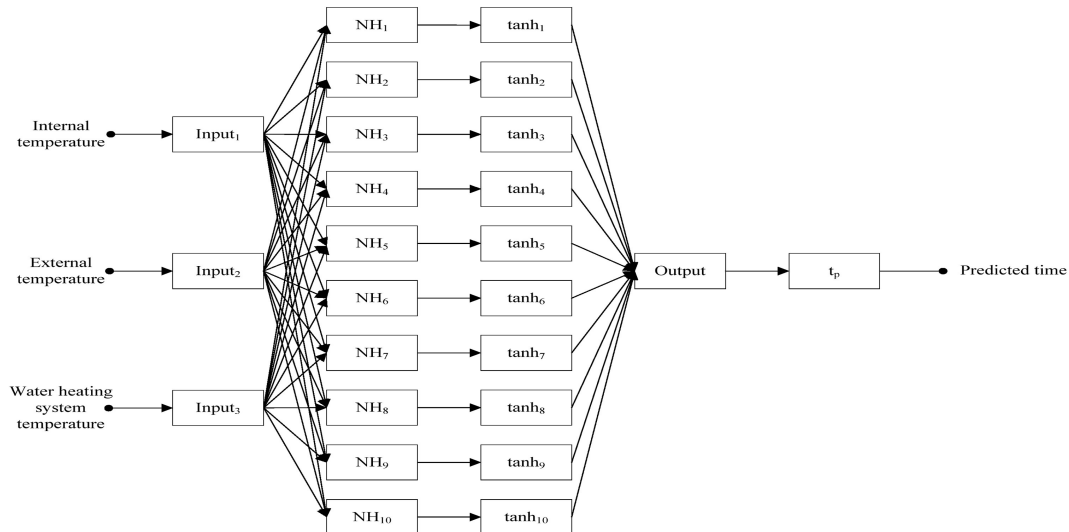


FIGURE 2.6: Artificial neural network implementation [53].

ANN performance. Additionally, the importance of training data size is discussed in [56, 84], both concluded that larger the training data sample is, the better the performance of ANN model.

Normally, residential buildings have non-constant occupancy and maintenance of thermal comfort for whole day leads energy wastage. Hence prediction of unoccupied hours was performed by [54] by using ANN algorithm and prediction of time required for restoration of indoor temperature to set-point temperature using another ANN model. Multi-Objective Genetic Algorithm (MOGA) controller have been efficient technologies in attaining balance between energy consumption and thermal comfort [85] and with hybrid MOGA author achieved around 31.6% energy management efficiency and 71.8% comfort index efficiency. Triple objective controller using particle swarm optimization (PSO) has been developed by [48], which achieved 19.8–33.3% decrease in annual cooling energy, while increasing in annual heating and lighting: 1.7–4.8% and 0.5–2.6% respectively. Final optimization resulted 1.6–11.3% reduction in annual electricity consumption for four climate regions in Iran. Whereas, O'Neill et al. [86] developed Bayesian networks (BNs) [87] model to predict hourly building energy performance with associated uncertainties. The BNs-based building energy performance prediction system can be applied in various scenarios: (1) Retrofitting buildings; (2) Model-based optimization systems; and (3) Energy diagnostics.

Occupancy's thermal comfort sensation of hot or cold mainly depends on subjective parameters (metabolic rate and clothing insulation) and physical ones (mean radiant temperature, air temperature, air velocity, and relative

TABLE 2.2: Overview on black-box models [39].

Type of model	Model structure	Parameter estimation	Example	
Steady-state	Linear	Linear regression (Least Squares method)	Energy signature of weekly values	
	Non-linear	Polynomials Any non-linear function	Linear regression (Least Squares method) Iterative process, Levenberg Marquardt	
Dynamic	Linear	Transfer function models (ARMA, ARMAX, etc.)	Heat flow through a plane wall	
	Non-linear	Neural networks (sigmoid, wavelet, radial basis networks)	Damped gauss-Newton back-propagation	Arbitrary non-linear systems
		Polynomials (Wiener /Hammerstein model, Volterra model)	Linear regression (Least Squares method)	Linear systems with steady-state non-linearities at the input or output (control element with saturation behavior)

humidity) as described by Fanger’s predicted mean vote (PMV) and predicted percentage of dissatisfied (PPD) model-ISO 7730. This method was developed in 1960–1970 and is still used as a baseline model for comfort measurement. Fanger’s base model advancements over the last 40 years are critically reviewed in [88]. An existing HVAC system can optimize PMV index with conventional controller, however, a fuzzy logic-based system is integrated to existing HVAC system to maintain PMV, CO₂, and energy consumption for efficient building performance [89]. This fuzzy logic’s member function together with rule selection were then tuned by multi-objective evolutionary algorithms (MOEA-GA) to minimize number of rules and thus maximizing system performance. This proved to be the best combination for FLC’s with reduced number of rules to maintain PMV and optimizing energy consumption. Table 2.3 gives the standard values for thermal sensation scale of PMV in which +3 being very hot and –3 being very cold. It is always suggested that the PMV value should be maintained within –0.5 to +0.5 to achieve better thermal comfort. The comfort classification based on relationship between PMV and PPD is shown in Table 2.4 [90]. Chen et al. [91] developed data-driven state-space Weiner model to evaluate the dynamic relation between dry bulb temperature variation and occupant thermal sensation. Later they compared developed model to dynamic thermal sensation (DTS). The DTS model is a reactive thermal comfort system with constantly changing its values based on the dynamic variation of weather conditions and occupant preferred thermal sensation votes delivered by an extended Kalman filter (EKF) with feedback system. Furthermore, predicted mean vote

and dynamic thermal sensation models were compared by developing MPC-DTS and MPC-PMV. Results indicated that the MPC-DTS achieved better thermal comfort and energy optimisation than the MPC-PMV model, but both efficiently maintained thermal comfort compared to the baseline model using proportional integral (PI) controller. However, they assumed that there is a feedback system in BEMS, which actually is not the case. Later, Chen et al. [92] conducted the same experiment to investigate the performance difference between MPC-DTS and MPC-PMV with real time actual mean vote feedback values, in addition, authors detailed the probable reasons for performance difference.

The above-mentioned researches mainly focus on optimization techniques used to achieve comfort measurement. However, the accuracy of subjective and physical parameters measurement taken from sensors has a significant impact on the PMV index evaluation. These measurement uncertainties can be evaluated using efficient tools such as: Monte Carlo analysis (MCA) [93], guide to the expression of uncertainty in measurement (GUM) [94], and sensitivity analysis (SA) [90]. These studies show that the proper handling of measurement uncertainties is essential in PMV index model.

TABLE 2.3: Thermal sensation scale of PMV.

PMV	Sensation
+3	Hot
+2	Warm
+1	Slightly warm
0	Neutral
-1	Slightly cool
-2	cool
-3	cold

TABLE 2.4: Comfort classification based on ISO-7730.

Class	Percentage of Dissatisfied (%)	Predicted Mean Vote
A	<6	$-0.20 < \text{PMV} < 0.20$
B	<10	$-0.50 < \text{PMV} < 0.50$
C	<15	$-0.70 < \text{PMV} < 0.70$
-	>15	$\text{PMV} < -0.70$ or $\text{PMV} > 0.70$

Black box models are less complex, does not need complete data of building physical parameters, efficient performance, and easy to build. Nevertheless, they require huge building operational and environmental parameter data for training in order to have efficient prediction values. These data are however difficult to obtain, while low quality data can cause huge prediction

error. Even though, these models are accurate and less complex, the lack of knowledge/explanation of the inner processes from the point of view of physics, there is some reluctance towards black box model implementation over physics-based model.

2.4.3 Gray Box Models

The third category of BEMS is known as gray box models. These are hybrid ones combining simplified physics-based models and data-driven ones. In a gray box model, the process is expressed in mathematical expression that may be based on the physics and/or thermodynamics laws. They consist expressions that have physical explanation (e.g., resistor capacitance network) and a part of the model may be obtained through regression from the available data.

A gray box model is a balanced model between the white box model and black box model. This combination ensures that the non-linearities in white box model can be handled using black box models and lack of laws of physics reasoning in black model can be represented through white box models, but extra effort is required to design and develop these models. However, selection of suitable gray box model structure for developing a good performance system is still a difficult task. Bacher and Madsen, ref. [24] proposed an approach to find appropriate heat dynamics of a building. Indeed, a set of different RC network models have been configured and compared using likelihood ratio tests. The study concludes that significant improvements can be obtained as the model order increases, while no further notable improvements can be expected beyond a model order of 3. Široký et al. [95] proposed an experimental analysis of a heating system using lumped capacitance network in a university building and analysis was carried out for two months. Through this approach they were able to achieve around 15% and 28% energy savings. The experimental analysis not only investigated the performance of MPC but also detailed the issues that can be encountered in its application.

Figure 2.7 illustrates the basic principle of MPC model structure [95], the inputs of the systems are time varying parameters: energy price can be taken from energy market, comfort conditions set by the occupants, occupancy prediction, and environmental parameters. The MPC system formulates the optimization of an objective function by using building dynamic model, a cost-function and constraints. After each time sample formulation, feedback from

occupants and weather conditions are fed back to MPC for the formulation of next time sample, which ensures that unanticipated disturbances are taken in consideration through feedback loop.

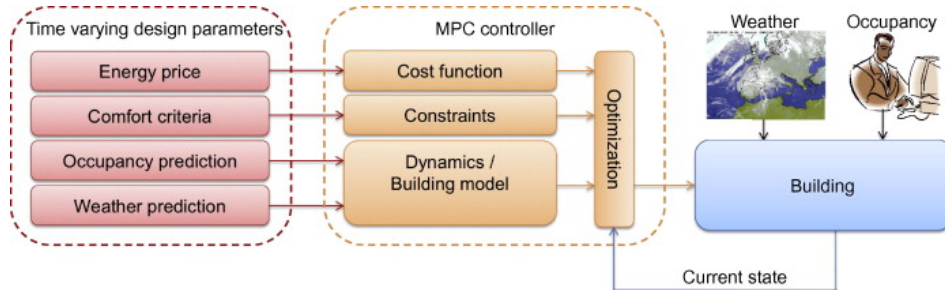


FIGURE 2.7: Basic principle of model predictive control for buildings [95].

A simplified low order gray box modelling has been introduced in [96]. The study considered a whole building as single zone building (Figure 2.8) neglecting the inter-zone heat exchange. Most of the studies in literature did not take account of inter-zone thermal interactions as it increases the complexity of the model and includes numerous uncertainties. In addition, the model performance declines with the increase of the number of zone. However, Cai and Braun [97] proposed a resistance capacitance thermal network model for multi-zone buildings (Figure 2.9) with a unique three-step estimation approach to reduce the complexity of the model and thus improving the performance of BEMS system, through:

- De-grouping weakly linked zones and grouping strongly linked zones.
- Sensitivity analysis to identify and eliminate non-influential variables.
- Correlation analysis to eliminate Non-correlated variables.

Performance of BEMS system is significantly increased because of the above-considered three steps, which have simplified the estimation problem by eliminating non-influential parameters. In general, gray box models can be used for predictions of energy consumption, thermal comfort conditions, occupancy, and heating/cooling load of buildings. These applications leads to use gray box modelling to building in smart Grid context for dynamic load management and energy storage. The reduced order gray box model for buildings connected to smart Grid was investigated in [57], where it is applied on two buildings types (insulated and uninsulated). Furthermore, Sharma et al. [98] presented a study of MPC controller implementation for buildings in centralized energy management system framework (CEMS). In

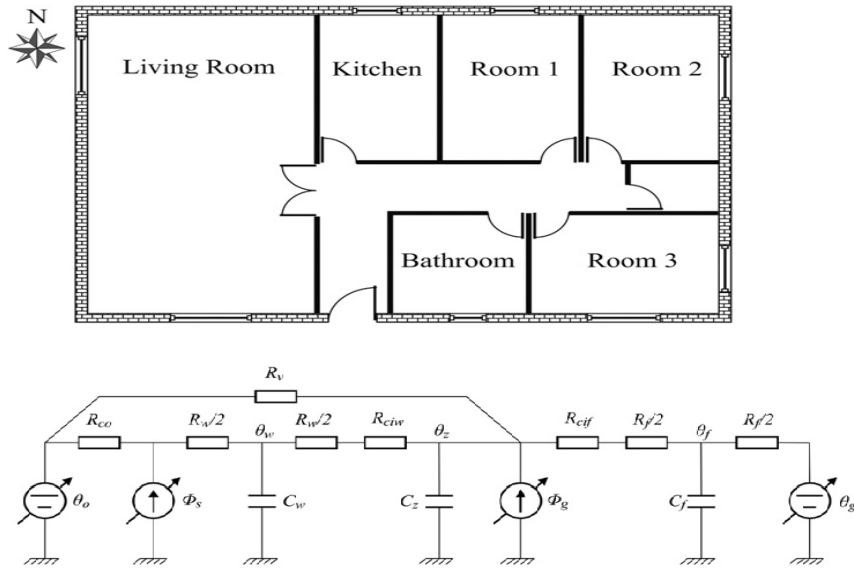


FIGURE 2.8: RC thermal network for single zone building [96].

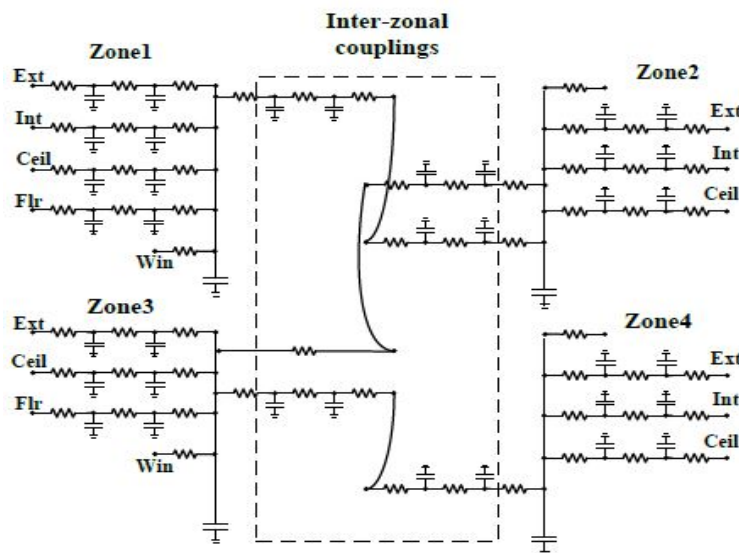


FIGURE 2.9: Resistor capacitance thermal network for multi-zone building [97].

addition, the insulated buildings opens the possibilities of enabling demand-side management (DSM) by exploiting heat capacity flexibility in building thermal wall mass. Harb et al. [99] developed gray-box models for forecasting the building thermal response. The analysis was conducted on four gray box models and data from three building. Building areas varied from 3000 to 30,000 m² and data duration from 39 to 110 days. To determine thermal behavior of the building, three forcing functions were used in this paper:

- Radiative building environment is expressed as the solar irradiation.

- Building thermal environment is represented by the outdoor air dry temperature.
- Various heat sources consists of heating elements.

From the above a three-function input vector is constructed:

$$\mathbf{U} = [T_a \quad Q_{irrad} \quad \phi_h]^T \quad (2.15)$$

where T_a —outdoor dry bulb temperature, Q_{irrad} —global solar radiation on horizontal surface, and ϕ_h —Building thermal consumption.

Four gray box model structures were developed in this paper: (1) 1R1C—the simplest structure characterizes the whole building into a single parameter (Figure 2.10); (2) 3R2C—consists of three resistors and two capacitors. Three resistors indicate convective and radiative heat exchange, and heat exchange between interior to environment, two capacitor indicates interior and exterior thermal mass (Figure 2.10); (3) 4R2C—extension of the 3R2C structure with additional indoor node (Figure 2.11); and (4) 8R3C-extension of the 4R2C considering all type of heat exchanges between interior, exterior, heating elements, and indoor air (Figure 2.11).

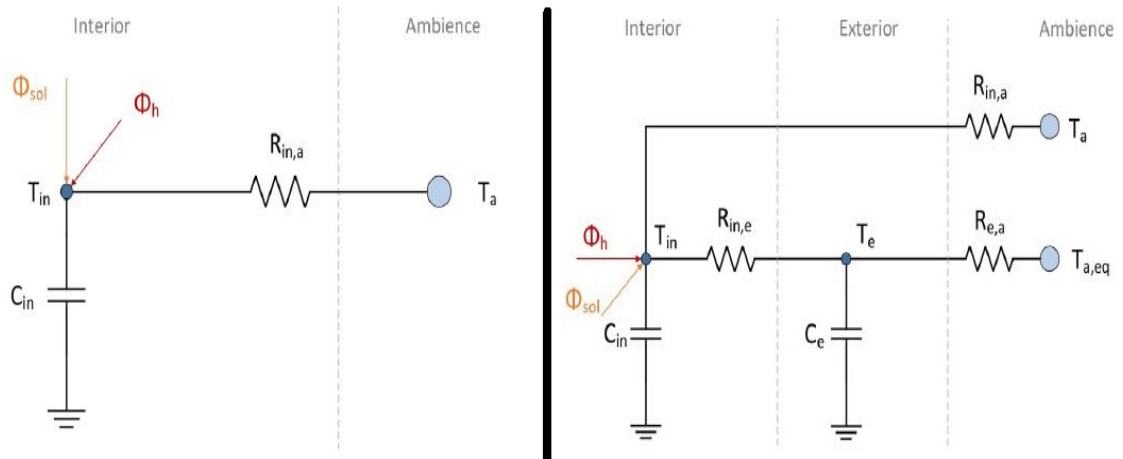


FIGURE 2.10: Building thermal structures—1R1C and 3R2C [99].

The achieved results show that the 1R1C model produced more harmonics in the prediction values due to its simple structure, the 3R2C have produced similar disturbances in indoor air temperature prediction, due to the lack of consideration of heat exchange between indoor and outdoor air temperature. The 4R2C produced accurate prediction in daily indoor temperature prediction, due to the consideration of heat exchange between various parameters.

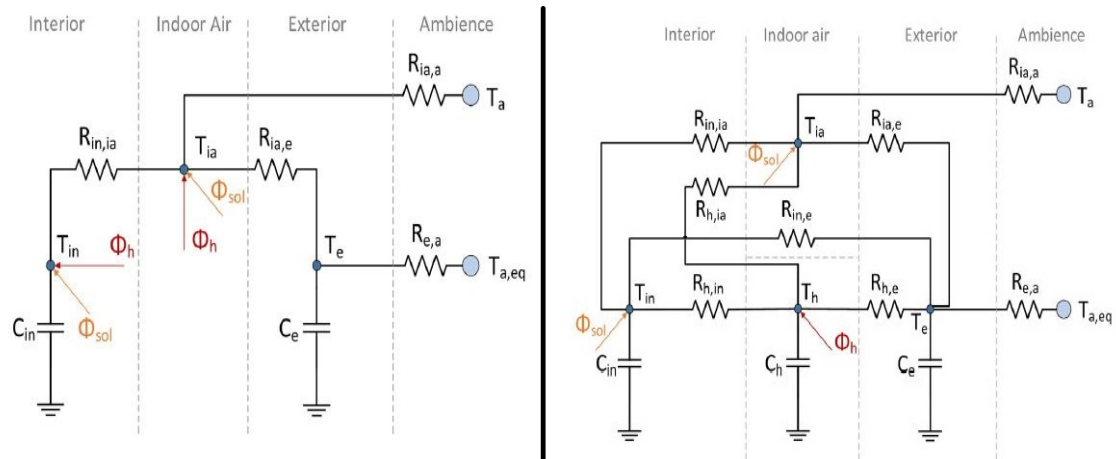


FIGURE 2.11: Building thermal structures—4R2C and 8R3C [99].

The 8R3C produced similar accurate prediction values with no significant improvements in the results despite the detailed model. The 4R2C model can thus be considered as the suitable structure for implementation because of its accuracy and low complexity. From the achieved results, it can be concluded that the addition of indoor air temperature node (4R2C and 8R3C) provides stable prediction values compared to model without indoor air temperature node (1R1C and 3R2C).

Meanwhile, application of MPC systems for building energy and comfort management has gained larger attention, Sturzenegger et al. [100] applied MPC strategy on commercial building of 6000 m² area for energy and comfort control. The results are later compared with existing rule-based control systems. The analysis of MPC implementation proved that energy savings were around 17% with an improved comfort level.

The above-described studies have shown that gray box models are robust, accurate, and applicable to complex buildings. However, these models possess high computational cost making them only profitable in applications for commercial buildings. Further investigations are needed to ensure adaptability and application for small buildings.

2.4.4 Building Models Comparative Analysis

The three modeling techniques comparison analysis has been performed based on reviewed papers for different scenarios. Furthermore, some assumptions are made for this analysis:

- Buildings in the context of smart-grid are considered as residential ones.

- Apartments with large commercial space are considered as non-residential buildings.
- Grid is considered to be a supply source for papers without specific indication on the supply source.
- Demand side management and load shifting are considered as dynamic pricing.

Based on the above-given assumptions, the following observations have been made. The carried out review shows that research majority is conducted on non-residential buildings, around 66%, and residential ones, being 34% (Figure 2.12). Non-residential buildings include: institutional, public, office, swimming pool, hospital, and hotel buildings. This lack of research may be due to the unavailability of data or controller systems. Figure 2.13 illustrates control strategies applied for both building types, where black box models are dominating with 74% and 67% of the overall applied controllers for residential and non-residential buildings, respectively. Significant researches have therefore been conducted on black box models due to their ease of application. Around 21% and 27% gray box models were applied to residential and non-residential building, respectively, while gray box models were less used in residential cases compared to non-residential ones mainly because of their high computational and design costs. Simulation tools combined with other control strategies are used for building energy performance analysis but the stand-alone use is low because of their complexity and high data acquisition cost.

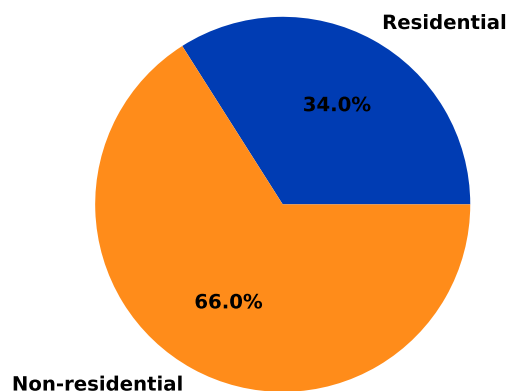


FIGURE 2.12: Research conducted on type of building.

In the context of comfort parameters, thermal comfort acquired more importance in both non-residential and residential buildings, whereas, other

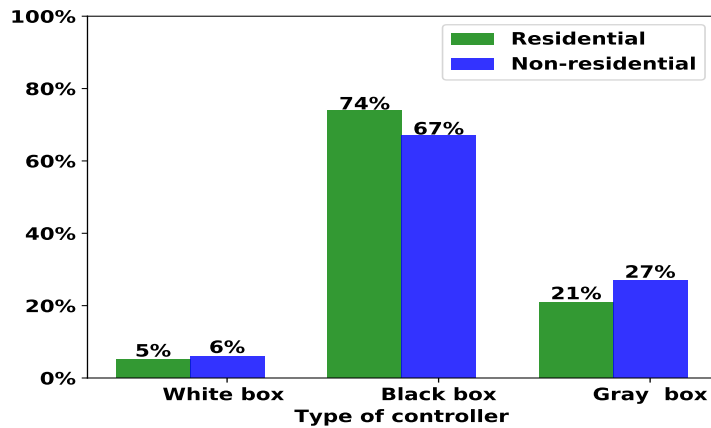


FIGURE 2.13: Controller application on both type of buildings.

parameters are taken into consideration in few papers (Figure 2.14). This indicates the significance of thermal comfort in overall indoor comfort sensation and optimization of thermal energy leads great amount of overall energy consumption reduction in comparison to other comfort variables energy consumption optimization. There is a major lack in consideration of indoor air quality and lighting control. However, regulations and standards urge maintenance of CO₂ and luminance level in order to keep occupants good health and productivity, hence more research on this topic is necessary. Only 5% of the papers have developed controller for all four comfort parameters control. This shows the difficulties in implementation of controller for overall indoor comfort management.

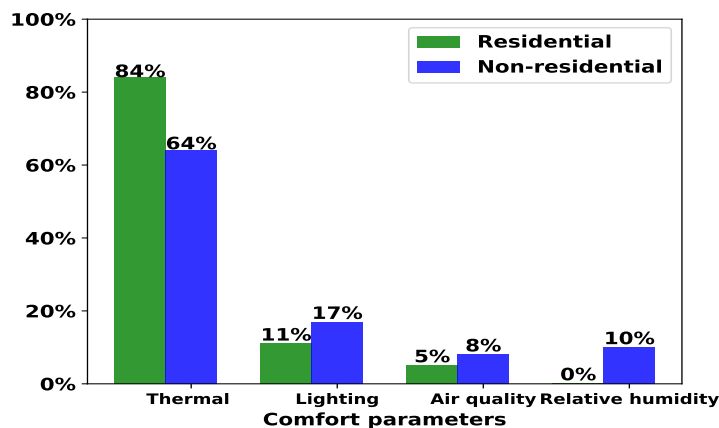


FIGURE 2.14: Controller application on comfort parameters.

Towards sustainable development, installation of renewable energies are important. This factor has also been considered in the literature review. The literature review highlights 16% and 23% renewable energies integration into

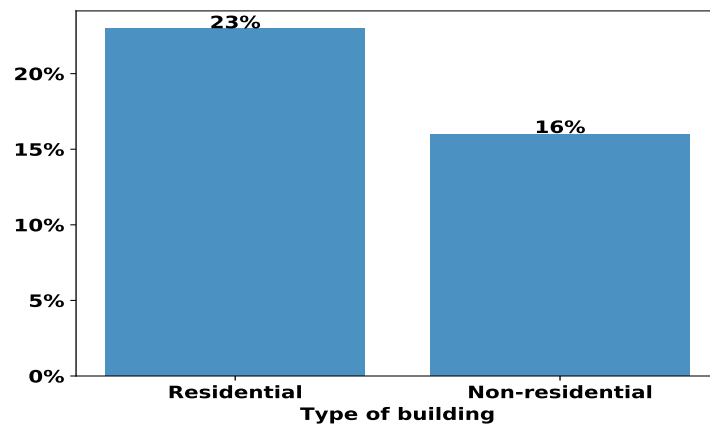


FIGURE 2.15: Renewable energy sources integration in both type of buildings.

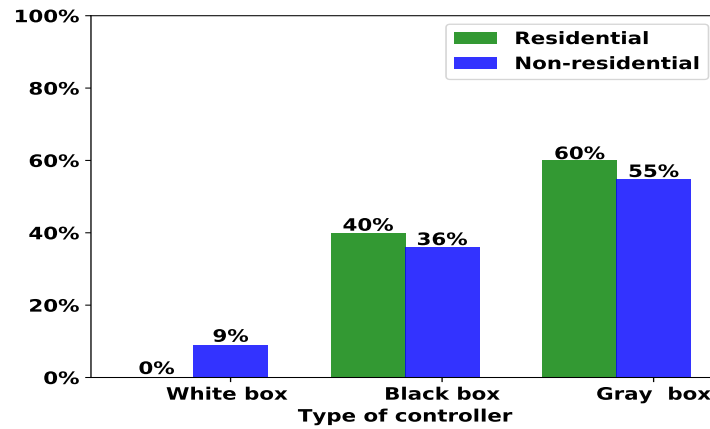


FIGURE 2.16: Controller used for demand response application in non-residential and residential buildings.

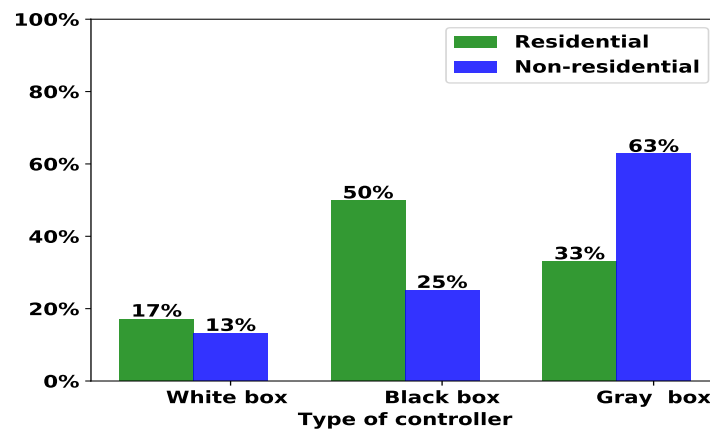


FIGURE 2.17: Controller used for renewable energy sources integration in non-residential and residential buildings.

non-residential and residential buildings, respectively (Figure 2.15). Most of RES integration is observed in smart grid and in big buildings context. The dynamic response in energy consumption by loads is an effective way of maintaining grid balance, grid durability, and cost optimization. Around 22% of non-residential and 25% of residential buildings have adopted DR. In Figure 2.16, it can be noticed the controller types used for DR application in both building types. Gray box modelling has higher implementation percentage because of the high flexibility for multi-objective optimization. Controllers used for RES integration are shown in Figure 2.17, where it should be noticed that black box models have higher percentage of implementation in residential buildings and gray box modelling in non-residential ones. This difference can be justified as follows: (1) Gray box models are characterized by high accuracy and higher computational cost that limit their usage only for large buildings; while (2) black box models are characterized by high accuracy and lower flexibility of MIMO that limit their application to multi-objective optimization purpose. In the literature review, it had been found that black box models includes controllers such as fuzzy logic, artificial neural networks, genetic algorithms, decision trees, particle swarm optimization, reinforced learning, etc., while gray box models includes lumped capacitance model, model predictive controller, hybrid systems, etc.

2.5 Model Predictive Control

2.5.1 Introduction

Most of the existing buildings are equipped with simple set-point temperature control building management systems, without giving importance to reducing the energy consumption, leading to waste huge amount of energy for maintaining thermal comfort. A promising solution for building energy management and comfort control is Model Predictive Control (MPC) [101–103], developed based on the building models. MPC has the capabilities to handle multi-objective control, with consideration of weather parameters, occupancy schedule, dynamic pricing for thermal comfort control. It also optimizes the energy consumption while maintaining the required temperature, and able to handle the constraints on input, output, and states of the system. MPC is the only control methodology that can systematically take into account future predictions during the controller design stage while satisfying the system operating constraints [103]. These features of MPC make

it ideal for building energy management systems.

MPC offers an attractive framework for model-based optimal control of dynamical systems. MPC allows optimizing a cost function subject to state and input constraints. In the context of optimal control of building, we are interested in optimizing the cost function being the energy consumption or cost of energy and constraints are imposed on states such as room temperature, and on inputs such as air mass flow and operational limitations of HVAC components.

MPC General Form

MPC is a multi-objective controller that is based on the system model and used to obtain sequence of control signals to minimize/maximize the cost/objective function by considering applied constraints.

A finite horizon optimal control problem is formulated and solved over a finite future window during each sampling interval. The final result is a future trajectory of inputs and states that respects the building's dynamics and constraints while optimizing the given objectives. In the context of buildings, the control signal trajectory is obtained for future finite horizon at the current control step. Apart from inputs the predicted disturbances, dynamical costs, and input and state constraints can be included in the optimization.

A generic framework is given by the following finite-horizon optimization problem:

$$\min_u \sum_{j=0}^{j=N-1} Q(x_{t+j|t}, u_{t+j|t}, d_{t+j|t}) \quad (2.16)$$

$$\text{subject to } x_{t+j|t} = f(x_{t+j|t}, u_{t+j|t}, d_{t+j|t}), \forall j = 0, 1, \dots, N-1, \quad (2.17)$$

$$y_{t+j|t} = g(x_{t+j|t}, u_{t+j|t}, d_{t+j|t}), \forall j = 0, 1, \dots, N, \quad (2.18)$$

$$u_{t+j|t} \in U, \forall j = 0, 1, \dots, N-1, \quad (2.19)$$

$$y_{t+j|t} \in Y, \forall j = 0, 1, \dots, N \quad (2.20)$$

where $x_{t+j|t}$ is read as "the state variable x at time $t + j$ predicted at time t ", N is the prediction horizon, x is the system state vector, u is the controllable input variables vector, d is the uncontrollable inputs vector, i.e., disturbances

of the system, $f(x, u, d)$ is the function allows to predict the building states based on the current conditions of x , u , and d ,

Each component of the MPC formulation is essential and how they influence the performance are detailed below. For more insights on the MPC formulations, components applicability, and their influence on the performance readers can refer [104].

Objective Function

The main purpose of the objective function is to guarantee the stability of the system while achieving minimum/maximum cost (Equation 2.21).

- **Stability:** The structure of the objective function is commonly chosen so that the optimal cost forms a Lyapunov function for the closed loop system, guaranteeing stability. In the context of buildings, which have slow dynamics, the cost is purely determined based on the performance.
- **Performance target:** This the objective of the function. Generally, in buildings, the objective will be to optimize energy consumption while maintaining the comfort.

$$Q(x_{t+j|t}, u_{t+j|t}, d_{t+j|t}) = (y_t - y_{r,t})^T Q_t (y_t - y_{r,t}) + R_t u_t \quad (2.21)$$

Dynamics The system model is an essential part of the MPC controller. It is the mathematical model of the building. A LTI model is always preferred as the system model. These system dynamics from the thermal network model can be represented using the state-space formulation.

$$\begin{aligned} X(k+1) &= AX(k) + Bu(k) + B_1 d(k) \\ y(k) &= CX(k) + Du(k) + D_1 d(k) \end{aligned} \quad (2.22)$$

Here the real matrices A , B , B_1 , C , D , D_1 are so called system matrices and are of appropriate dimensions. This is the most common model type and the only one that will result in a convex and easily solvable optimization problem.

Constraints The MPC controller's major advantage is the ability handle the given constraints. These can be applied on both the states and the output, as

well as the input. The most frequent sort of constraint is a linear constraint, which is used to set upper and lower boundaries on system variables.

$$u_{min,t} \leq u_t \leq u_{max,t}, \quad (2.23)$$

or generally formulated as

$$G_t u_t \leq g_t \quad (2.24)$$

The constraints can be similarly defined for system states and outputs.

The objective function 2.17 allows to minimize the energy consumption for given set of operational constraints. A large amount of research studies has been demonstrated MPC applied for efficient building management/control. MPC controllers significant advantage is taking into consideration measurable disturbances (weather, occupancy, uncontrollable heating systems, etc.), and then producing the optimal control strategy, while better handling constraints impacting operating conditions [105]. MPC can be applied to specific parameter of building systems such as: building cooling systems [103], indoor air quality [106], heating systems [107], ventilation [108], and energy management [109].

2.5.2 HVAC Systems

In the previous sections, it was noticed that thermal comfort is essential for both residential and commercial buildings to keep occupants' healthy and productive. In general, the HVAC systems are centralized and have same air conditioning in the whole building. There has been gradual development of HVAC systems from complete building to individual zones independent of other zones in the same building. Such systems (called as "multi-split air conditioning systems") focuses on zone specific comfort management, the overall comfort conditions increase significantly at the same time reducing the energy consumption from the zones in which heating is not required [110–112].

Air-Conditioning System

The air-conditioning system is consisted of a central constant volume supply fan that supplies conditioned air to all the local variable air volume terminal boxes through a network of ducts. Quantity and temperature of the mixture of the air which is delivered to each room is designed based on the room sensible load, the quantity and temperature of the outdoor air in the mixture,

and space thermostat setting. Additional part of the air that is not needed for conditioning each space is bypassed into a common return air path and after getting mixed with the return air from all the other spaces goes back to the air handling unit as return air stream usually with the help of a return/exhaust fan. Terminal units are also equipped with hot water reheat coils or electrical strips that are designed for either heating or dehumidification of the discharged air to each space.

The cooling or heating capacity, Q , is the product of airflow, times the difference in temperature between the supply air to the zone and the return air from the zone.

$$Q = \dot{m}_{s,air} c_{pa} (T_{s,air} - T_{zone}) \quad (2.25)$$

Where $\dot{m}_{s,air}$ is the air mass flow through the ducts into zone, c_{pa} is the specific heat of air, $T_{s,air}$ is the temperature of the chilled air or hot air that comes into the zone through the ducts, and T_{zone} is the zone temperature.

Heating System - Air Source Heat Pump - Variable Refrigerant Flow Systems

A multi-split air conditioning system consist of one outdoor unit and multiple indoor units, the refrigerant flowing in the system varies flow rate (variable refrigerant flow - VRF) based on the heating or cooling load requirement of each zone with the help of variable speed compressor and electronic expansion valves (EEVs). There are many different heat pumps available in the market based on their type of thermodynamic cycle (type of refrigerant liquid) and type of source. There are mainly three types of source available in the nature:

- Air source heat pumps (ASHP),
- Ground source heat pumps (GSHP), and
- Water source heat pumps (WSHP).

The most common and widely used heat pump is air source heat pump and it generally follows the principle of the reversed Carnot cycle [113]. In ASHP, heat is absorbed from the surrounding air and then transports it into the indoors during winter season for heating and reverses its operation from indoor to outdoor during summer for cooling purposes. The major benefit of

using an ASHP is that useful heat is extracted from air, which is abundant in nature and free. ASHP implemented with variable refrigerant flow is called ASHP-VRF system. A typical ASHP-VRF system having multiple indoor units and one outdoor unit is presented in Figure 2.18.

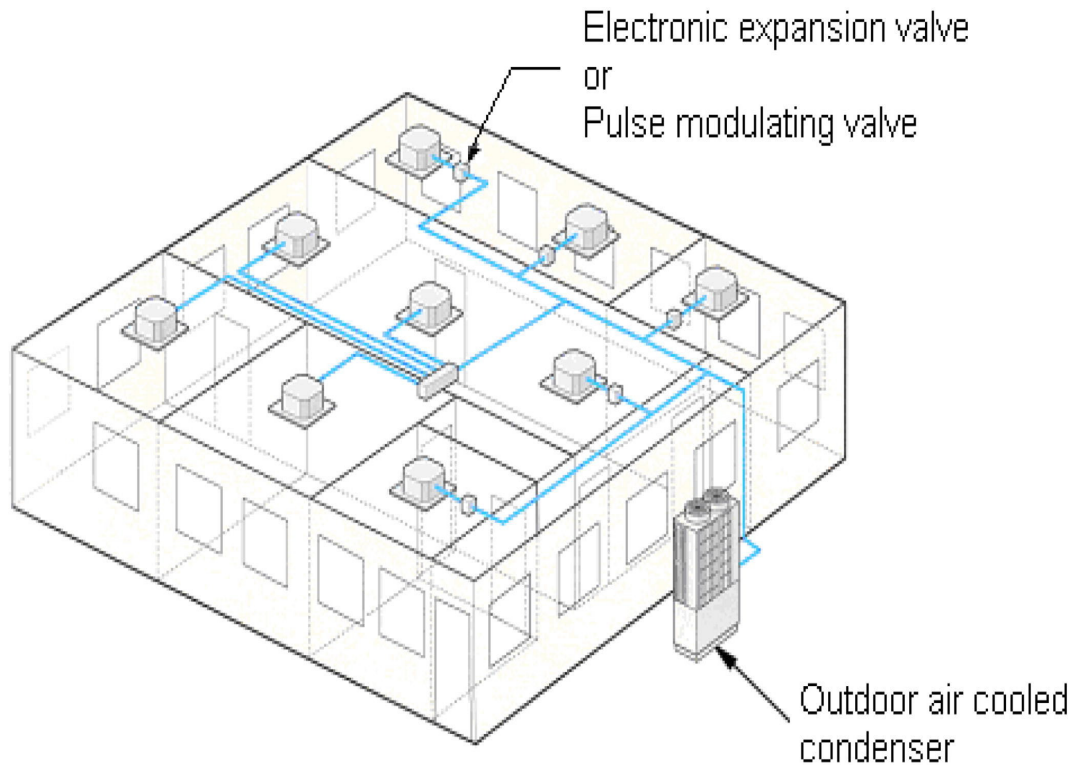


FIGURE 2.18: ASHP-VRF system with multiple indoor units [110].

This system can be used for both cooling and heating purposes by reversing its operation. In the heating mode, the heat absorbed from the outdoor unit increases the temperature of the refrigerant and converts into superheated vapor at low-pressure thus acting as evaporator, this superheated refrigerant enters compressor and leaves at high-pressure. The discharged high-pressure refrigerant enters the indoor unit heat exchanger to heat up the room (used as condenser). Then, the low temperature, high-pressure refrigerant passes through electronic expansion valves (EEV) to obtain low temperature, low-pressure refrigerant. This is again fed back to evaporators, and the cycle completes [114–116]. In ASHP-VRF system, the refrigerant flow is controlled by the variable compressor speed, thus changing its mass flow rate to match the required heating/cooling loads of all indoor units. Although, with many benefits of ASHP-VRF systems, there is only a limited number of studies can be noticed in the open literature. The high variation in loads

from different indoor units, operational conditions, and operational parameters greatly influence modeling difficulty and complexity. In general, the performances of the simulated systems greatly differed from the measured values [117]. Many studies have been carried out to develop a generic model by considering the indoor temperature as constant and steady-state simulation techniques [118]. In addition, there is no standard simulation tool to use for VRF performance analysis. Considering this huge gap in literature, this study attempts to design and develop a generic model for ASHP-VRF systems.

2.6 Conclusions

This chapter has dealt with a state of the art review of recent developments on building energy and comfort management, and the related control. The carried out investigations includes explanation of conventional controllers and their up-gradation to the current challenging applications and new methods viz., black and gray box modelling. These models have been compared and critically reviewed on the basis of comfort conditions, RES integration, DR application, and building type. The proposed critical review depicts in-depth representation of the methodologies and will be helpful in selection of suitable controller methods for BEMS model based on various conditions. In addition, the following observations, comments, and recommendations should be helpful.

- All the comfort parameters (thermal, visual, air quality, and relative humidity) need to be controlled in the building to ensure occupants' health and productivity. However, thermal comfort control remains dominant as the other parameters have a minimal impact on energy consumption. In addition, these parameters inclusion may introduce complexity in the controller model and leads to poor performance.
- White box models have been investigated as preliminary models for building energy performance analysis and were found to be used for low scale application. However, the white box application is restricted only for initial analysis and is not efficient to implementation due to its limitations.
- Black box models have high accuracy, low computational cost, and higher flexibility for building non-linearities. These models have gained

significant attention in recent years. Constant developments of new algorithms ensures the improved efficiency and suitable for multi-objective applications. Nevertheless, these applications have restricted implementation due to lack of physics-laws explanation and huge amount of data is required for model training.

- Gray box models are found out to be more feasible for multi-objective optimization, predictive/adaptive, and cost-optimization applications.
- Finally, the heat pump and VRF models are detailed and the operation principle is presented.

Based on the findings, model predictive controller based on gray box model implementation looks feasible in our case due its advantages over other models in the case of data unavailability. The first step in this work is to develop a model to replicate the heat transfer dynamics of the building. The selection of models for representing the whole-building and its parametric identification is detailed in the following chapters.

Chapter 3

Lumped Parameter Thermal Network Modeling

The objective of this chapter is to provide a brief introduction on the energy/heat transfer dynamics in buildings and its behavior. Different heat transfer methods that are used in developing simulation tools, modeling techniques, and control purposes are discussed here. This chapter contains review on the different modelling techniques and building climate control strategies. Some comments on adaptability, implementability, and advantages and disadvantages of these modeling techniques are given.

The chapter divided into two parts, first part is introduction to the importance of the lumped parameter thermal network models and some review of various studies from the literature. A physical model based on heat balance equation was presented using its equivalent analogy to electrical systems. Furthermore, we discussed on different configurations of thermal network models that are well-established, this section was the basis for selection 3R2C model for our thesis. Later, we have also introduced analytical and numerical methods to solve heat equation. A comparison has been given between analytical and numerical model, in order to develop reference model for parameters identification we selected numerical Crank-Nicolson FDM because of its simplicity, stability, and accuracy over other FDM and analytical models.

Finally, the simulations were carried for different configurations of composite walls and their parameters identified using PSO, the optimal model is compared against other two models. The comparison models have different R and C values. It has been observed that the model with optimal value performed well and followed the dynamics of the reference model. The proposed method is then validated against an analytical model from literature.

3.1 Introduction

In the literature review (Chapter 2), it was highlighted that the grey box models are dominant in the case of multi-objective controller applications. The most used models for these controllers were lumped parameter thermal network models (LPTNM), due to their simplified reduced order, computational efficiency, reliability, and acceptable accuracy. These characteristics of the LPTNM reduces enormous amount of simulation complexity over the simulation tools, these models also offer best solution for short time period controller application [11, 19, 22, 33, 119, 120]. The thermal network methods help to obtain simplified/reduced state space models of the buildings

thermal dynamics model. Building reduced models are often developed on the basis of linear networks with lumped parameters [121–125]. The principle idea is to have an analogy between two different domains, which can be described by the equivalent mathematical equations. Applying this analogy, building models with the help of lumped parameters are expressed as electrical circuits and state-space equations are deduced from these circuits. The LPTNM can be mathematically modeled by using Ordinary Differential Equations (ODE). Thermal - Electrical system analogy is given in Table 3.1.

TABLE 3.1: Thermal to Electrical system analogy.

	Thermal System	Electrical System
Source	Temperature (T)	Voltage (V)
	Heat flux (ϕ)	Current (I)
Element	Thermal conductivity (k)	Conductivity (σ)
	Thermal resistance (R)	Electrical resistance (R)
	Thermal capacity (C)	Electrical capacitance (C)

The equivalent thermal network circuit of a zone is determined by incorporating models of building envelope such as: walls, windows, and internal mass, etc. In thermal RC network model, the building is split into a network of nodes with interconnecting paths, through which the energy flows [126, 127]. The application of this method differs primarily based on the choice of nodes on which energy balance is applied. These models can be developed for two categories:

1. Model for a building envelope (walls, floors, roofs, etc.). These models are then used to develop complete zone model.
2. Model for a complete zone.

Whilst, there is not huge difference between two methods, the model for a complete zone is developed by aggregating the individual envelope models into a single model. Whereas, the specific model for building envelope are significant in knowing surface temperatures, analysis of individual envelope dynamics, etc.

3.2 Lumped Parameter Thermal Network Model (LPTNM)

In most of the cases, the simulation of the thermal model response of the building must be performed at high time resolution. For example, experiments on the transient response of HVAC plant; study of control system responses; control system optimization; and design analysis of smart controllers. Previous approaches (analytical and numerical approaches), while suitable for longer-term studies related to heating/cooling load prediction, but these are usually not well suited for models that require short-time response. An approach that offers reasonable accuracy over short time horizon simulations and, by its simplicity, exhibits low computational demands, can be accomplished by considering each building element as one or a small number of 'lumps' in which a uniform thermal response is assumed.

The LPTNM approach is used to simplify the complex modeling of building dynamics, and to obtain reduced order simplified models of the buildings based on state-space equations. Lorenz and Masy [128] proposed among the early implementations of a thermal network model of configuration 2R1C (two resistors and one capacitor) to represent building envelope. The model also includes various heat sources, such as space heating ($Q_{heating}$), heat gains from solar radiations (Q_{s-sur} and Q_{s-air}), and the gains from occupancy (Q_{occu}). The energy grains from the occupancy includes gains from electrical appliances and occupants. The thermal network proposed in this study is presented in Figure 3.1.

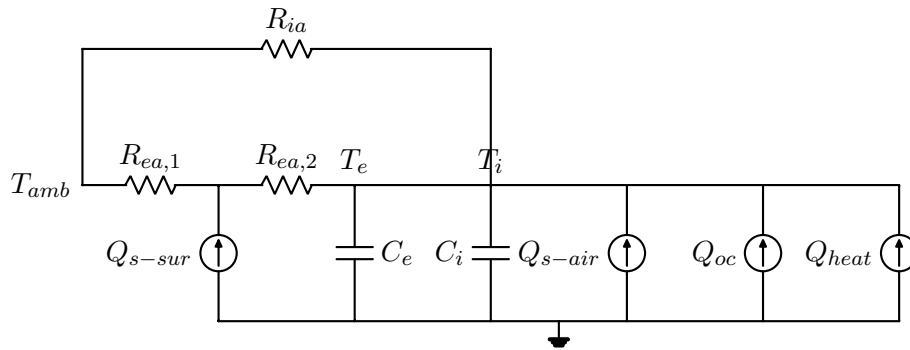


FIGURE 3.1: Thermal network model for whole building [128].

Davies [129] proposed lumped parameter methodology for single layer and multi-layer walls. In this paper for a single layer two resistors and one capacitor model is selected (see Figure 3.2), where T_r , T_w , and T_o represent room, wall, and outside air temperature, respectively. The thermal resistance is

3.2. Lumped Parameter Thermal Network Model (LPTNM)

equally divided into two r_r and thermal capacitance is represented as C . The corresponding mathematical equations can be described as follows:

$$(T_o - T_w)/r = C \frac{dT_w}{dt} + (T_w - T_r)/r \quad (3.1)$$

$$C = \rho C_p LA \quad (3.2)$$

$$R = L/kA \quad (3.3)$$

They have proposed four resistors three capacitor (4R3C) model for seven layer wall. They concluded that proposed methodology is comparatively simple and direct, and the results are very close to those found using the frequency domain method.

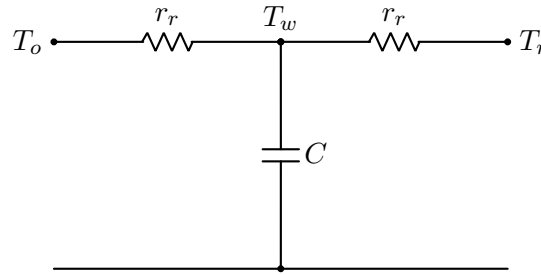


FIGURE 3.2: Simplified thermal network model - 2R1C [129].

Gouda et al. [21] proposed improvised model of configuration 3R2C to obtain accurate models by non-linear optimization. The paper presented multi-order models from 2R1C to 21R20C. The model parameters were determined using an optimization technique by fitting the thermal response of 2nd order model (3R2C) with the reference 20th order model (21R20C). The results of 3R2C model is more accurate than the 2R1C model with the slightly more computational cost. The paper concluded that 3R2C model with proper parameter values is best suited for practical applications in comparison with 2R1C model.

Fraisse et al. [19], proposed a technique to evaluate resistors and capacitors values analytically, and then analyzed the performance of various RC combinations (2R1C, 1R2C, 3R2C, and 3R4C). These parameter values can be used to develop a reduced order model to realize thermal behavior of buildings while considering radiative and convective loads from the internal and external sources. The models were compared in time and frequency domains

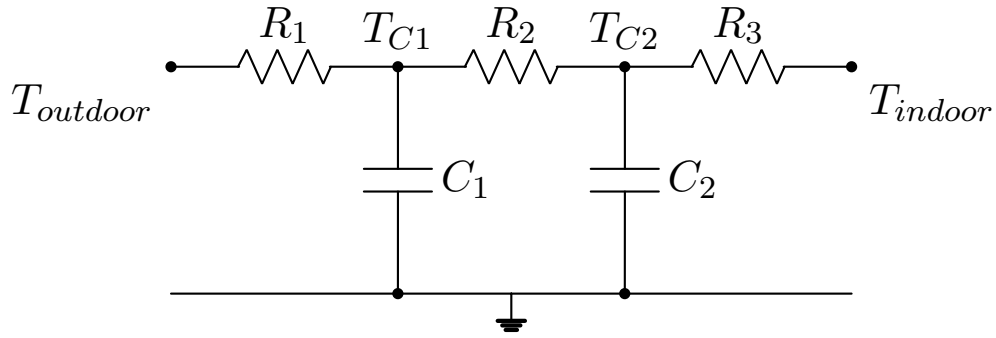


FIGURE 3.3: Simplified thermal network model - 3R2C.

and results were analyzed. Among all models, the 3R4C model is more reliable since it considers the thermal inertia of the inside surface of the wall. The 3R4C model was then added to the zone model that consists of windows, roof, floor, internal walls and partition walls.

Harb et al. [119] developed models for forecasting the building thermal response. The analysis was conducted on four models and data from three building. Building areas varied from 3000 to 30,000 m² and data duration from 39 to 110 days. To determine thermal behavior of the building, three forcing functions were used in this paper:

- Radiative building environment is expressed as the solar irradiation.
- Building thermal environment is represented by the outdoor air dry temperature.
- Various heat sources consists of heating elements.

From the above a three-function input vector is constructed:

$$\mathbf{U} = [T_a \quad Q_{irrad} \quad \phi_h]^T \quad (3.4)$$

where T_a —outdoor dry bulb temperature, Q_{irrad} —global solar radiation on horizontal surface, and ϕ_h —Building thermal consumption.

Four model structures were developed in this paper: (1) 1R1C—the simplest structure characterizes the whole building into a single parameter (Figure 3.4); (2) 3R2C—consists of three resistors and two capacitors. Three resistors indicate convective and radiative heat exchange, and heat exchange between interior to environment, two capacitor indicates interior and exterior thermal mass (Figure 3.4); (3) 4R2C—extension of the 3R2C structure with additional indoor node (Figure 3.5); and (4) 8R3C-extension of the 4R2C considering all

3.2. Lumped Parameter Thermal Network Model (LPTNM)

type of heat exchanges between interior, exterior, heating elements, and indoor air (Figure 3.5).

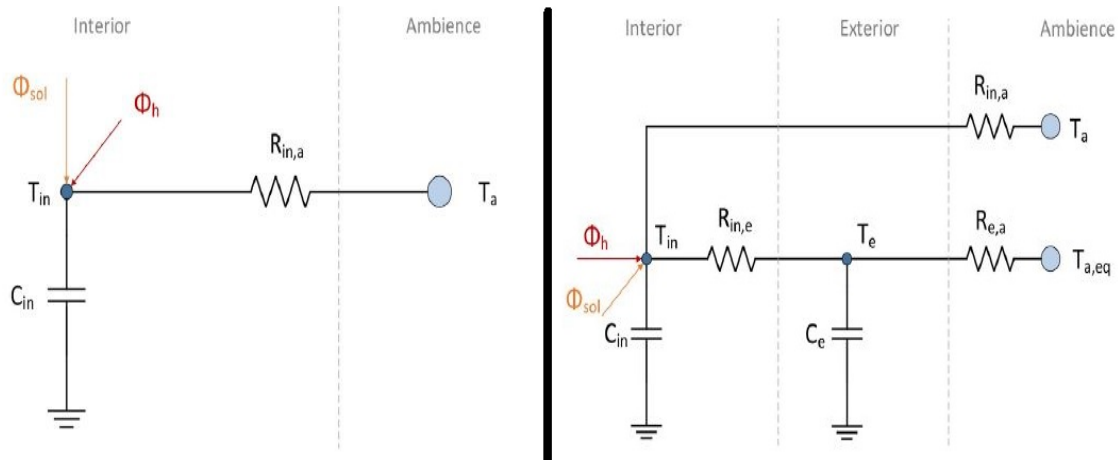


FIGURE 3.4: Building thermal structures—1R1C and 3R2C [119].

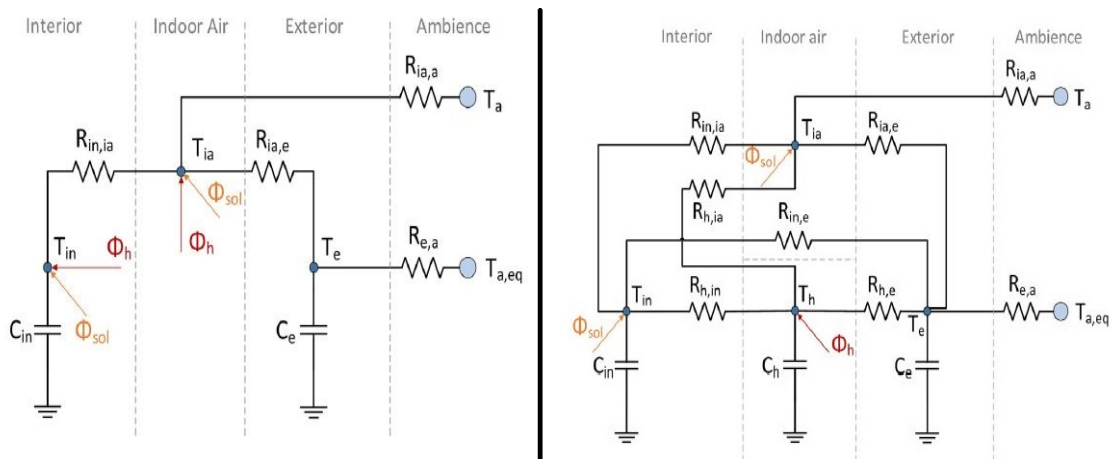


FIGURE 3.5: Building thermal structures—4R2C and 8R3C [119].

The achieved results show that the 1R1C model produced more harmonics in the prediction values due to its simple structure, the 3R2C have produced similar disturbances in indoor air temperature prediction, due to the lack of consideration of heat exchange between indoor and outdoor air temperature. The 4R2C produced accurate prediction in daily indoor temperature prediction, due to the consideration of heat exchange between various parameters. The 8R3C produced similar accurate prediction values with no significant improvements in the results despite the detailed model. The 4R2C model can thus be considered as the suitable structure for implementation because of its accuracy and low complexity. From the achieved results, it can be concluded that the addition of indoor air temperature node (4R2C and 8R3C) provides

stable prediction values compared to model without indoor air temperature node (1R1C and 3R2C).

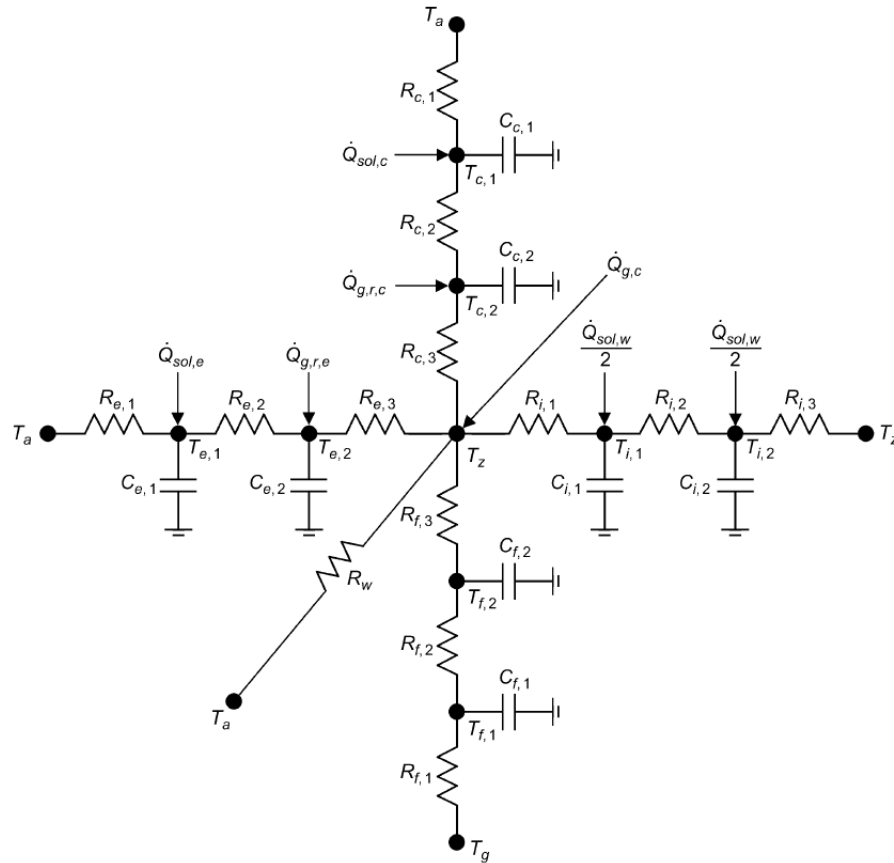


FIGURE 3.6: Thermal Network for Overall Building Model [130].

The reduced order modeling methodology for the buildings using the LPTNM has been well suited for buildings. Cases of low-energy buildings for which thermal insulation and mass delivery are improved have been studied. Hazyuk et al. [131] developed a thermal network model for whole building and the envelope is represented by 2R1C configuration. The resistance value of wall is equally distributed to the two resistors and they have proposed a 2R1C thermal network for slab as well. Parameters values are identified by inverse method. Xu and Wang [127] presented a study of an alternative simplified building energy model that combines both lumped parameter model of configuration 2R2C with the conduction transfer function (CTF) model. Where, the envelope models were represented by CTF and internal mass model was represented by 2R2C. Same authors [132] proposed another method to develop 3R2C building envelope model based on frequency response models and the parameters of this model were identified and optimized using

genetic algorithm with short-term monitored operation data. Braun and Chaturvedi [130] proposed an inverse model development, they used 3R2C thermal network configuration to represent each of the building elements and represented whole building linking each 3R2C network of each element, such as external walls, roof, slab, and internal partitions (see Figure 3.6). Similarly, Ramallo et al. [133] proposed 3R2C model with dominant layer approach. This method does not require complex numerical operations, but is obtained using a simple analysis of the relative influence of the different layers within a construction on its overall dynamic behavior.

Despite the robustness, reliability, and modeling simplicity of the thermal network models. There are great difficulties in development of such models as its performance mainly depends on the optimal values of network parameters: resistors and capacitors. Composite walls have multi-layers with different thermo-physical characteristics, hence positing of resistors and capacitors with proper values is complex task. The parametric values can be identified using three ways:

- Direct method: These methods are similar to white box models. The parameter values are identified using analytical methods such as: CTF, response factor, etc.
- Inverse method: These methods are similar to black box models. The parameter values are identified by curve fitting method. The collected data from the building is used to identify the parameter values.
- Hybrid method: In this method, the parameter values are identified using curve fitting. However, data collected from the building is not required for curve fitting. The data can be obtained from the reference models such as: analytical methods, and numerical method.

Parametric identification from analytical approach is complex in designing and simulation. Whereas, inverse methods are simple to use. The parameters values identified using inverse method can over estimate the value as compared to the values calculated using thermo-physical properties. This overestimation can cause reduction in the performance accuracy. However, the accuracy of these models are still under acceptable range hence inverse methods are mostly used where performance data from the building is available.

In the case of developing building model to analyze the performance of the new buildings, such performance data will not be available to implement

inverse method. To overcome this problem, hybrid models are developed. These models use reference models to replicate the thermal dynamics of the building using the thermo-physical values of the materials. Reference models can be analytical or numerical methods. As described in the previous section, solving heat transfer dynamics analytically becomes complex. Whereas, the numerical methods are efficient and easy to implement to solve heat transfer dynamics. These numerical methods are computationally inefficient, but the parameter values identified once and same values are used for rest of thermal network simulations hence these methods can be considered for developing reference models.

This section summarizes that the development of thermal network model methodology for building thermal response simulations are well-established and the most of the building elements are represented by 3R2C thermal model network. It has been observed that this 3R2C model is more accurate and computationally efficient only with the optimized parameter values. Many studies have proposed the inverse modeling method but in the case of conventional buildings where data is not collected application of such models become difficult. Furthermore, many of the studies, which have shown forward method have used analytical models as reference models. In analytical approach, the parametric values will be obtained by using set of algebraic equations and in numerical methods, an approximation of RC values are achieved by using optimization techniques. Numerical approaches have shown greater accuracy than the analytical approach because of their optimization techniques and limitation of analytical approaches for few combinations.

3.3 Building Envelope Modeling

Heat transfer through building envelope includes several heat and mass transfer processes. Conduction, convection, and radiation heat transfer through buildings are some major factors to be considered in model development. One of most important types of heat transfer in buildings is heat conduction through building envelope mainly through walls, floors, and roofs.

The conduction heat transfer in a wall under steady-state conditions can be defined using Fourier's law of heat conduction [134]:

$$\dot{Q}_{cond} = -kA \frac{dT}{dx} (W) \quad (3.5)$$

3.3. Building Envelope Modeling

where \dot{Q}_{cond} —conduction heat transfer through building envelope (W),

k —thermal conductivity of the material (W/m·K),

T —temperature (K),

A —surface area of the wall (m²), and

x —spatial coordinate (m)

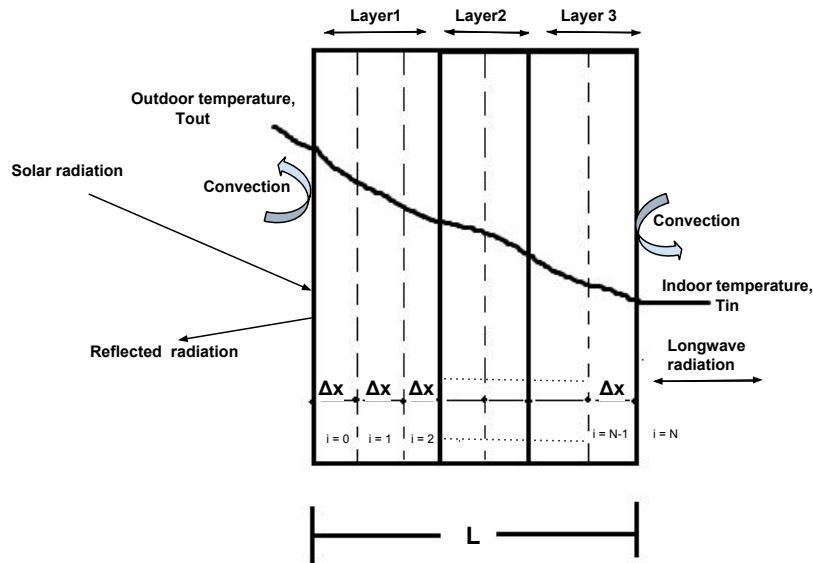


FIGURE 3.7: Heat flow through wall.

The thermal energy flow through multilayer homogeneous wall is shown in Figure 3.7. Equation for the heat transfer through building envelope can be obtained by making these assumptions:

- Thermal energy flow is considered in only spatial x coordinate, because the ratio between height and thickness is very large that results in negligible amount of thermal flow along other directions, i.e., y and z directions [135],
- There is no heat source or sink within the wall,
- Effects of thermal bridge are neglected, and
- Thermal energy distribution in the material is isotropic in nature and thermal properties are temperature independent.

The temperature at any given point is the function of space x and time t , i.e., $T = T(x, t)$. By making above assumptions the heat transfer Equation

(3.5) becomes:

$$\frac{\partial T(x, t)}{\partial t} = \alpha \frac{\partial^2 T(x, t)}{\partial x^2} \quad \text{for } 0 < x < L, t > 0, \quad (3.6)$$

where $\alpha = \frac{k}{\rho C_p}$ —thermal diffusivity (m^2/s),

L —thickness of the wall (m),

k —thermal conductivity of the material ($\text{W}/\text{m}\cdot\text{K}$),

ρ —density (kg/m^3),

C_p —heat capacity of the material ($\text{J}/\text{kg}\cdot\text{K}$).

Equation (3.6), requires to be solved with boundary conditions at two surfaces of the envelope, and initial conditions. Due to the effect of movement of air near the wall surfaces results in convective heat transfer, hence convective boundaries are formulated as follows:

$$\begin{aligned} k \left(\frac{\partial T}{\partial x} \right)_{x=0} &= h_c [T_s(t) - T_{x=0}(t)] \\ k \left(\frac{\partial T}{\partial x} \right)_{x=L} &= h_c [T_{x=L}(t) - T_i(t)] \end{aligned} \quad (3.7)$$

The partial differential equation (PDE) (3.6), along with convective boundary conditions (3.7), can be solved analytically, by using well-established methods [33, 136, 137]: Laplace transforms or Separation of variables or others. Nevertheless, heat transfers in buildings are time dependent and are generally difficult to model by analytical methods. Numerical approaches are therefore preferred to approximate solutions, because of their complexity handling capabilities.

3.3.1 Numerical Modeling

The analytical methods have sound intuitive appeal and are computationally efficient, but they can seriously complicate the smooth solution of the building space model, which may require both heat and mass transfer, forced and natural convection with field-dependent laminar and turbulent characteristics, and contact with the plant. An alternative solution is to consider the transient thermal conduction equation as a nodal problem and to solve it numerically, thereby allowing this each node of the problem to participate as part of a larger building envelope problem. Consideration is then

provided to the treatment of heat exchange on room surfaces, including the treatment of long-wave and short-wave radiant exchanges, followed by the closing of surface, source and room air exchanges resulting in room space heat exchange.

The development of high-speed digital computers has greatly improved the use of computational methods in various fields of science and engineering. Many complex problems can now be overcome at a relatively low cost even in a very limited period using the available computational resources. Presently, the finite difference method (FDM), the finite volume method (FVM), and the finite-element method (FEM) are widely used for the solution of partial differential equations of heat, mass, and momentum transfer [138].

There is a great deal of research on the use of these approaches to solve heat transfer problems. Each approach has its benefits, depending on the design of the physical problem to be solved, but there is no perfect way to solve all the problems. For eg, the dimension of the problem is an significant aspect that needs some attention, since an efficient approach for one-dimensional problems cannot be so appropriate for two-or three-dimensional problems.

FDMs are easy to formulate and can quickly be generalized to two-or three-dimensional problems. In addition, FDM is very straightforward to learn and refers to the solution of partial differential equations found in the simulation of engineering problems with basic geometries. Whereas, In the case of problems containing irregular geometries in the solution domain, the FEM is proven more compact since the area near the boundary can easily be separated into sub-regions. The main drawback of FDM used to be its difficulties in efficiently solving problems over arbitrary complex geometries due to the interpolation between the boundary and the inner point, in order to develop finite differences of expression for nodes next to the boundary. Recently, with the emergence of numerical grid generation approaches, FDM has become equivalent to FEM in the handling of irregular geometries, while retaining the flexibility of standard FDM [138–141]. In this thesis, FDM is used for solving conduction heat transfer equation because of its simplicity and reliability.

3.3.2 Finite Difference Method

The FDM for solving a differential equation is based on the assumption that when the spatial and temporal domains are divided into a uniform finite

number of slices and uniform finite time steps, respectively, at a specific time step, the state of the temperature, within each slice can be expressed by the state at the same time. In addition, the variation of the state between each pair of adjoining slices is assumed to be linear, as shown in Figure 3.7. Mainly three methods can be used to derive the finite difference equations for describing the time evolution of the nodal temperatures.

1. Explicit (Forward difference) FDM
2. Implicit (Backward difference) FDM
3. Crank-Nicolson (Combined) FDM

Factors such as stability and convergence are critical in determining the suitable FDM method. The simple explicit FDM method is very simple computationally for solving one-dimensional heat equation. However, during stability analysis it was observed that it has some restrictions with respect to maximum size of the time step. The solution became unstable with increasing the time step. If calculations are to be carried out over a long period of time, the amount of steps — hence the amount of calculations — needs can become prohibitively high. In order to minimize this complexity, a finite difference scheme has been established that is not restrictive of the scale of the time step Δt . That method is implicit FDM.

As compared to the explicit FDM, each time step required further calculation using the implicit FDM. The implicit finite difference approximation is stable for all values of the time step Δt . However, Δt must be kept significantly fine to obtain results sufficiently close to the exact solution of the conduction heat equation. This has increased number of time steps and computational cost. Hence, Crank and Nicolson [142] proposed an alternative solution of combining the both implicit and explicit methods to form a single method. In Crank-Nicolson FDM (CNFDM), there was speed of convergence of explicit method and stability of implicit method. The finite difference Crank-Nicolson method is therefore implemented to approximate solutions at finite time and space, due to its proven ability to solve PDEs and its unconditional stability.

In order to formulate heat transfer model using CNFDM, the multilayer wall of Figure 3.7 is discretized into equal segments of spatial width Δx along its thickness. Therefore, a set of algebraic equations are developed by discretizing the governing Equations (3.6) and (3.7) corresponding boundary conditions, using unconditionally stable CNFDM. The general form of CNFDM is

3.3. Building Envelope Modeling

detailed as follows:

$$T_i^{(t+\Delta t)} - T_i^{(t)} = \Psi[(T_{i-1}^{(t+\Delta t)} - 2T_i^{(t+\Delta t)} + T_{i+1}^{(t+\Delta t)}) + (T_{i-1}^{(t)} - 2T_i^{(t)} + T_{i+1}^{(t)})] \quad (3.8)$$

$$\Psi = k\Delta t/2\rho C\Delta x^2$$

Equation (3.8) applied for interior nodes is expressed as:

$$(2 + 2\Psi_l)T_i^{(t+\Delta t)} = (2 - 2\Psi_l)T_i^{(t)} + \Psi_l(T_{i-1}^{(t)} + T_{i+1}^{(t)} + T_{i-1}^{(t+\Delta t)} + T_{i+1}^{(t+\Delta t)}) \quad (3.9)$$

where $\Psi_l = k_l\Delta t/2\rho_l C_l\Delta x^2$ for sublayers $l = 1, 2, 3, 4 \dots n$, discretized equal segments of the wall. Nodes at the boundary of two intermediate layers (node between $i = 2$ and $i = 3$ in Figure 3.7), the thermo-physical properties of these two material layers have an impact on the transient heat transfer. The corresponding equations from CNFDM approach are as follows:

$$(2 + \Psi_{l1} + 2\Psi_{l2})T_i^{(t+\Delta t)} = (2 - \Psi_{l1} - 2\Psi_{l2})T_i^{(t)} + \Psi_{l1}T_{i-1}^{(t)} + \Psi_{l2}T_{i+1}^{(t)} \quad (3.10)$$

$$+ \Psi_{l1}T_{i-1}^{(t+\Delta t)} + \Psi_{l2}T_{i+1}^{(t+\Delta t)}$$

$$\Psi_{l1} = \frac{\lambda_{l1}\Delta t}{(\rho_{l1}C_{l1} + \rho_{l2}C_{l2})\Delta x^2} \quad (3.11)$$

$$\Psi_{l2} = \frac{\lambda_{l2}\Delta t}{(\rho_{l1}C_{l1} + \rho_{l2}C_{l2})\Delta x^2} \quad (3.12)$$

The convection boundary conditions at node $x = 0$ and $x = L$ are formulated as listed below:

$$(2 + 2\Psi + 2H)T_1^{(t+\Delta t)} = (2 - 2\Psi - 2H)T_1^{(t)} + 2\Psi(T_2^{(t)} + T_2^{(t+\Delta t)}) + H(T_e^{(t)} + T_e^{(t+\Delta t)}) \quad (3.13)$$

$$(2 + 2\Psi + 2H)T_N^{(t+\Delta t)} = (2 - 2\Psi - 2H)T_N^{(t)} + 2\Psi(T_{N-1}^{(t)} + T_{N-1}^{(t+\Delta t)}) + H(T_e^{(t)} + T_e^{(t+\Delta t)}) \quad (3.14)$$

$$H = h_c\Delta t/\rho C\Delta x \quad (3.15)$$

T_e = ambient temperature for boundary at $x = 0$, and zone air temperature for boundary at $x = L$.

The set of CNFDM equations of energy conservation can be expressed in tridiagonal matrix.

$$AT_{1..n}^{(t+\Delta t)} = BT_{1..n}^{(t)} \quad (3.16)$$

where A is the matrix with future values and B is the matrix with present values with respect to time coefficients $(t + \Delta t)$ and (t) , respectively. T is the temperature vector at (t) and $(t + \Delta t)$. By applying Thomas algorithm with the given initial and boundary conditions, the future temperature values can be determined [143].

3.4 Optimization Techniques

The application and brief introduction was given in the Introduction chapter Section 2.4. In this section, a constrained optimization technique capable of identifying optimal parameters of the thermal network model is described.

Parameters R and C identification through optimization techniques will enhance the performance of the building 3R2C thermal network model-based controllers. The heat conduction through composite wall with multilayer materials, which have different thermo-physical properties is expected to behave as the reference model (building envelope real behavior). Hence, it is important to obtain proper distributed values for each resistor and capacitor of the 3R2C model matching the building envelope real dynamics.

The optimization theory formed from a series of analytical and numerical approaches aimed at identifying the right candidate within a group of alternatives without the need to analyze any of these choices. In certain cases, optimization problems are presented as the optimal search for functions, i.e. the search for the values of the variables that make the function find its global minimum or maximum value. The function to be optimized is called the objective or cost function, and the variables are the decision variables. Some of the optimization algorithms are:

- Genetic algorithms
- Particle Swarm optimization algorithms
- Artificial immune systems
- Evolutionary algorithms, etc.

In this thesis, a Particle Swarm optimization (PSO) algorithm is applied for parameter values identification of a building thermal network model. PSO is

a population-based stochastic algorithm [144–146], and is suitable for discontinuous non-linear systems with convergence behavior and robustness as key features. The particles of PSO update themselves with the velocity, they even have a memory of the preceding location. In addition, PSO particles have individual best position and move towards global best position by sharing information with other particles. This characteristics makes PSO to converge faster compared to other algorithms for example GA (crossover) [147]. Therefore, PSO can be found well suited to parametric optimization processes when compared to other evolutionary algorithms.

3.4.1 Particle Swarm Optimization

The particle swarm optimization (PSO) algorithm is a population-based search algorithm based on the simulation of the social behavior of birds within a flock. The original purpose of the particle swarm idea was to graphically model the graceful and chaotic choreography of the bird flock, with the goal of finding patterns that rule the ability of birds to fly synchronously, and to spontaneously change direction by regrouping in an optimum configuration. From this initial goal, the idea has developed into a simple and effective optimization algorithm.

In PSO, individuals, referred to as particles, are “flown” through hyper-dimensional search space. Changes to the position of particles within the search space are based on the socio-psychological propensity of individuals to imitate the performance of others. Therefore, modifications to a particle inside the swarm are affected by the experience or awareness of its neighbors. Thus, a particle’s search activity is influenced by that of other particles inside the swarm (PSO is therefore a kind of cooperative symbiotic algorithm). The effect of modeling this social behavior is that the search process is such that particles return to previously successful regions in the search space stochastically.

A PSO algorithm maintains a particle swarm, where a possible solution is represented by each particle. A swarm is similar to a population in contrast to evolutionary computing concepts, while a particle is similar to an entity. Simply stated, the particles are ‘flown’ into a multidimensional search space where, according to their own knowledge and that of their neighbors, the location of each particle is adapted. Let $x_i(t)$ denote the position of particle i in the search space at time step t . The position of the particle is changed by

adding a velocity, $v_i(t)$, to the current position, i.e.

$$x_{i,j}^{t+1} = x_{i,j}^t + v_{i,j}^{t+1} \quad (3.17)$$

It is the velocity vector that drives the optimization process, and reflects both the experiential knowledge of the particle and socially exchanged information from the particle's neighborhood. The experiential knowledge of a particle is generally referred to as the cognitive component, which is proportional to the distance of the particle from its own best position (referred to as the particle's personal best position) found since the first time step. The socially exchanged information is referred to as the social component of the velocity equation. The PSO can search for local best $lbest$ and global best $gbest$.

For the global best PSO, or gbest PSO, the neighborhood for each particle is the entire swarm. The social network employed by the gbest PSO reflects the star topology. For the star neighborhood topology, the social component of the particle velocity update reflects information obtained from all the particles in the swarm. In this case, the social information is the best position found by the swarm, referred to as $Gbest(t)$.

$$v_{i,j}^{t+1} = wv_{i,j}^t + c_1r_1(lbest_{i,j}^t - x_{i,j}^t) + c_2r_2(Gbest_j^t - x_{i,j}^t) \quad (3.18)$$

where $v_{i,j}^t$ is the velocity of particle i in dimension $j = 1, \dots, n_x$ at time step t , $x_{i,j}^t$ is the position of particle i in dimension j at time step t , c_1 and c_2 are positive acceleration constants used to scale the contribution of the cognitive and social components respectively, and r_1, r_2 are random values in the range $[0, 1]$, sampled from a uniform distribution. These random values introduce a stochastic element to the algorithm. The velocity calculation as given in equation 3.18 consists of three terms:

- Previous velocity, $v_i(t)$, which acts as a memory of the previous direction, i.e. acceleration in the immediate past. This memory concept can be seen as a momentum that stops the particle from dramatically shifting direction and from bias against the current direction. The component is often referred to as the inertia component.
- The cognitive component, $c_1r_1(lbest_{i,j}^t - x_{i,j}^t)$, which quantifies the performance of particle i relative to past performances. The result of this term is that the particles are attracted back to their own better positions,

3.4. Optimization Techniques

resembling the propensity of individuals to return to circumstances or areas that have most pleased them in the past.

- The social component, $c_2 r_2 (Gbest_j^t - x_{i,j}^t)$, which quantifies the performance of particle i relative to a group of particles, or neighbors. Conceptually, the social component resembles a group rule or ideal that individuals seek to accomplish. The consequence of the social aspect is that each particle is therefore drawn to the best location in the vicinity of the particle.

The PSO to find $gbest$ is summarized in below algorithm 1:

Algorithm 1: PSO $gbest$ algorithm.

Create and initialize an n_x -dimensional swarm;

repeat

for each particle $i = 1, \dots, n_s$ **do**

 //set the personal best position **if** $f(x_i) < f(lbest)$ **then**

 | $lbest = x_i$;

end

 //set the global best position **if** $f(lbest) < f(gbest)$ **then**

 | $gbest = lbest$;

end

end

for each particle $i = 1, \dots, n_s$ **do**

 | update the velocity; update the position;

end

until stopping condition is true;

The Figure 3.8, shows the position updates with reference to the task of minimizing a two-dimensional function with variables x_1 and x_2 using $gbest$ PSO. The global minimum is at the origin, indicated by the X symbol. In the Figure 3.8(a), the initial position of eight particles are shown along with the global best particle's position. In the Figure 3.8(b), the particles have moved in the direction of global minimum and attaining new global best position.

PSO can handle constraints optimally by rejecting infeasible solutions. A constrained PSO will not allow infeasible particles to be selected as personal best or neighborhood global best solutions. In reality, infeasible particles can never affect other particles in the swarm. Infeasible particles are, however, pushed back to workable space due to the fact that the best personal and neighborhood locations are in feasible space. This method will only be useful if there is a combination of amount of infeasible particles to viable particles are thin. If this ratio is too high, the swarm will not have enough

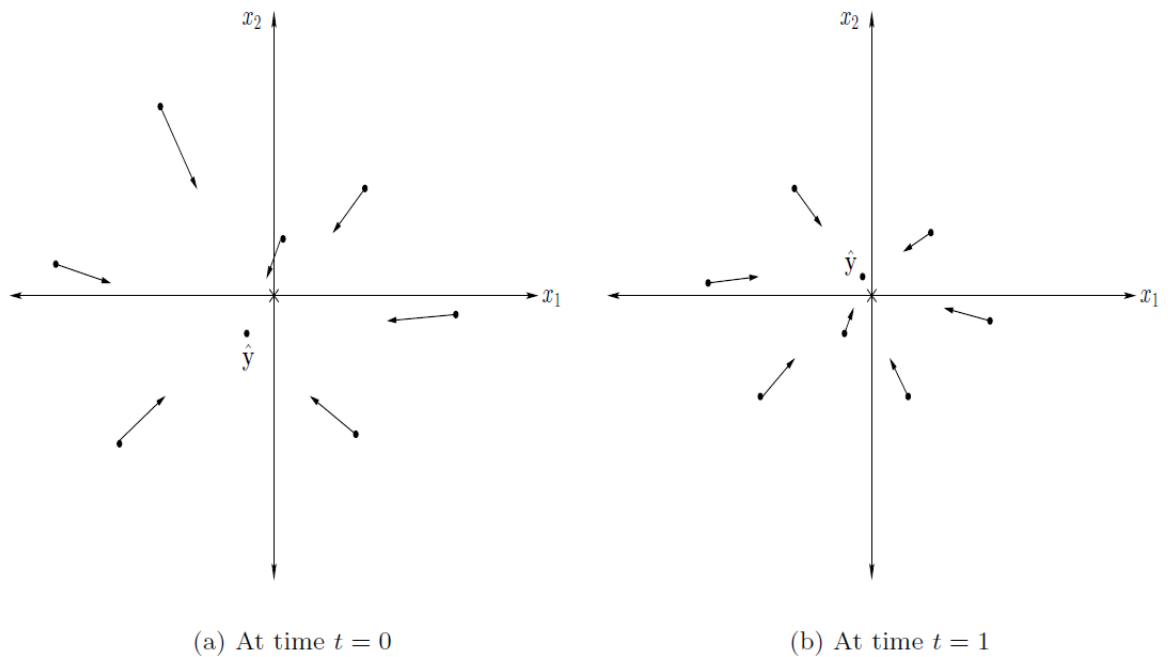


FIGURE 3.8: Multi-particle gbest PSO Illustration [148].

diversity to efficiently fill (feasible) space. An alternative to the above solution is by replacing infeasible particles with their feasible personal best positions [149]. By doing so, the infeasible particles are brought back feasible space efficiently.

3.5 Building Envelope Model Development and Parameters Identification

This section proposes a method for parametric identification of thermal network model (3R2C) by using constrained particle swarm optimization (PSO) algorithm [150].

3.5.1 Thermal Network Model Comparison

Based on the thermal balance equation and different configurations from literature study, we modeled our envelope as a first order (2R1C), a second order (3R2C), and a third order (4R3C) lumped parameter thermal network model. Furthermore, the results from these models are compared with each other. For this analysis, only heat load from heating system is given. The multi-layer wall data and corresponding input and output temperatures data are obtained from Hensen's model [151].

3.5. Building Envelope Model Development and Parameters Identification

TABLE 3.2: Thermo-physical properties of the wall.

Material	Thickness (mm)	Density (kgm^{-3})	Conductivity ($Wm^{-1}K^{-1}$)	Specific heat capacity ($Jkg^{-1}K^{-1}$)
Plasterboard	13	720	0.16	840
Concrete block	100	2096	1.63	920
Insulation	50	91	0.04	840
Air gap	20	1	0.11	1005
Brick	100	1920	0.87	800

First Order Model - 2R1C

The first order lumped parameter model consist of two resistors and one capacitor (1R1C), the model is shown in Figure 3.9. The value of C_{th} is the total thermal capacitance of the wall and R_1 are identified using the above given parametric identification method.

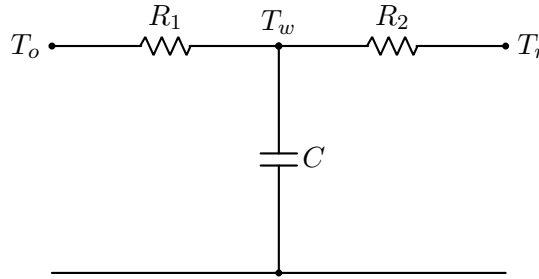


FIGURE 3.9: First order lumped parameter model - 2R1C

Second Order Model - 3R2C

The second order lumped parameter model consist of three resistors and two capacitors (3R2C), the model is shown in Figure 3.10. The parameters R_1 , R_2 , and R_3 are resistors of wall thermal resistivity, and C_1 and C_2 are capacitors representing thermal capacitances of the composite wall. Same parametric identification method used to obtain the parameters values. Similarly, a third-order model is developed for comparison purposes.

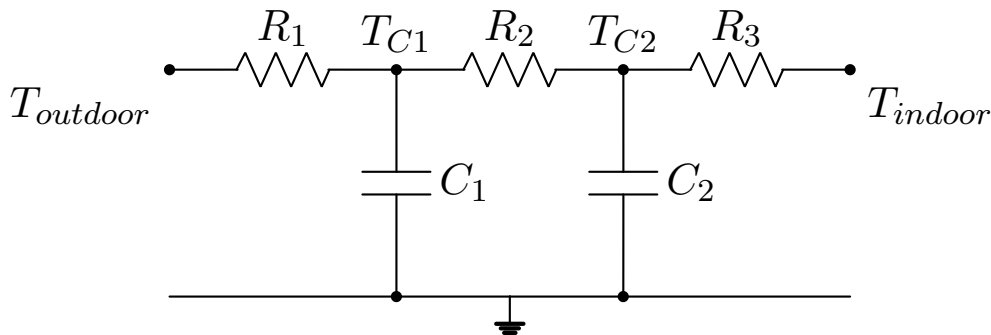


FIGURE 3.10: Simplified thermal network model - 3R2C.

In order to select the best suitable lumped parameter model, we firstly simulated above three different configuration models for a five layer composite wall. The simplification of these thermal networks is done through state-space equations. The values of RC values are unknown parameters and obtained from the parametric identification method detailed in the following section. These different models output is compared with each other and with the reference model [151].

RC Models Comparison Analysis

The above given models are simulated by using same input and initial conditions. The simulation is performed for 7 days and compared with the reference model output data.

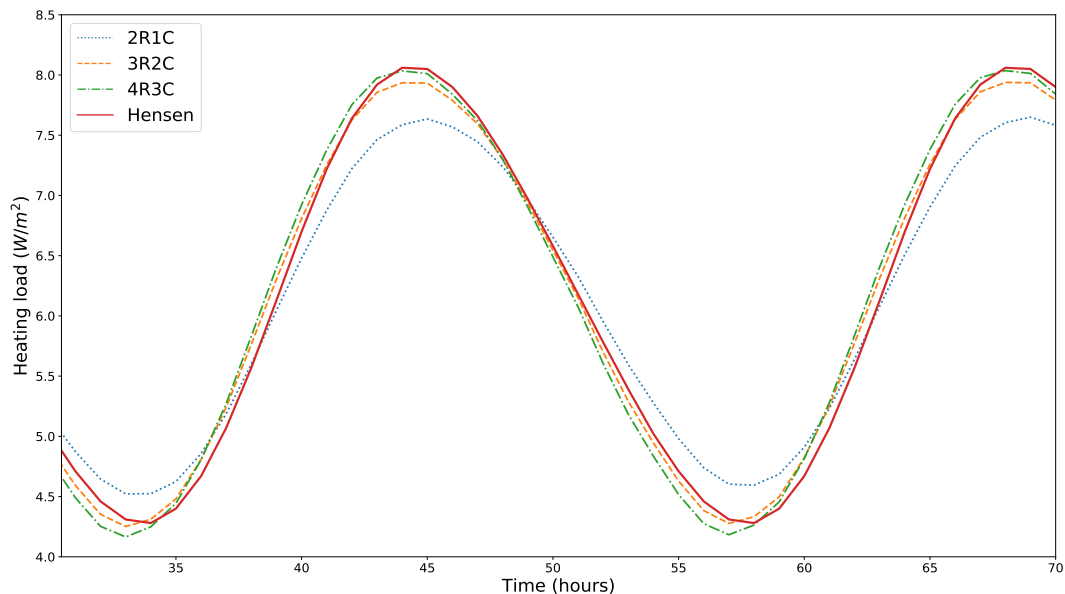


FIGURE 3.11: Comparison of simulated heat load from RC models and reference model.

Figure 3.11 presents the simulated output from three different RC models are compared with reference model. All three models have good fitting and follows the dynamics of the reference model. The first order model output has higher deviation compared to the other two models, the low R_1 value obtained from the parameter optimization method has higher influence on the heat load prediction. Furthermore, it is noticed that prediction accuracy is increased as the model order is increased. The symmetric mean absolute percentage error (sMAPE) between the RC models and reference model is given in Table 3.3.

3.5. Building Envelope Model Development and Parameters Identification

All three models have similar prediction behavior since it is a simple model applied for just one wall. The 2R1C model has high computational efficiency and good fitting with the reference model. This model can be used for simple building because of its simplicity. However, considering the sMAPE error criteria, 3R2C and 4R3C model are more accurate than the 2R1C model. Among the 3R2C and 4R3C models, the 4R3C model has the best accuracy. Furthermore, the difference between these two models is very low ($\approx 0.1\%$). However, the computational cost of 3R2C is greater than 6% compared to 4R3C model. Therefore, simulating multiple zone building models with 4R3C model will constitute for high computational cost and increases the design complexity.

From this comparison, it can be concluded that the 3R2C model has the acceptable range accuracy and high computational efficiency. However, if accuracy is the main concern 4R3C model can be used for such purposes.

It is important to notice that 4R3C model has very low sMAPE, however difference between 3R2C and 4R3C model is also very low and 3R2C model accuracy is in acceptable range. All three models have high computational cost for one wall simulation.

TABLE 3.3: Symmetric mean absolute percentage error (sMAPE) between reference and RC models.

RC model	sMAPE	Run time
First-order model	0.03716	4.86 (<i>ms</i>)
Second-order model	0.02008	4.97 (<i>ms</i>)
Third-order model	0.01891	5.2 (<i>ms</i>)

3.5.2 Simulation Model

A simplified model (3R2C) is developed to represent building envelope for predicting its thermal response. As discussed in the previous sections the model parameters can be determined using two ways: analytical and numerical. In our study, we selected numerical stochastic optimization algorithm (PSO) to identify optimal parameter values. The constrained PSO can be adapted to find parameters by finding the global minimum error value between the two models: 3R2C thermal network model and a reference model. A reference model is developed using well-established Crank-Nicolson finite difference method (detailed in section 3.3.2) to represent the energy flow through the building envelope [138].

In literature, parameters are identified by comparing simplified model with the reference model response for a step excitation of input variables [125,130, 132, 133]. However, in reality the input variables vary dynamically, for example the output temperature varies periodically. Therefore, in this study, a step and a periodic input excitation given and responses are then compared between reference model and second-order thermal network models. Subsequently, PSO algorithm is applied to minimize the root mean square error (RMSE) between the reference and thermal network models.

The thermal network model approach is used to simplify the complex modeling of building dynamics, and to obtain reduced order simplified models of the buildings based on state-space equations. The 3R2C network model consists of three R and two C representing resistances and capacitances of composite homogeneous wall, respectively. The application of 3R2C model can be seen regularly in the literature due to its performance accuracy and low computational cost. In 3R2C model (see Figure 3.10), R_1 , R_2 , and R_3 are resistors of wall thermal resistivity, and C_1 and C_2 are capacitors representing thermal capacitances of the composite homogeneous wall. The degree of differential equations is equal to the number of capacitors in the network. Consequently, second-order differential Equations (3.19) and (3.20) are obtained from 3R2C model.

$$\frac{dT_{c1}}{dt} = \frac{T_{out}}{R_1 C_1} - \frac{T_{c1}}{R_1 C_1} - \frac{T_{c1}}{R_2 C_1} + \frac{T_{c2}}{R_2 C_1} \quad (3.19)$$

$$\frac{dT_{c2}}{dt} = \frac{T_{c1}}{R_2 C_2} - \frac{T_{c2}}{R_2 C_2} - \frac{T_{c2}}{R_3 C_2} + \frac{T_{in}}{R_3 C_2} + \frac{Q_{in}}{C_2} \quad (3.20)$$

The overall thermal capacitance per unit, C_{total} is calculated by adding thermal capacitance (3.24) of each layer of the wall, similarly overall thermal resistance, R_{total} is calculated by summing thermal resistance (3.22) of each layer of the wall.

3.5. Building Envelope Model Development and Parameters Identification

$$R_{total} = \sum_{j=1}^M R_{layer,m} \quad (3.21)$$

$$R_{layer} = \frac{l}{kA} \quad (3.22)$$

$$C_{total} = \sum_{j=1}^M C_{layer,m} \quad (3.23)$$

$$C_{layer} = \rho.C_p.l.A \quad (3.24)$$

where

l —thickness of the material layer (m),

m —number of layers of the wall,

k —thermal conductivity of the material (W/m·K),

ρ —density (kg/m³),

C_p —heat capacity of the material (J/kg·K), and

A —surface area of the wall (m²)

To obtain a simplified 3R2C network model, the overall thermal resistance to be distributed appropriately between R_1 , R_2 , and R_3 and the overall thermal capacitance between two capacitors C_1 and C_2 .

$$R_1 = x_1 R_{total} \quad (3.25)$$

$$R_2 = x_2 R_{total} \quad (3.26)$$

$$R_3 = x_3 R_{total} \quad (3.27)$$

$$x_3 = 1 - x_1 - x_2 \quad (3.28)$$

$$C_1 = x_4 C_{total} \quad (3.29)$$

$$C_2 = x_5 C_{total} \quad (3.30)$$

$$x_5 = 1 - x_4 \quad (3.31)$$

The coefficients x_1 , x_2 , x_3 , x_5 and x_4 values are important for the model performance accuracy, these values are optimally obtained from the optimization technique given in the following section. The second-order differential

equations can be expressed using state-space formulation and simulated using Python programming language:

$$\begin{aligned}\dot{T} &= AT + BU \\ y &= CT + DU\end{aligned}\tag{3.32}$$

where

T is the temperature vector,

U is the input vector,

y is the output vector,

A is the state matrix coefficients related to state vector,

B is the input matrix values related to input vector,

C is the output matrix values related to state vector, and

D is the direct transition matrix.

A constrained PSO algorithm (detailed in section 3.4.1) was developed to identify model parameter values by minimizing the RMSE between reference and 3R2C thermal network models. The two inputs of the system model, $T_{ambient}$ and T_{indoor} , are excited with sinusoidal periodic and unit step functions. Internal and external surface temperatures are predicted from reference CNFDM model and are compared with 3R2C model. The RMSE is minimized by using objective function (3.33) of the constrained PSO algorithm.

$$min f(x_1, x_2, x_4) = \sqrt{\frac{\sum_{k=1}^n (T_{fdm_k} - T_{sim_k})^2}{n}}\tag{3.33}$$

subject to constraints:

$$\begin{aligned}x_1 + x_2 + x_3 &= 1; \quad x_1, x_2, x_3 > 0 \\ x_4 + x_5 &= 1; \quad x_4, x_5 > 0; \\ 1 - (x_1 + x_2) &> 0; \quad 1 - x_4 > 0\end{aligned}\tag{3.34}$$

3.5. Building Envelope Model Development and Parameters Identification

R and C values of 3R2C model are obtained from below expressions:

$$\begin{aligned} R_1 &= x_1 R_{total}, \quad R_2 = x_2 R_{total}, \quad R_3 = x_3 R_{total}, \\ C_1 &= x_4 C_{total}, \quad C_2 = x_5 C_{total} \\ R_{total} &= \sum_{j=1}^M R_{layer,m}, \quad C_{total} = \sum_{j=1}^M C_{layer,m} \end{aligned} \quad (3.35)$$

where R_{total} is the total resistance and C_{total} is the total capacitance values of composite wall, $f(x_1, x_2, x_4) =$ fitness function to be minimized, $Tfdm_k$ and $Tsim_k =$ step and periodic input response temperature at interval of (k).

We have evaluated our model with different accuracy measure method (error calculation) methods.

- Root mean square error (RMSE)

$$RMSE = \sqrt{\sum_{i=1}^N \frac{(y_{measured,i} - y_{predicted,i})^2}{N}} \quad (3.36)$$

- Mean absolute error (MAE)

$$MAE = \frac{1}{N} \sum_{i=1}^N |(y_{predicted,i} - y_{measured,i})| \quad (3.37)$$

- Absolute percentage error (APE)

$$APE = \left| \frac{(y_{measured,i} - y_{predicted,i})}{y_{measured,i}} \right| \times 100\% \quad (3.38)$$

- Mean absolute percentage error (MAPE)

$$MAPE = \frac{1}{N} \sum_{i=1}^N \frac{|y_{predicted,i} - y_{measured,i}|}{y_{measured,i}} \times 100\% \quad (3.39)$$

- Symmetric mean absolute percentage error (MAPE)

$$sMAPE = \frac{1}{N} \sum_{i=1}^N \frac{|y_{predicted,i} - y_{measured,i}|}{(y_{predicted,i} + y_{measured,i})/2} \times 100\% \quad (3.40)$$

where N is the number of values, $y_{measured,i}$ is the i^{th} measured temperature value or the reference model temperature value and $y_{predicted,i}$ is the i^{th} predicted one.

3.5.3 Simulation Results of Parametric Identification

In this study, three types of building envelope datasets are used to demonstrate the suitability of proposed parametric identification approach. These datasets are light, medium, and heavy weight/thermal mass composite walls. Low thermal mass construction walls typically consist of either steel or timber layers with insulating materials. Typically, low mass wall systems are at least partly pre-assembled off-site this indicates that they are pre-fabricated in an industry/factory. With this option, we can construct building quicker than the heavy mass walls, as the construction work is less weather dependent. Low mass walls have lower amount of heat storage ability. Whereas, heavy mass walls generally built of precast concrete or concrete blocks. Properly insulated heavy mass walls can store significant amount of heat from sun, thus minimizing cooling and heating load while enhancing indoor comfort. Many of the conventional buildings are built using heavy mass walls. New buildings are recently using low mass walls. Therefore, the parameters identification approach is applied to different thermal mass walls.

The multilayer wall layer's thermo-physical properties and wall composition details are provided in Table 3.7. These thermo-physical properties and composition of layers data are obtained from the ASHRAE Handbook of Fundamentals [23]. In order to identify the parameter values of thermal network model and to validate the its dynamics, a reference model is developed. In addition, two other thermal network models (model (I) and (II)) are developed for comparison purposes. The resistors and capacitors values of model (I) are assigned in such a way that the total resistance and capacitance values are allocated equally for $R_1, R_2, R_3, C_1,$ and C_2 parameters. Whereas, the values of resistors and capacitors of model (II) are assigned same as the building envelope layer's thermal resistance and capacitance meaning that the layer (outside) value is assigned to resistor R_1 . Capacitors C_1 and C_2 values are allocated in the same way.

Furthermore, the CNFDM-based reference model is divided into 80 equal segments to have higher accuracy with initial conditions $T(x, t) = 0$ at $t = 0, \forall x \in [0, L]$, boundary conditions $T(x, t) = u(t) \forall t > 0,$ at $x = 0$ and $x = L, T(x, t) = T_e(t), \forall t > 0$. A unit step and periodic input is given to

3.5. Building Envelope Model Development and Parameters Identification

the models (optimized 3R2C model, model (I), and model (II)) and output indoor temperature is measured.

The minimization of the objective function by PSO algorithm is shown in Figure 3.12. The minimized fitness function value is plotted against the particle generations in which each generation consists of 100 particles. Initial particles are randomly generated within the bounded values, hence few particles in first few iterations have violated the given constraints, and those are omitted in the plot.

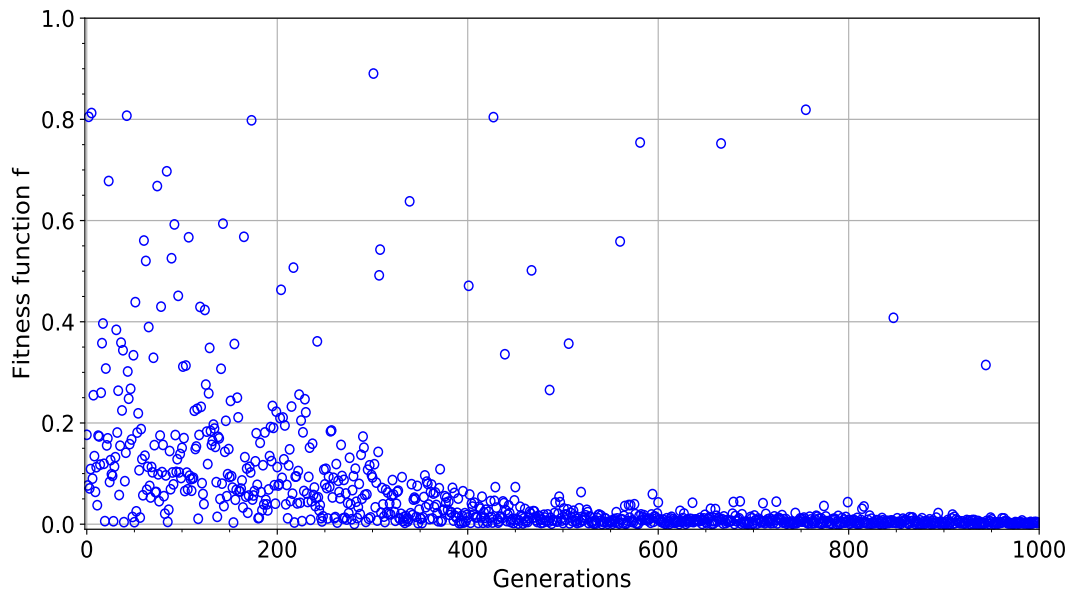


FIGURE 3.12: Minimized value of objective function for medium weight wall.

The simulation results of PSO in the Figure 3.13 shows the influence of the resistor and capacitor values on the performance accuracy. The global minimum values are obtained by using the PSO. Furthermore, small variation of the x_1 coefficient of R_1 is greatly affecting the accuracy. Whereas, the capacitor value is varied for almost 50 % but has the impact on accuracy as same as the resistor value. This observation show that optimal parameter values are essential for performance accuracy, particularly the resistor values.

The developed models were simulated in Python using the following computational facilities: Intel Core i5-7300U, CPU 2.60 GHz and 8 GB (RAM) under operating. Accordingly, the average execution time of PSO algorithm is 30.33 seconds (1000 maximum iterations). The 3R2C thermal network model was around 40% to 50% computationally faster over reference model.

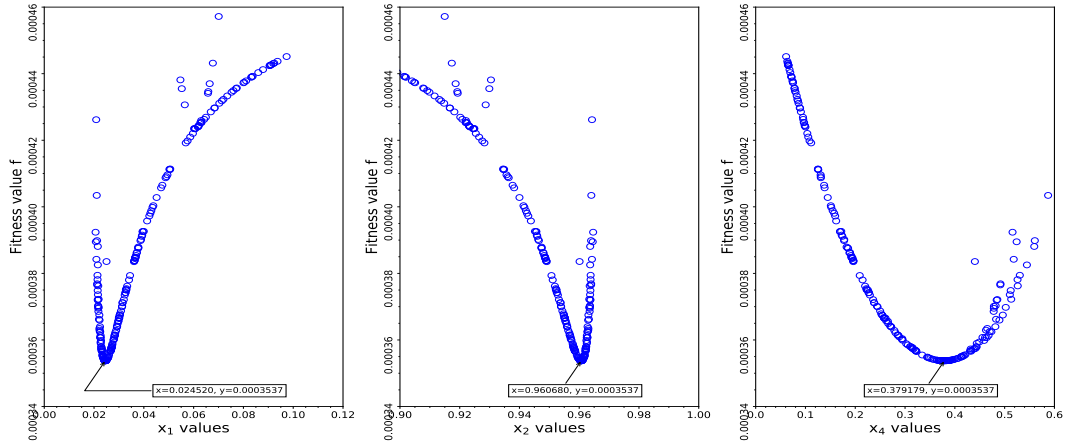


FIGURE 3.13: Optimized values of R_1 , R_2 , and C_1 coefficients (x_1 , x_2 , and x_4) with PSO algorithm.

The comparison between temperature responses of heat conduction transfer of the reference model and the thermal network model with optimal parameter values for different thermal mass walls is shown in Figures 3.14–3.18. For the better understanding and validation of the developed model, we have chosen to compare with other two models ((*I*) and (*II*)) that were used in the literature. For model (*I*), the resistor values are chosen such that the R_1 and R_2 are 33% of the total thermal resistance, and R_3 is 34% of the total thermal resistance. Capacitors C_1 and C_2 , each are given 50% of the total thermal capacitance value.

Similarly, the parameter values of the model (*II*) is chosen such that the R_1 , R_2 , and R_3 value taken as same value as the wall layer resistance value. This condition is implemented for the walls with three layers but for the four and more layers the R_1 and R_3 are equal to resistance value of first and last layer and R_2 is the cumulative value of the middle layers. Capacitors C_1 and C_2 , each are given 50% of the total thermal capacitance value.

Low Thermal Mass Wall

Low thermal mass wall indicate the walls with low weight materials such as: wooden walls, partition walls with plaster and insulation. The simulation results of this wall is shown in Figure 3.14. The model simulated for 2 days, the results show that model with optimal parameter values has great fitness to the reference model characteristics. The model (*II*) has acceptable accuracy but underestimated the dynamics. However, it reached steady-state just after the optimal model. Whereas, model (*I*) dynamics took more time to

3.5. Building Envelope Model Development and Parameters Identification

reach steady-state with big difference in response as compared to the reference model, hence produces large error in real application.

Meanwhile, the model (II) of the low thermal mass wall has shown relatively good accuracy with reference model. The parameter values of the model (II) are same as of the 3 layers in the low mass wall. The results show that for low thermal mass model (II) can be applied in real time applications due to its acceptable performance.

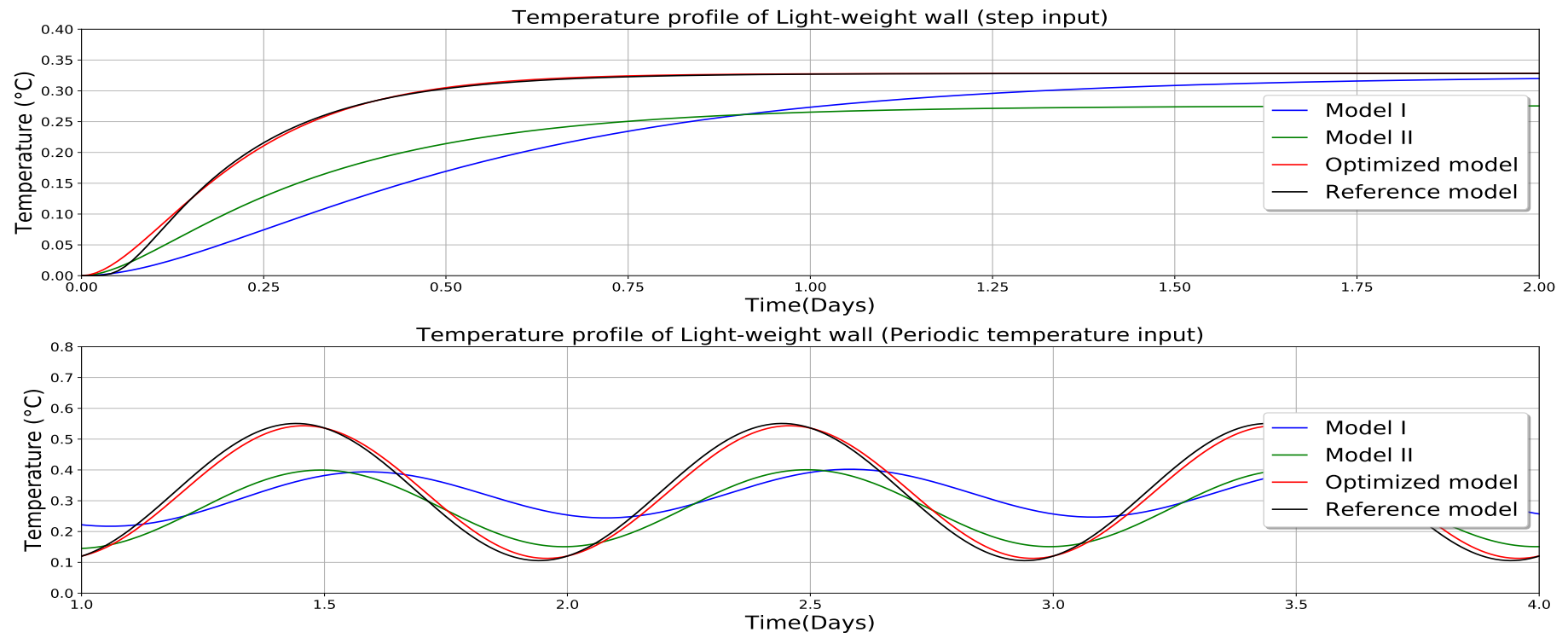
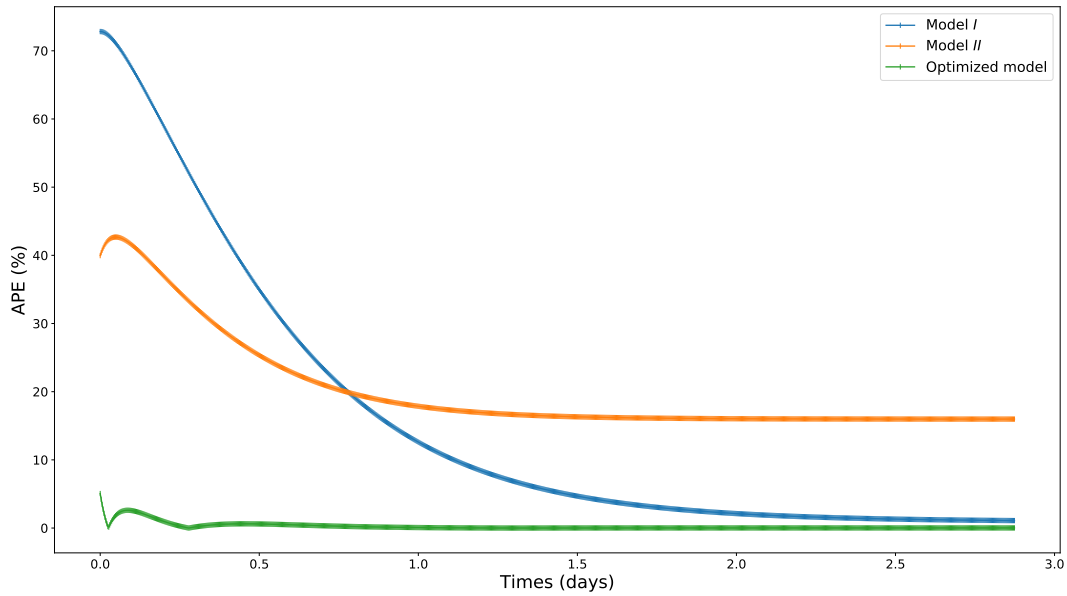
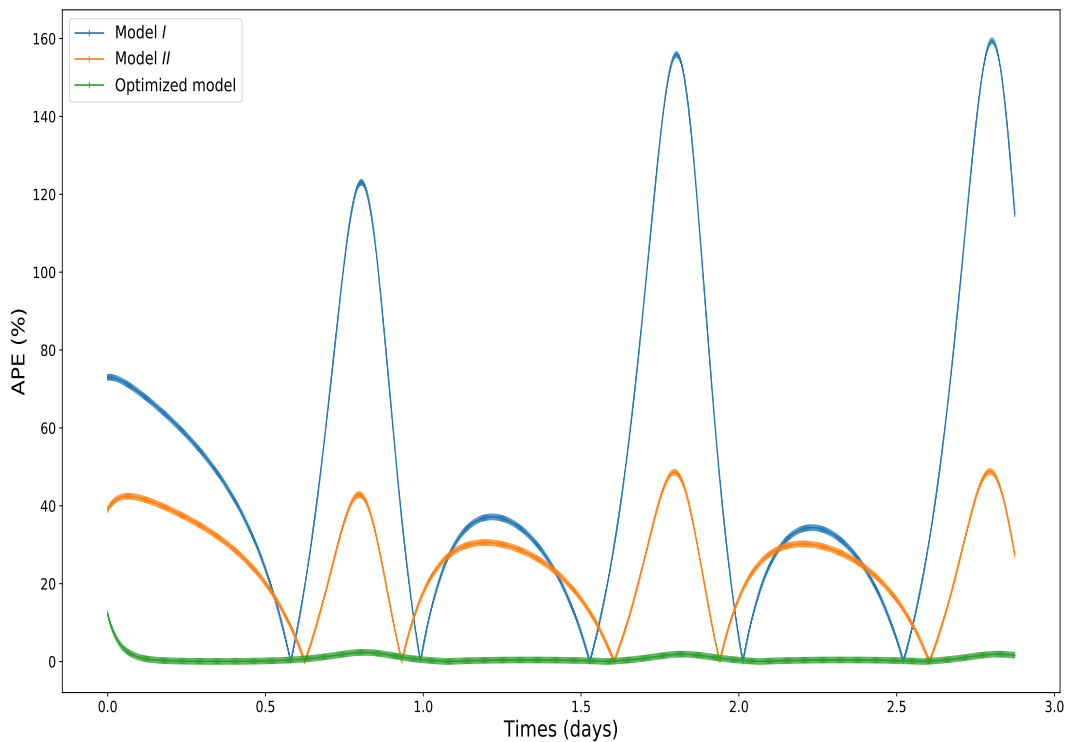


FIGURE 3.14: Temperature dynamics of reference, optimized and comparison models for light weight wall.

3.5. Building Envelope Model Development and Parameters Identification



(A) APE for step input function



(B) APE for periodic input

FIGURE 3.15: Evolution of APE of the low thermal mass wall.

The different error methods are used to verify the model performance accuracy. The evolution of APE is shown in Figure 3.15. This method is used to validate the accordance of the model with the reference model. We studied models with both step and periodic inputs. The values APE are much bigger in the beginning due to the fast dynamics of the thermal network model

as compared to the reference model. The maximum error is noticed in the model (*II*). There is $\pm 5\%$ difference between the optimized parameter values obtained for thermal network model when both step and periodic input function applied. However, we observed that there is small difference in error values between step and periodic input model performance. For low thermal mass walls, the values obtained for step or periodic input models can be used in the modeling. Both the models are well under the accepted accuracy. Their corresponding MAE, MAPE, and sMAPE are given in Table 3.4.

TABLE 3.4: Low thermal mass wall performance evaluation results.

Input methods	Models	MAE	MAPE (%)	sMAPE (%)
step input	Optimized	0.00102	6.11	3.69
	Model (<i>I</i>)	0.05907	22.54	25.09
	Model (<i>II</i>)	0.04215	17.33	23.64
periodic input	Optimized	0.00210	6.86	4.34
	Model (<i>I</i>)	0.15257	59.11	56.12
	Model (<i>II</i>)	0.15900	65.26	61.32

Medium Thermal Mass Wall

Medium thermal mass wall indicate the walls with medium weight materials such as: brick walls, partition walls with plaster, brick, and insulation. We obtained optimal parameters for the thermal network model representing the medium thermal mass wall by using the PSO optimization. The performance of the model is compared with the reference model and other two models: model (*I*) and model (*II*). Figure 3.16 illustrate the thermal dynamics of all three models in comparison with reference model. The temperature response of model with optimal parameter values has best fitting with the reference model response in both step and periodic input methods. Other two models have poor fitting with the reference model, model (*II*) underestimated the temperature, whereas model (*I*) is slow and steady-state is not reached in 4 days.

3.5. Building Envelope Model Development and Parameters Identification

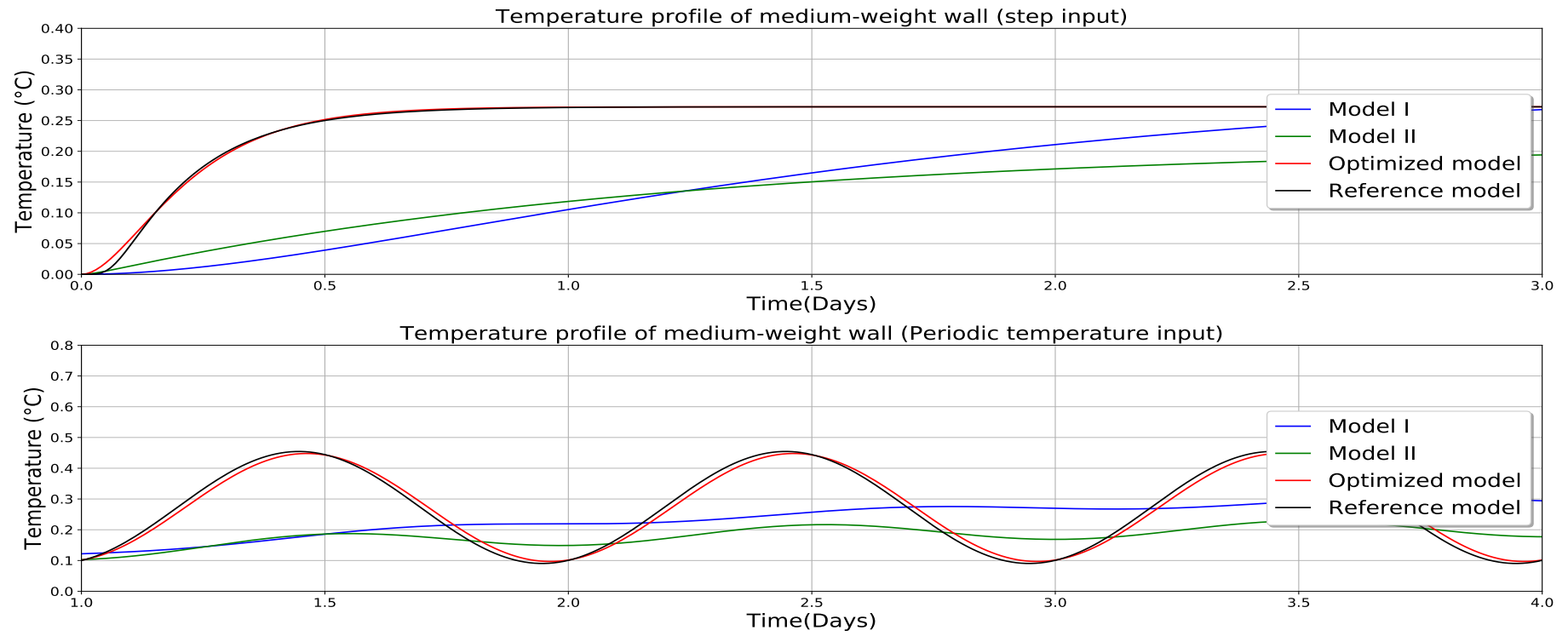
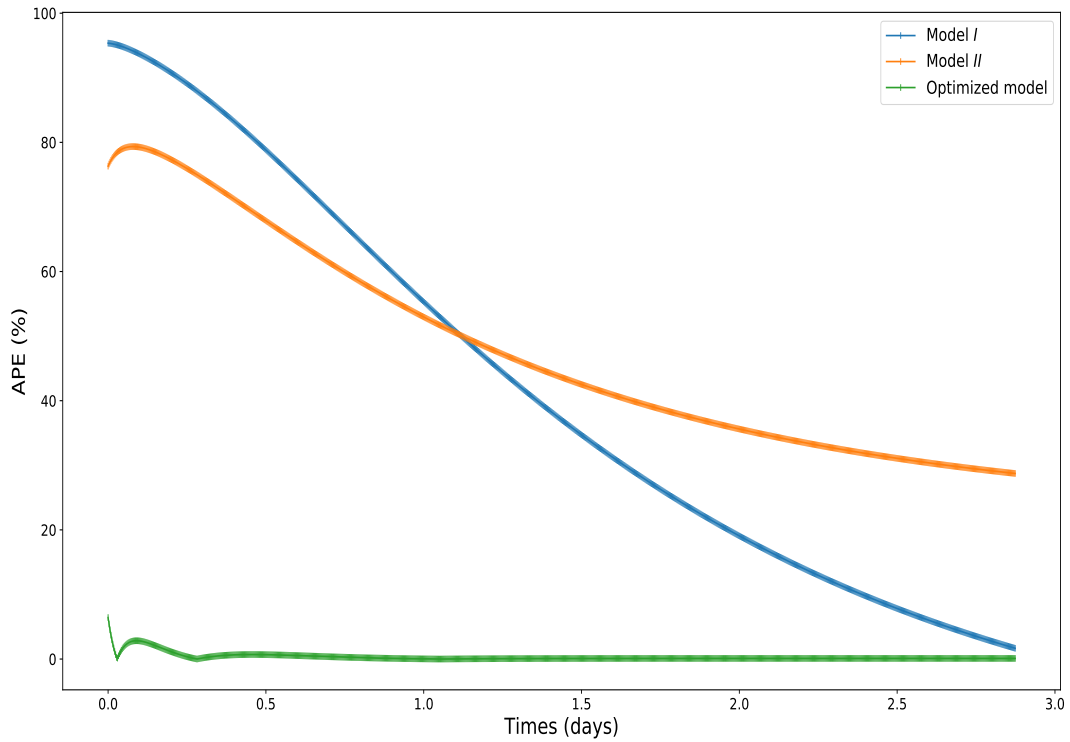
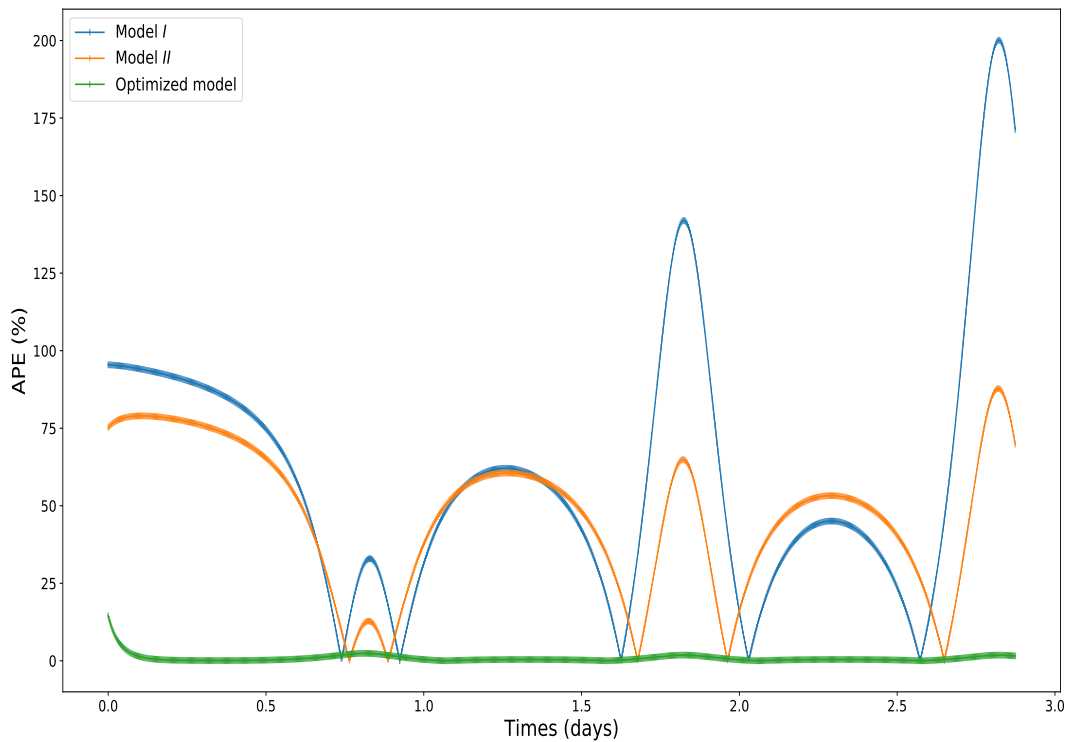


FIGURE 3.16: Temperature dynamics of reference, optimized and comparison models for medium weight wall.



(A) APE for step input function



(B) APE for periodic input

FIGURE 3.17: Evolution of APE of the medium thermal mass wall.

The APE evolution of these two models and optimized model is depicted in

3.5. Building Envelope Model Development and Parameters Identification

Figure 3.17. Similar to low thermal mass results, at the beginning there is greater difference between reference and other models. The optimized parameter model has maximum APE of 10 % at the beginning, and sMAPE of 3.94 %. The error is high in the periodic input method as compared to the step input method. Moreover, model (I) has worst performance accuracy and its error increasing at every successive period in the periodic input method. It shows the importance of the parameter values on the thermal network model performance and the need of the optimized parameters model. Other error methods are listed in Table 3.5.

TABLE 3.5: Medium thermal mass wall performance evaluation results.

Input methods	Models	MAE	MAPE (%)	sMAPE (%)
step input	Optimized	0.00101	7.48	3.94
	Model (I)	0.11753	49.32	68.23
	Model (II)	0.10083	43.84	67.71
periodic input	Optimized	0.00188	8.29	4.58
	Model (I)	0.13530	47.98	62.98
	Model (II)	0.14796	61.09	74.46

Heavy Thermal Mass Wall

We studied the application of thermal network model with optimal parameter values for heavy thermal mass wall. The dynamics of optimized model along with models (I) and (II) are compared with that of reference model (Figure 3.18). The chosen multi-layer wall has 4 layers. Similar to the low and medium thermal mass walls, the optimized model has good fitting with the reference model dynamics. Whereas, model (II) reach steady-state within 2 days but it underestimated the dynamics. The model (I) has poor performance accuracy and does not reach steady-state within 4 days. However, there is great difference between the performance accuracy of the optimized model for step and periodic input.

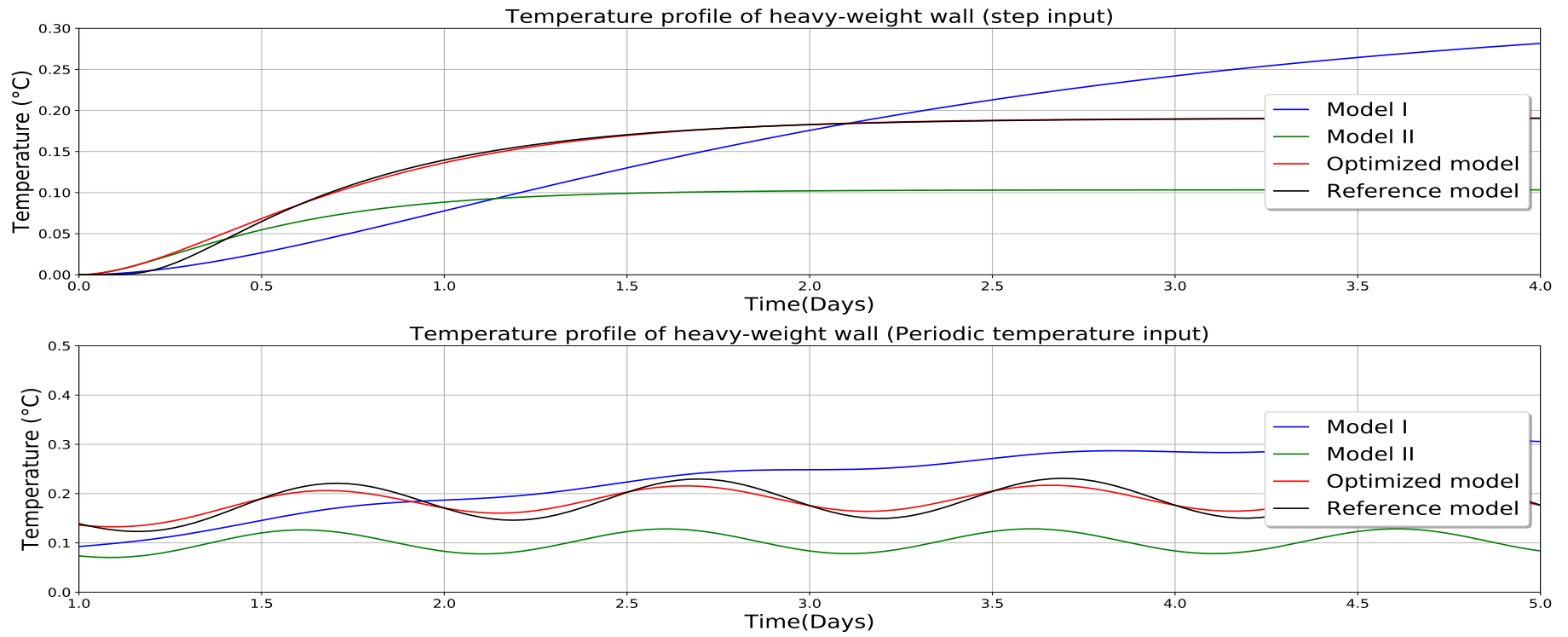
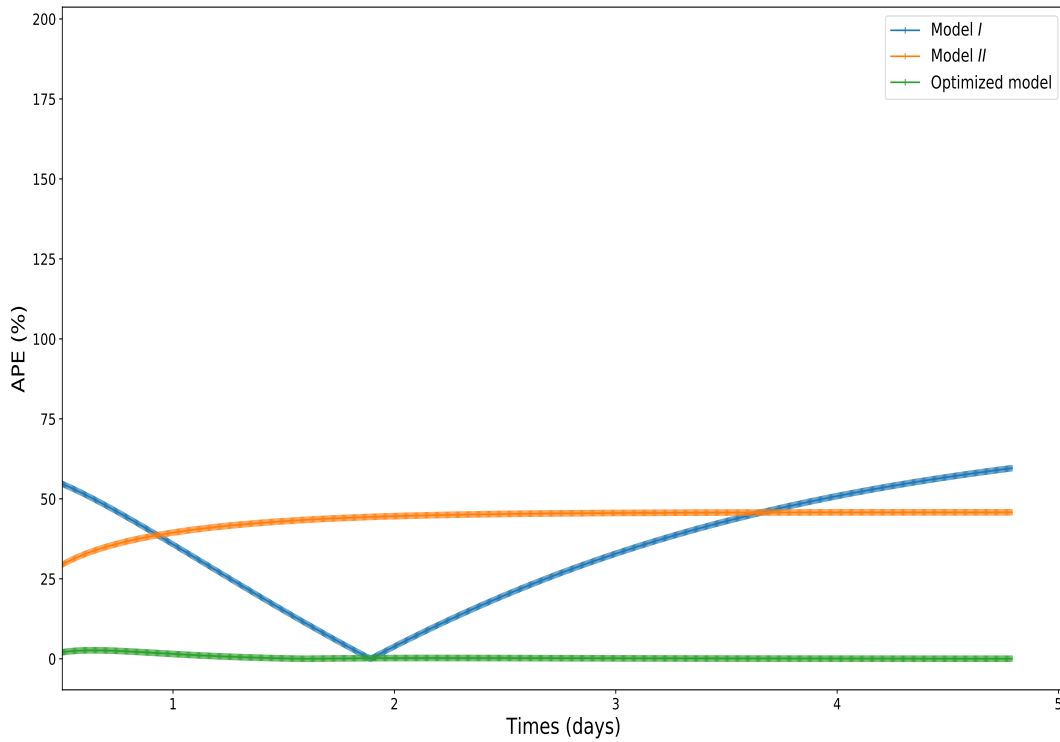
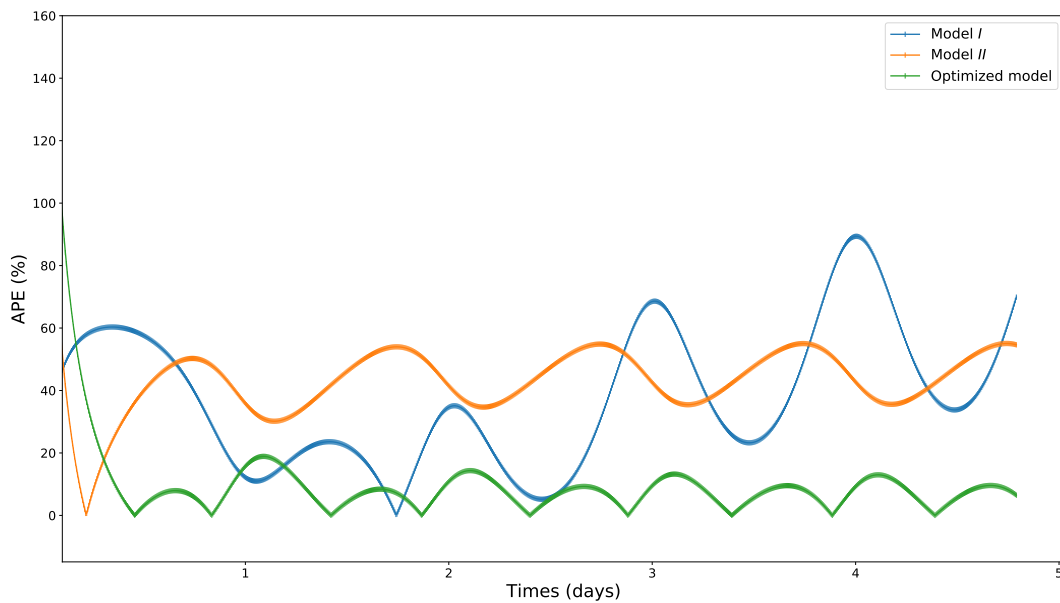


FIGURE 3.18: Temperature dynamics of reference, optimized and comparison models for heavy weight wall.

3.5. Building Envelope Model Development and Parameters Identification



(A) APE for step input function



(B) APE for periodic input

FIGURE 3.19: Evolution of APE of the heavy thermal mass wall.

The APE evolution for heavy thermal mass wall is shown in Figure 3.18. Model (*I*) has the poor performance among other models, model (*II*) underestimated the temperature response. Performance of the optimized model in step input method has best fitting, however the error is more in periodic input method. The values of the step input for heavy thermal mass provides

false representation of the performance. Therefore, validating models with the periodic input method is essential to enhance the performance accuracy. The root mean square error (RMSE) for different construction class walls are given in Table 3.8 and other error evaluations are given in Table 3.6.

Furthermore, the temperature response of model with optimized parameter values has closely followed the reference model response dynamics in both cases of step and periodic excitation. In this context, the proposed 3R2C model with optimal parameter values is strongly recommended because of its increased accuracy and computational efficiency.

The Figures 3.14–3.18 shows that the time-lag difference between the different thermal mass walls, the time response of the model is less in low mass wall compare to other two walls. The time-lag in the heavy mass wall is almost 2 days to reach the steady state.

TABLE 3.6: Heavy thermal mass wall performance evaluation results.

Input methods	Models	MAE	MAPE (%)	sMAPE (%)
step input	Optimized	0.00139	15.48	9.43
	Model (<i>I</i>)	0.06944	70.59	57.91
	Model (<i>II</i>)	0.05482	66.57	39.53
periodic input	Optimized	0.0139	28.81	17.14
	Model (<i>I</i>)	0.07389	80.73	60.32
	Model (<i>II</i>)	0.05990	63.9	39.75

3.5. Building Envelope Model Development and Parameters Identification

TABLE 3.7: Multilayer wall classification, thermal properties, and optimized R and C values.

Construction Class	Thermal Properties				Parametric Values R ($\text{m}^2 \cdot \text{K}/\text{W}$) and C ($\text{kJ}/\text{m}^2 \cdot \text{K}$)							
	Thickness	Conductivity	Density	Specific Heat	R_{total}	C_{total}	R_1	R_2	R_3	C_1	C_2	
	mm	$\text{W}/(\text{m} \cdot \text{K})$	kg/m^3	$\text{kJ}/(\text{kg} \cdot \text{K})$								
Light-weight (LW)												
Stucco	25.00	0.692	1858	0.84	3.1498	76.852	0.29477	2.7812	0.07383	20.694	56.157	
Insulation (batt)	125.00	0.043	91	0.96								
Plaster/Gypsum	20.00	0.727	1602	0.84								
Medium-weight (MW)												
Brick	101.60	0.89	1920	0.79	3.8238	183.724	0.0937	3.6735	0.0565	69.664	114.059	
Insulation board	50.80	0.03	43	1.21								
Air space	50.00	0.02514	1.205	1.00								
Gypsum	20.00	0.727	1602	0.84								
Heavy-weight (HW)												
Brick	101.60	0.89	1920	0.79	2.1917	402.102	0.1417	1.9018	0.1481	205.196	196.906	
Heavyweight concrete	203.2	0.53	1280	0.84								
Insulation board	50.80	0.03	43	1.21								
Gypsum	20.00	0.727	1602	0.84								

TABLE 3.8: Root mean square error (RMSE) between reference and simplified thermal network model.

Construction Class	Step Excitation	Periodic Excitation
Light-weight(LW)	1.239×10^{-3}	1.651×10^{-2}
Medium-weight(MW)	1.311×10^{-3}	1.365×10^{-2}
Heavy-weight(HW)	1.495×10^{-3}	2.208×10^{-2}

As expected and observed in the PSO results (Figure 3.13) the middle resistor dominated the resistance values obtained from the optimization technique, this is largely due to the presence of high thermal resistance insulation inner layers as compared low resistance outer layers. It was noticed (Figure 3.13) that the resistor values variation has greater influence on the thermal network model accuracy. In order to know the influence of each parameter on the model performance, we performed a sensitivity analysis on the 3R2C model parameters using SALib Python library [152].

The sensitivity analysis is done for both first-order and total-order indexes. The influence of each parameter on the model performance is given in Table 3.9. The resistance values have much higher influence on the performance than capacitance values. Particularly, the R_2 and R_3 resistors have greater influence on the model. The influence of resistors are almost 70 % - 80 %, whereas capacitors have 2 % - 10 % of influence on the model performance. This indicates that the using of proposed optimization technique is essential to obtain optimal value of all high influential parameters value.

TABLE 3.9: Sensitivity analysis results of the 3R2C model parameters.

Parameters	First-order index	Total-order index
R_1	0.023846	0.161070
R_2	0.185691	0.387125
R_3	0.137046	0.291419
C_1	0.000245	0.016622
C_2	0.007953	0.023883

3.5.4 Comparison with Conduction Transfer Function (CTF) Model

There are various methods to simulate the performance of a building. These methods can be put into two categories: (1) Analytical, and (2) Numerical. In this paper, numerical finite difference method has been chosen to develop

3.5. Building Envelope Model Development and Parameters Identification

reference model. Many simulation tools are developed based on the finite difference approach [135]. However, many recent well-established simulation tools (EnergyPlus, TRNSYS, etc.) use analytical conduct transfer function (CTF) method to perform calculations.

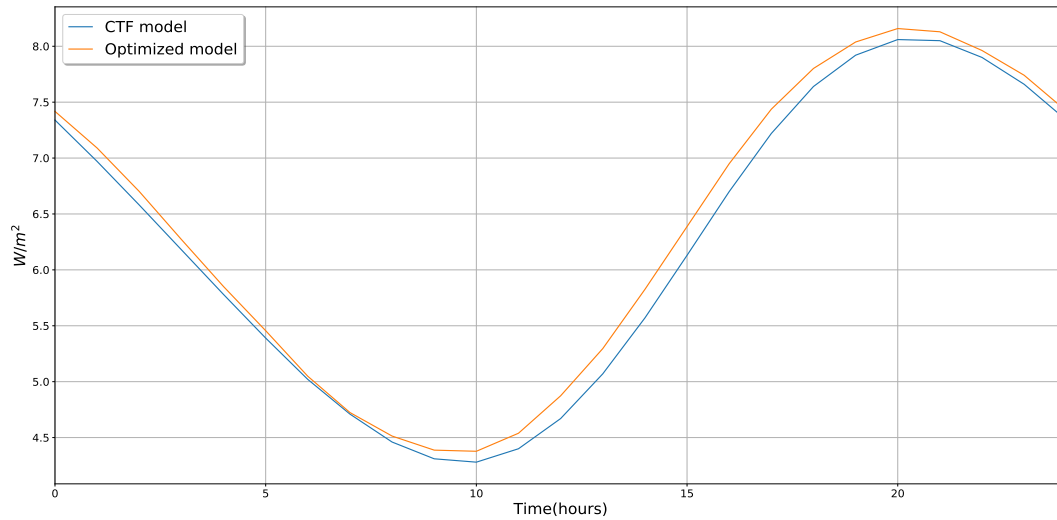


FIGURE 3.20: Comparison between CTF and simplified thermal network model.

The parameters of simplified thermal network model are identified by comparing it with the finite difference model. Furthermore, a comparison simulation has been conducted to compare thermal network performance with the analytical conduction transfer function method. The CTF method was introduced by Mitalas and Stephenson [136]. A transient conduction calculations performed on multilayer wall using CTF method is detailed in [151], all coefficients for this wall was provided along with cooling load output, and input outdoor and indoor temperatures. Applying the parameters identification technique detailed in Section 3.5.3 on example wall, the resistor and capacitor values are obtained. The simplified thermal network model is then developed for the example wall and compared with the CTF model in Figure 3.20. A very good agreement can be noticed between optimized thermal network and CTF model. The symmetric mean absolute percentage error (sMAPE) between the both models was found to be 0.02008 ($\approx 2\%$). The developed parametric identification method based on CNFDM, presents very good prediction accuracy when compared with CTF model.

3.6 Conclusion

The objective of this chapter was to establish a lumped parameter thermal network model for a composite wall consists of multi-layers including high insulation layer. An improved method for the simplified thermal network modelling for thermal response of building envelope elements was proposed and validated against the reference model. The thermal network model selected was 2nd-order model, it consists of three resistors and two capacitors (3R2C). An unconditionally stable reference Crank-Nicolson model is developed for the heat conduction equation with convective and radiative boundary conditions. The model parameter values have significant impact its performance. A stochastic constrained PSO algorithm has been adopted to determine the parameters set that provides the optimal approximation of the proposed low-order model dynamics with respect to the reference model dynamics. The constraints for the PSO algorithm were chosen such that the parameter values are not more than the total material resistance and capacitance. The temperature inputs are excited stepwise and periodically. The developed model has been verified for three different wall configurations. The performance of the simplified thermal model with optimized parameters has computational efficiency 40% to 50% higher compared to reference model.

The chapter is divided into two parts, in the first part, we have introduced the importance of the lumped parameter thermal network models and some review of various studies from the literature. A physical model based on heat balance equation was presented using its equivalent analogy to electrical systems. Furthermore, we discussed on different configurations of thermal network models that are well-established, this section was the basis for selection 3R2C model for our thesis. Later, we have also introduced analytical and numerical methods to solve heat equation. A comparison has been given between analytical and numerical model, in order to develop reference model for parameters identification we selected numerical Crank-Nicolson FDM because of its simplicity, stability, and accuracy over other FDM and analytical models.

Finally, the simulations were carried for different configurations of composite walls and their parameters identified using PSO, the optimal model is compared against other 2 models. The 2 other models have different R and C values. It has been observed that the model with optimal value performed well

3.6. Conclusion

and followed the dynamics of the reference model. The proposed method is then validated against an analytical model from literature.

Chapter 4

Case Study Building

4.1 Introduction

In the chapter 1 we detailed fundamentals of building models, types of different models and compared each model with their advantages and disadvantage. This gave insights into the building's thermal modeling, factors influencing building performance, occupants comfort parameters, and intelligent control systems for buildings. In Chapter 2 appropriate modeling techniques, difference between envelope and whole building modeling were presented. Furthermore, we have detailed how to select thermal network model, their parameters identification, and development of a thermal network model for composite wall. In the next chapter, we validate the proposed methodology of simplified thermal network with parameters identification with the measured data from a container building. In order to validate the model, first the whole building model has to be developed using thermal networks of building elements. The objective of this chapter given as follows:

- Introduction of the off-site container building, the developed model is validated with the measured data from this building,
- To present a the HVAC system of the building, and
- To detail the scheduling and the data collection methods.

This chapter provides a brief detail on selected case-study building, its materials, HVAC systems, and scheduling.

4.2 Case Study Building Description

The CESI smart container building is a multi-purpose building, the rooms are used as classrooms and laboratories, located in the CESI Campus of Nanterre, France (see Figure 4.1). This building is constructed under the program French Programmes d'Investissement d'Avenir (PIA-France). The building meets the French energy standard BBC (Bâtiment à Basse Consommation) [153].

Figure 4.2 shows the CESI smart building (Nanterre, France). It is an intelligent and connected building built in partnership with companies CISCO, Philips Lighting and Vinci Energies. The 200 m² building is constructed using 16 recycled maritime containers. The Smart Building integrates different technologies and data sensors to detect various physical parameters. These include LED lights powered and controlled by POE (Power Over Ethernet),

4.2. Case Study Building Description



FIGURE 4.1: Building site top view.

opening sensors, POE temperature and humidity sensors in each room, POE cameras and the presence of a weather station on the roof.



FIGURE 4.2: CESI smart building.

Thus, the demonstrator allows the collection of data on brightness, temperature, humidity, presence, sash opening, energy consumption and occupancy. The server is capable of controlling the systems and modifying the thermal and luminous ambiances. The heating and cooling energy is supplied to indoors through installed heat pump and ventilation system. The building is

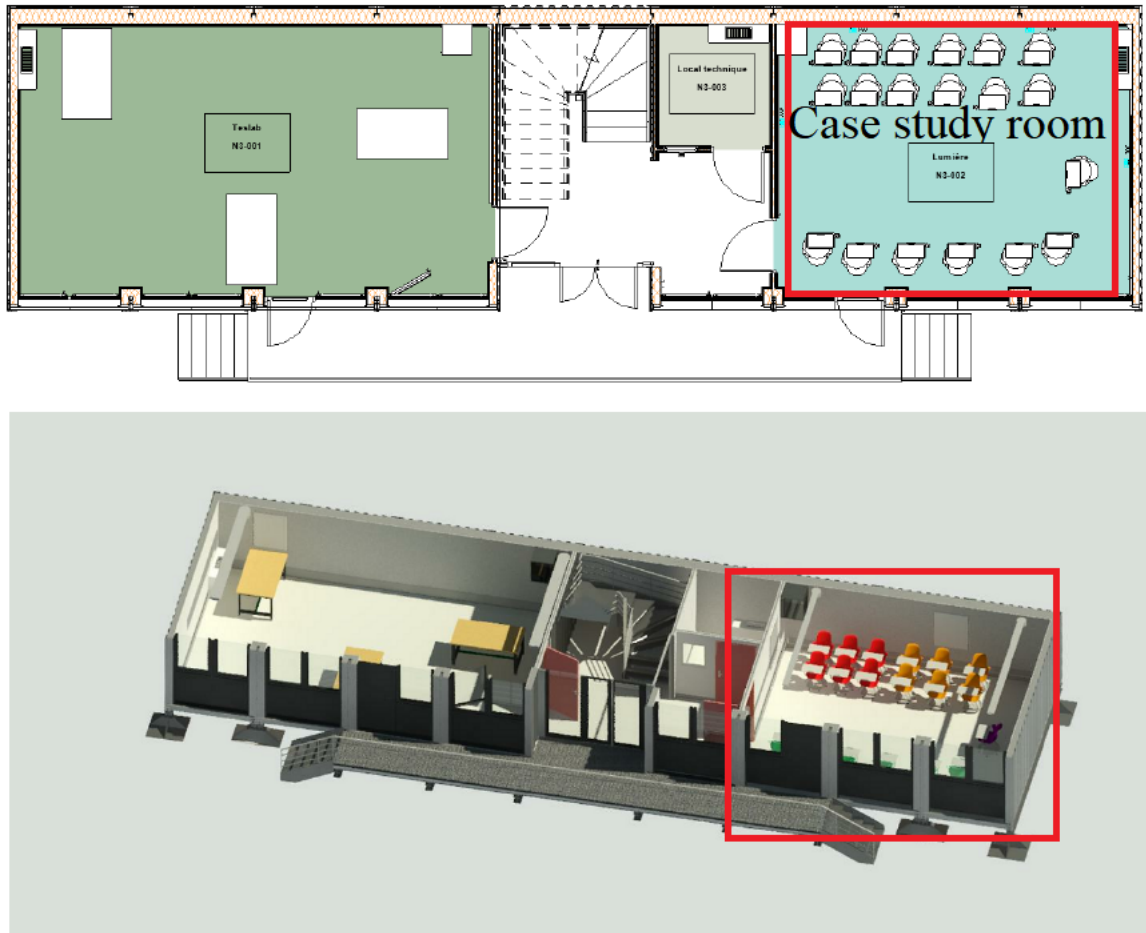


FIGURE 4.3: CESI smart building and the case study room.

south facing with a door opening, and south wall is almost covered with windows. Table 4.1 lists physical dimensions of each room of the reference building. The zone in the case-study building are all of the same dimension. However, two classrooms at the first floor have small offices within them. For our study, a classroom was selected as a case study room (see Figure 4.3). The objective is to develop a simplified thermal network model using the parametric identification and validate it against the measured temperature values. Similar approach can be applied to other rooms, as they are similar to the case study one.

4.2. Case Study Building Description

TABLE 4.1: Building wall and windows physical dimensions.

Zone	Height (m)	Direction	Wall surface (m ²)	Window surface (m ²)	volume (m ³)
4 zones	2.6	East	15.756	-	61.917
		West	15.756	-	
		North	6.344	-	
		South	16.200	9.17	

4.2.1 Data Collection

Temperature Data Collection

The building is equipped with advanced technology sensors. TO measure zone temperature, each room is equipped with the wall mount thermometer. This device can measure both temperature and humidity. This sensor is mounted on the north wall of the case-study room (shown in Figure 4.4). The range of this temperature sensor is -10 to 80°C and has accuracy of $\pm 0.8^{\circ}\text{C}$. Similarly, the accuracy for humidity measurement is $\pm 5\%$.



FIGURE 4.4: Wall mount temperature installed in the building.

Weather Station

An outdoor meteo station is installed on the roof of the building. This meteo station is used to measure environmental parameters such as: outdoor dry

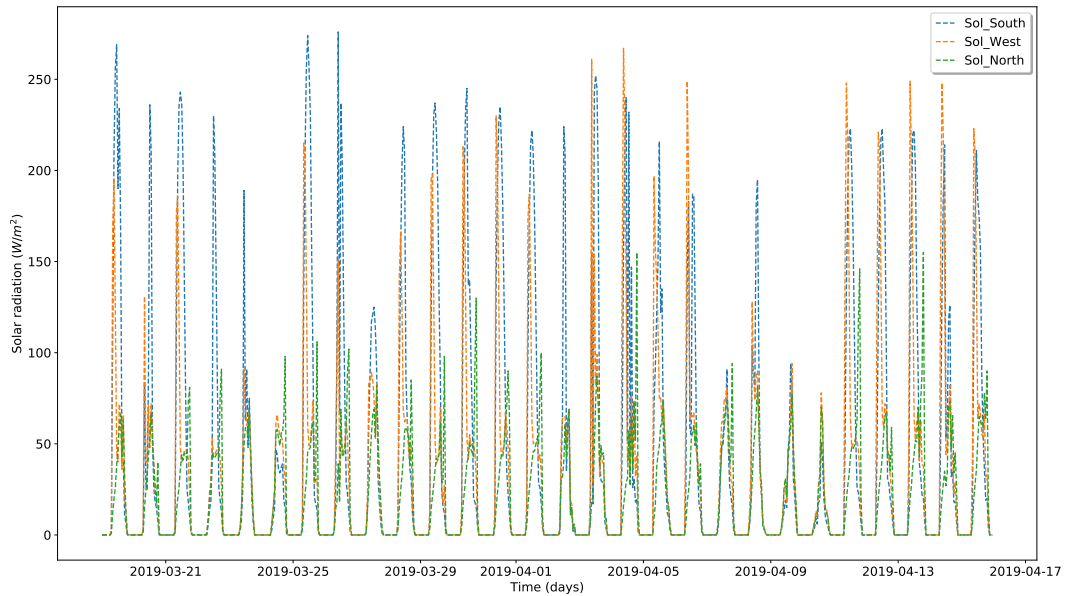


FIGURE 4.5: Measured solar radiation incident on wall surfaces.

bulb temperature, humidity, solar radiation, luminosity levels, wind speed, and wind direction. Pyrometer is capable of measuring the overall solar radiation on different walls (Figure 4.5). A sampling time of 60 seconds and 3600 seconds chosen to collect all the data from the weather station (Figure 4.6).

The measurement ranges and associated error ranges of the installed sensors are listed in Table 4.2.

TABLE 4.2: Measurement and associated error ranges of sensors.

Sensors	Measurement Range	Error Range
Outdoor temperature	-40 to +75	± 1
Indoor temperature	-10 to +80	± 1
Indoor illuminance	50 lx to 20,000 lx	$\pm 20\%$
Relative humidity	5% to 95%	$\pm 5\%$

HVAC Systems

The building is also equipped with the sensors such as: occupancy sensor, electrical power consumption meter, sash opening sensors, and indoor luminosity sensors. To meet the building heating/cooling load two HVAC systems are installed: VRF system and ventilation system. All these systems

4.2. Case Study Building Description



FIGURE 4.6: Installed weather station and VRF system heat pump setup on the building.

along with the sensors are connected to server and these systems are controlled by human machine interface (HMI) (Figure 4.7). However, the building is used as classrooms, standard schedules are applied and only authorized persons can change the set parameters. The HMI is used for displaying present condition of the room.

We have collected all data from the building. However, data regarding occupancy was not available due to the malfunction of the system. We have considered occupancy based on the time-table of the case-study room. When the class took place in the room, we considered occupants number as per strength of the class and if the class strength is more than room capacity, we considered occupancy to the limit of the room occupancy 18 students plus one teacher. The ventilation system power consumption for each room is shown in Figure 4.8. Similarly, heat gains from the occupants are calculated and shown in Figure 4.9



FIGURE 4.7: HMI installed in each room of the building.

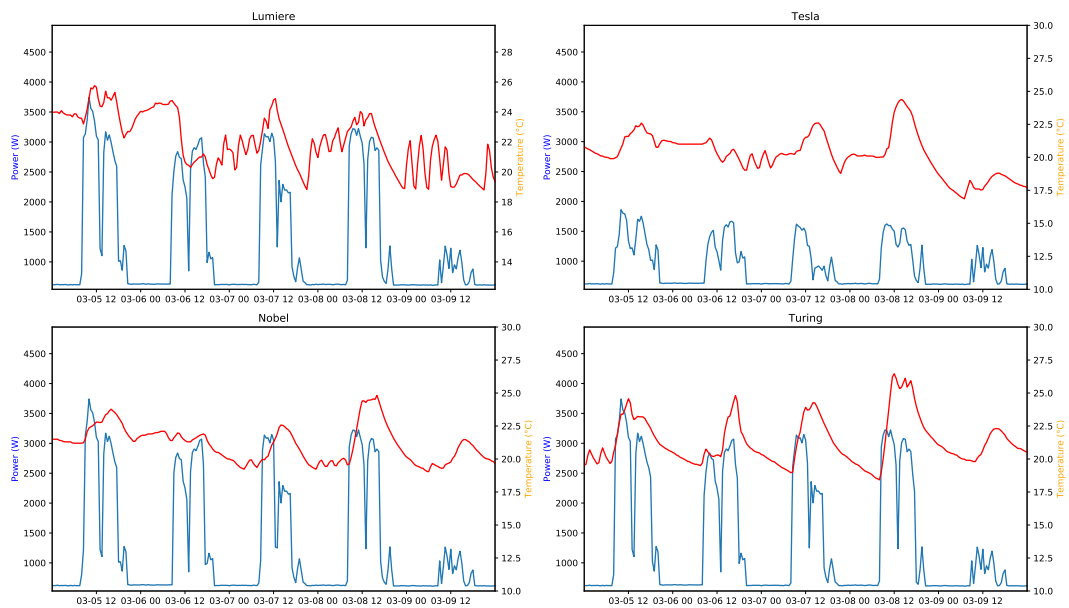


FIGURE 4.8: Power consumed by the ventilation system.

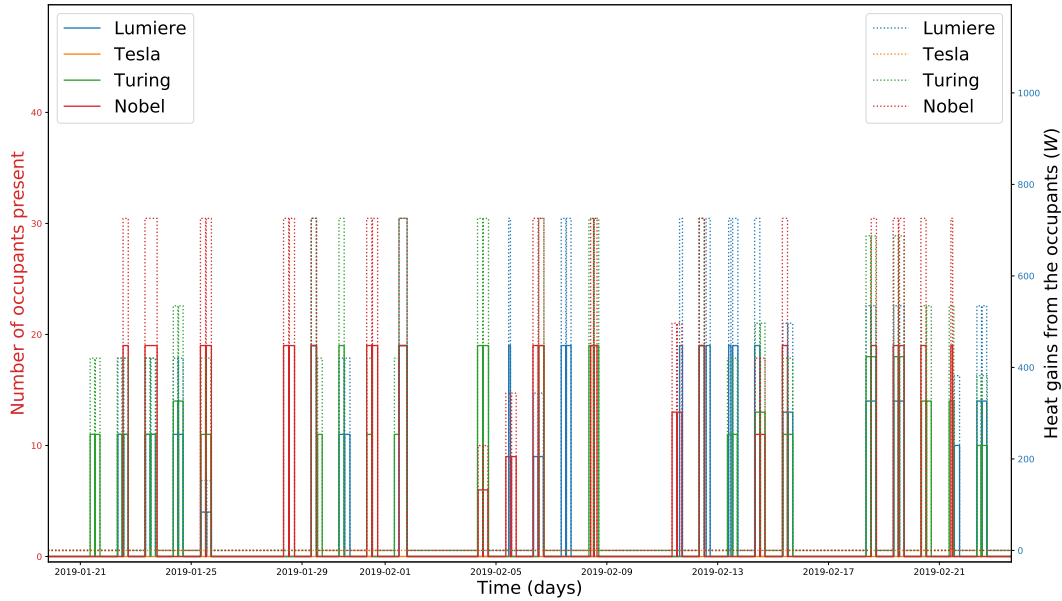


FIGURE 4.9: Heat gains from the occupants.

4.3 Air Source Heat Pump - Variable Refrigerant Flow Heating System Model

In the chapter 2, we have given brief introduction to ASHP-VRF systems. In this section, an attempt has been made to develop a generic model for simulation of ASHP-VRF systems. The system model is cumulative of major individual subsystem models such as compressor, condenser, EEVs, and evaporator. This method of designing increases the complexity, however model reduction studies will be carried out once after developing a quasi-accurate model. We have considered only two rooms for the modeling purposes.

Variable Speed Compressor

In general, a polytropic process and steady-state compression is considered for the compressor modeling, as the compressor transient characteristics can be neglected as compared to a condenser and evaporator [154,155]. The compressor speed is considered to be reaching its desired speed instantly. In this study, scroll compressor is considered, because this motor is used in the installed VRF system of the building. The modeling is majorly adapted from the studies [154–157]. The mass flow rate of the compressor is represented as:

$$m_{com} = \frac{n\eta_{com}V_{s,th}}{\gamma_{r1}} \quad (4.1)$$

where

n is the rotational speed,

η_{com} is the volumetric efficiency,

$V_{s,th}$ is the swept volume, and

γ_{r1} is the refrigerant specific volume of the suction vapor.

The volumetric efficiency of the variable speed compressors, the ratio of actual volume of the refrigerant entering the compressor to the geometric displacement of the compressor. In the scroll compressors, we can consider that the volumetric efficiency to be 100 % as there is almost negligible leakage in the scrolls. There the above equation becomes:

$$m_{com} = \frac{nV_{s,th}}{\gamma_{r1}} \quad (4.2)$$

The values of the $V_{s,th}$ and n are obtained from the data sheet from the manufacturer. The electrical work of the variable speed scroll compressor is given by:

$$P_{e,compressor} = \frac{m_{com}(h_3 - h_2)}{\eta_{iso}} + (\Delta P)m_{com}v_{real} \quad (4.3)$$

where

h_3 and h_2 are enthalpy values at point 2 and 3 in the $\log(p, h)$ Figure 4.10,

ΔP is the difference between exhaust pressure and suction pressure,

η_{iso} is the isentropic efficiency, and

v_{real} is the actual volume at the point 3 in Figure 4.10.

Evaporator

The evaporator is a type of heat exchanger, in our study, we considered it as fin-tube type with counter flow heat exchanger. The low-pressure refrigerant liquid enters evaporator and leaving refrigerant is superheated before entering compressor. The evaporator model is divided into two sections: superheated and two-phase. The two-phase section is further divided into many control volumes.

In general, the evaporator model can be developed using three approaches: lumped-parameter model [158], distributed-parameter model and multi-zone

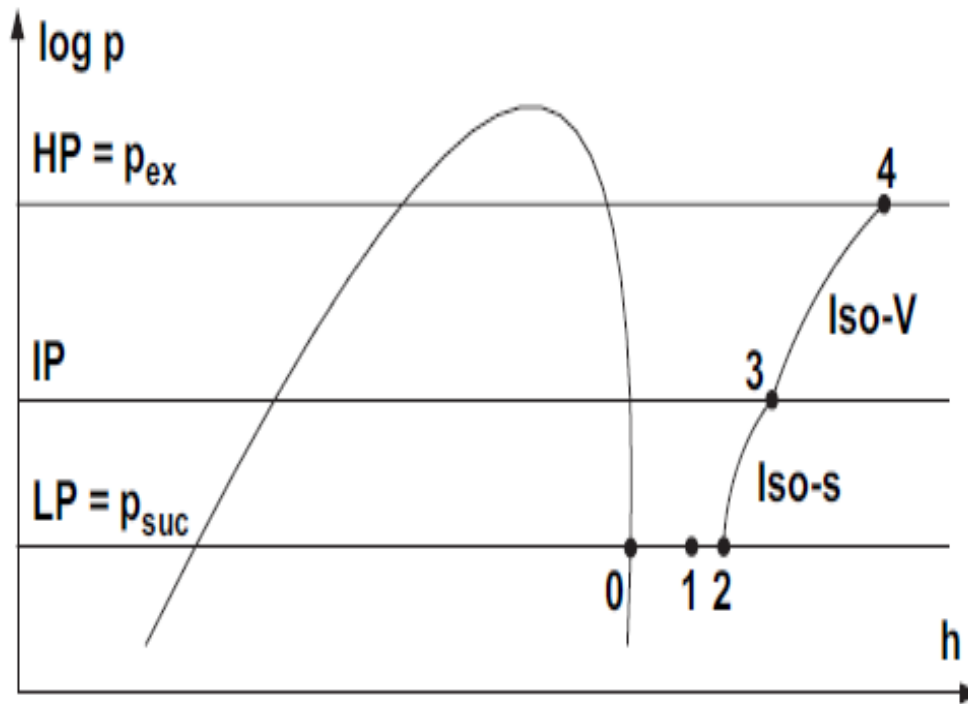


FIGURE 4.10: Thermodynamic process $\log(p, h)$ diagram [154].

model. The lumped parameter model is the most simple modeling approach but it fails to consider various heat transfers at various points of the thermodynamic process, therefore the error between predicted and the real models is high. Whereas, distributed-parameter model is complex, and design and computational costs are high [159, 160]. In our study, we used multi-zone model for evaporator modeling, because of the convergence and computational efficiency [157]. However, for the model simplicity, the control volumes of the two-phase section are modeled using lumped parameter model.

Before deriving equations for each section, some assumptions are made:

- Refrigerant flow is in one direction,
- Axial heat conduction is ignored,
- Refrigerant fluid and air thermal properties are considered homogeneous in any cross-section,
- The refrigerant liquid and vapor are in thermodynamic equilibrium in each control volume.

For refrigerant side, the equations are given as follows [157]:

The mass and energy balances for each control volume is given by:

$$m_r \Delta h - Q_r = 0 \quad (4.4)$$

$$Q_r = \alpha_r A_{cv} (T_w - T_{rm}) \quad (4.5)$$

where

m_r is the mass flow of refrigerant,

A_{cv} is the internal heat exchange area,

Δh is the enthalpy difference between leaving and entering refrigerant, and

α_r is the convective heat transfer coefficient.

For the better performance of the model, fluid properties (R410A), heat transfer coefficients, and pressure drop in both air and refrigerant sides are essential. The R410a type refrigerant fluid is used in the installed VRF system in building. The properties of the fluid is calculated using open-source platform CoolProp [161] Python library. The convective heat transfer coefficient in single-phase refrigerant is given by [157]:

$$\alpha_{r,sp} = 0.023 Re_{r,sp}^{0.8} Pr_{r,sp}^{0.4} \frac{\sigma_{r,sp}}{D_i} \quad (4.6)$$

$$Re_{r,sp}^{0.8} = \frac{(1-x)w_{r,sp}\rho_{r,sp}D_i}{\mu_{r,sp}} \quad (4.7)$$

$$w_{r,sp} = \frac{m_{r,sp}}{\frac{\pi D_i^2}{4} \rho_{r,sp}} \quad (4.8)$$

Similarly, two-phase refrigerant convective heat transfer coefficient is given by:

$$\alpha_{r,tp} = \frac{3.0}{X_{tt}^{2/3}} \alpha_{r,sp} \quad (4.9)$$

where

Pr is Prandtl number,

X_{tt} is Martinelli number [162],

x is the refrigerant vapor mass ratio,

m is the refrigerant mass flow,

μ is viscosity of the refrigerant,

Airside of the evaporator can be modelled the same way as the refrigerant side model with some changes in correlation methods [157].

Electronic Expansion Valve (EEV)

Generally, EEVs are controlled by stepper motors. The low temperature high-pressure refrigerant enters the EEV and leaving out as low temperature low-pressure refrigerant. The refrigerant mass flow through EEV is represented by using its opening diameter and pressure differences [163]:

$$m_{eev} = c_{eev} A_f \sqrt{2\rho_{eev,in}(P_{in} - P_{out})} \quad (4.10)$$

$$A_f = \frac{\pi D^2}{4} \quad (4.11)$$

$$c_{eev} = 0.02005\sqrt{\rho_{eev,in}} + 0.634v_{eev,out} \quad (4.12)$$

where

c_{eev} is the correlation coefficient,

D is the orifice diameter,

$v_{eev,out}$ is the volume of refrigerant leaving EEV, and

P_{in} and P_{out} are the refrigerant pressures at EEV inlet and outlet.

Condenser Model

In the multi-split VRF system outdoor unit and indoor units work as both evaporator and condenser based on the seasons, therefore the model for evaporator can be readily used for condensers except there is no dehumidification in the airside.

The VRF system coefficient of performance is improvised by sub-cooling the refrigerant exiting from condenser. Therefore, refrigerant in condenser is divided into three regions: two-phase, vapor, and subcooled region. The vapor and subcooled belongs to the single-phase region, hence single-phase calculations of evaporator model can be used here.

4.3.1 VRF System Model - Results

To validate the system model performance, a simulation is performed and compared with the measured data from the case study building. It is implemented for two rooms, each having heating and cooling capacity of $2.5kW$

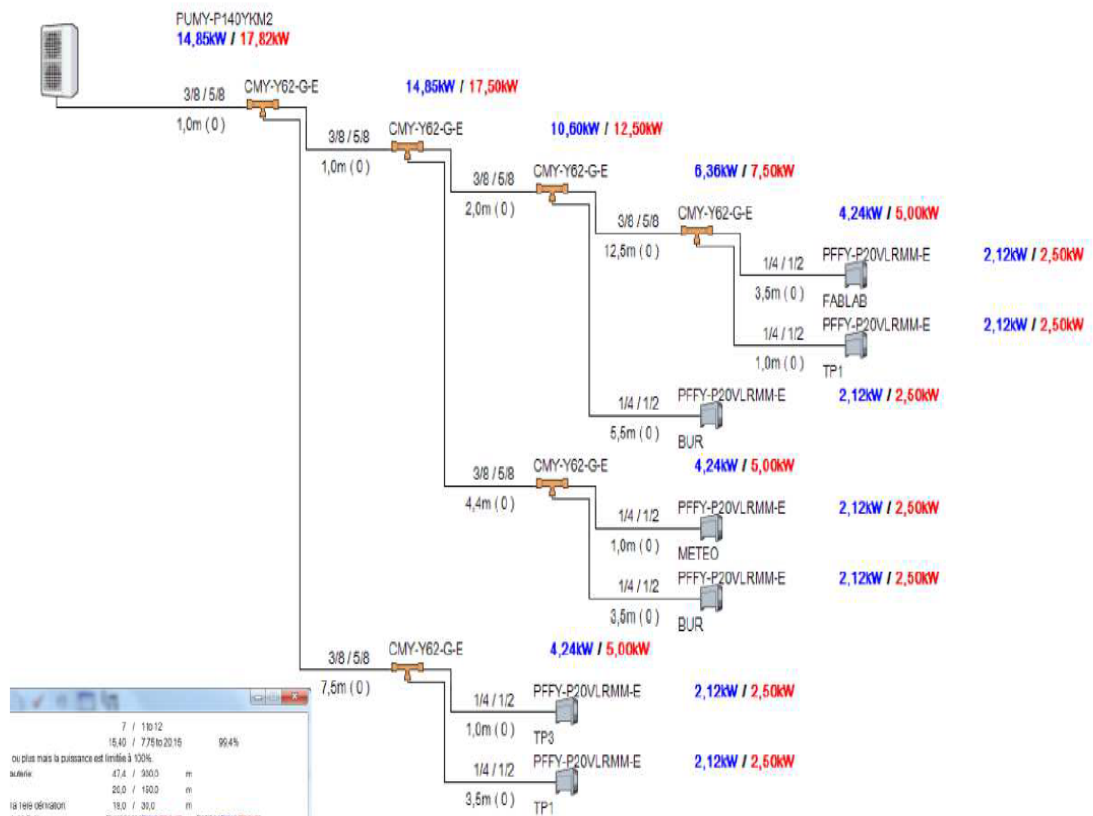


FIGURE 4.11: VRF system installed in the case study building.

and 2.12kW , respectively. The installed VRF system configuration is shown in Figure 4.11.

The compressor, heat exchangers, and EEV physical dimensions data, power ratings data, and operational data is collected from the data sheet from the manufacturer. Fluid properties are calculated directly from CoolProp library. The cooling load of the two rooms are calculated from the building model, internal heat gains, solar gains, and electrical equipment gains are given to the model. The room set temperature is 22°C for both the rooms.

Figure 4.12, presents the predicted power output of indoor units. The predicted power is well under the rated cooling capacity. Both of the rooms have similar trajectory of cooling capacity, this is due to the rooms are identically built. The COP of the simulated model is slightly lesser than the manufacturer's COP value. We have obtained average COP of 4.34. From simulation results, we can observe that during the time period between 7-8, the compressor is running in low speed thus low power consumed as there was low

4.3. Air Source Heat Pump - Variable Refrigerant Flow Heating System Model

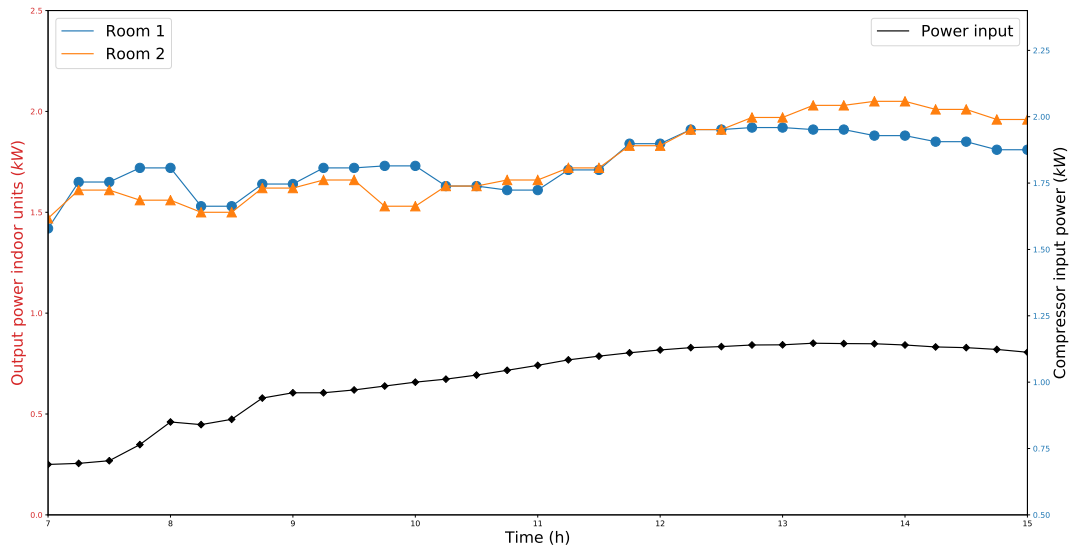


FIGURE 4.12: Cooling load output and electricity consumption of the VRF system.

cooling load required. Similarly, during mid-day the room heats up drastically due to the excessive solar gains. The compressor model is running in high speed to maintain room temperature under set temperature. In addition, the dynamicity of the predicted cooling load indicates the compressor is fast reactive to the load requirements.

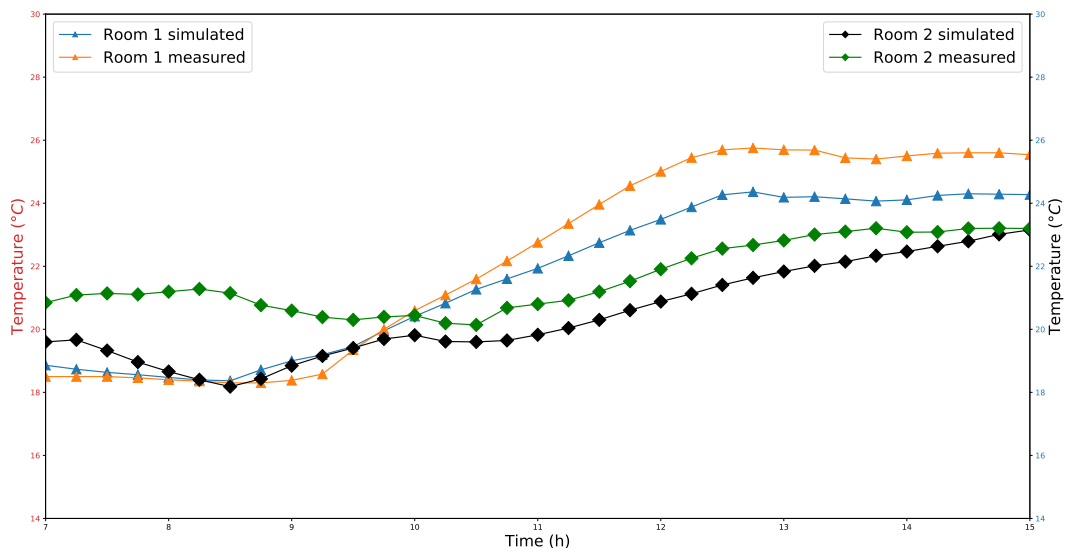


FIGURE 4.13: Comparison of room temperatures from VRF system with measured values.

Furthermore, the simulated room temperature for both the rooms are in figure 4.13. The predicted temperature for room 1 has followed the same trajectory as measured temperature, whereas room 1 model has high error between the predicted and the measured temperature values. In both the rooms there is difference of almost 2°C between predicted and the simulated, this may be due to the location of temperature sensor. The temperature sensors are installed on the wall that faces the window. Although the pipe losses are neglected in the simulation the COP of the model is lower than the actual COP and the system model of room 1 did not follow the trajectory in beginning. Therefore, there is a need of further study on this model, it has to be validated for more rooms and longer duration.

4.4 Conclusion

The objective of this chapter was to present development of thermal network model for whole building. Building elements were represented using 3R2C thermal network that we have simplified and validated in the previous chapter. Model thermal parameters resistor and capacitor values are determined using the method proposed in the previous chapter using constrained PSO.

In this chapter, we have validated our model with the measured temperature values of CESI LINEACT container building. The model was applied to a case study room but it can well extended to complete building. A model is developed and validated with the data of case study building. The model validation result has shown a second order thermal network model produce exact thermal behavior with a better accuracy. In this study, we observed that the presence of occupants and their activities has significant influence on the thermal performance of building. When occupants were present in the case study room, there was high variations in the predicted temperature profile, however, when the same room is simulated without occupants has shown much less variations. We have also proposed a well established but complex solar model for modeling solar gains. The isotropic model is straightforward and calculation of radiation on tilted surfaces becomes simple. However, it fails to take account of circumsolar diffuse and/or horizon brightening components on an inclined surface, this results in the underestimation of solar radiation (around 10 to 15%).

Finally, we established that the developed 3R2C network model is well suited for model-based controller application. A simple MPC model is implemented

4.4. Conclusion

for indoor thermal comfort control. The MPC has shown the ability to multi-objective control under given constraints, the average indoor temperature is always maintained within the lower and upper limits.

The energy consumption of the HVAC system for thermal comfort management during the 6 days was performed. The results indicate that the MPC system produces optimal control strategy, and offering reduced energy consumption in comparison, while the conventional controller is seen to be wasting energy and performing poorly. The presented MPC application has shown almost 31% of energy saving compared to the conventional controller. Indeed, it has reduced system states number, it is computationally efficient, and can be adapted to any type of buildings.

Chapter 5

Thermal Network Model for Whole
Building and Simulation Results

5.1 Introduction

In the chapter 1, we detailed fundamentals of building models, types of different models and compared each model with their advantages and disadvantage. This gave insights into the building's thermal modeling, factors influencing building performance, occupants comfort parameters, and intelligent control systems for buildings. In Chapter 2 appropriate modeling techniques, difference between envelope and whole building modeling were presented. Furthermore, we have detailed how to select thermal network model, their parameters identification, and development of a thermal network model for composite wall. In this chapter, we validate the proposed methodology of simplified thermal network with parameters identification with the measured data from a container building.

In order to validate the model, first the whole building model has to be developed using thermal networks of building elements. The objective of this chapter given as follows:

- Introduction of the off-site container building, the developed model is validated with the measured data from this building,
- To present a methodology to develop complete building model,
- To linearize the building model because the building model is non-linear when we take account radiative heat transfer between walls,
- Finally, to discuss the results of the developed model,

This chapter provides a brief detail on development of whole building model using the already developed building envelope model and its parameters identification method.

5.2 Thermal Network Model—CESI Smart Building

The heterogeneous nature of buildings and parameters that influence its performance makes modeling of a zone (case study room) highly complex. Particularly, modeling of building using analytical approach is infeasible because of its non-linear behavior.

The thermal network approach discretize the complex building into multiple zone, where each zone is assumed to have properly mixed well and the

building walls have uniform temperatures throughout its volume. The zones are then modeled by means of the network of nodes with interconnecting heat flow paths. The heat transfer can occur through conduction, convection, and radiation. Heat gains from different means: internal, solar radiation, etc., are lumped in the thermal network nodes, and the heat storage in building thermal mass is in thermal capacitances. Temperature and heat flows between the nodes are determined by energy balance approach as described in Chapter 3. The resultant formulations are a set of coupled ordinary differential and algebraic equations that can be solved using the state space equation.

The simplified thermal network model was developed by making the following assumptions:

- heat conduction occurs through the building envelope,
- convective heat transfer at building envelope surfaces and floors,
- solar gains through windows and solar radiation absorption in external walls,
- radiation heat transfer within the zone walls,
- effect of thermal bridge is neglected,
- heat storage is not considered in windows, and
- impact of wind velocity variation on the convective heat exchange coefficient of the wall surface is neglected, hence the convective resistances are considered constant.

The CESI container building external walls are built using variety of materials for different sides: east, west, north and south. Therefore, 3R2C model is developed individually for each side of external walls, floor, and roof.

Considering all the above hypothesis, a thermal model is developed with 6 sets of 3R2C networks and the equations obtained by energy balance at each node from the schematic shown in Figure 5.1:

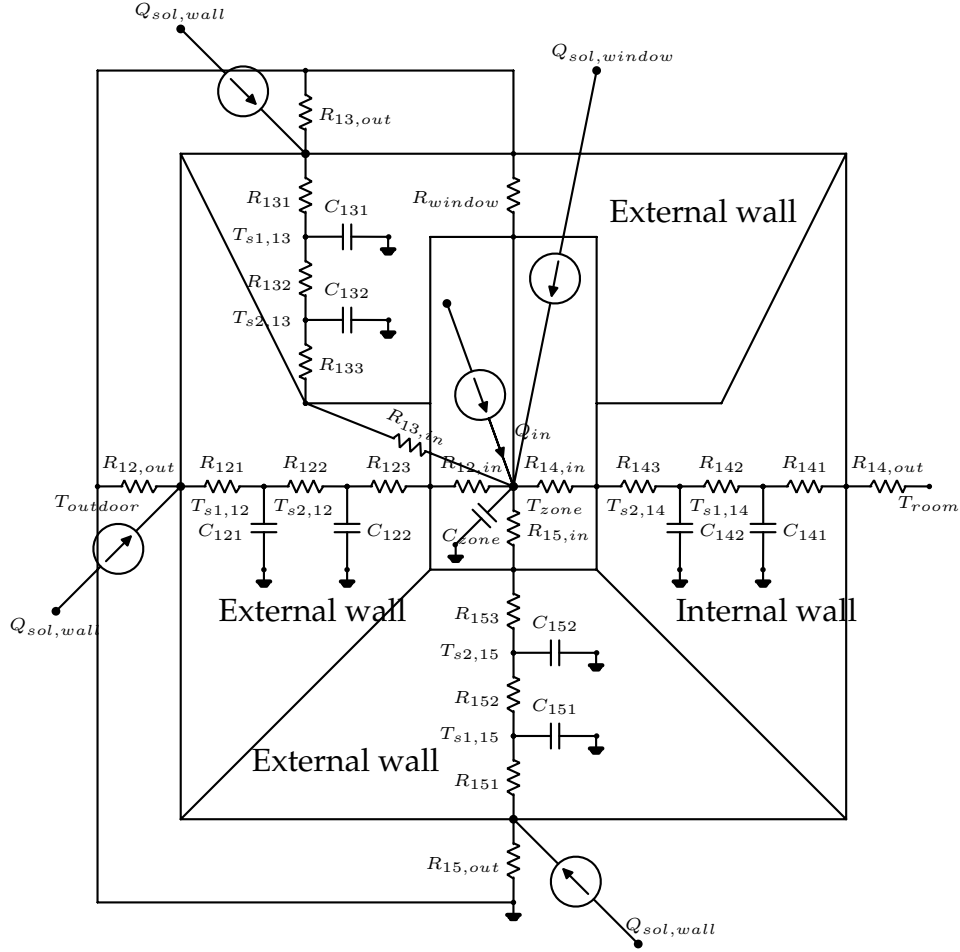


FIGURE 5.1: Equivalent thermal network model of the case study building.

$$\frac{dT_{s1,12}}{dt} = -\frac{T_{s1,12}}{C_{121}} \left(\frac{1}{R_{122}} + \frac{1}{R_{12,cout}} \right) + \frac{T_{s2,12}}{R_{121}C_{121}} + \frac{T_{out}}{C_{121}R_{12,cout}} + \frac{\dot{Q}_{12}}{C_{121}} \quad (5.1)$$

$$\frac{dT_{s2,12}}{dt} = \frac{T_{s1,12}}{R_{121}C_{122}} - \frac{T_{s2,12}}{C_{122}} \left(\frac{1}{R_{122}} + \frac{1}{R_{12,cin}} \right) + \frac{T_z}{C_{122}R_{12,cin}} \quad (5.2)$$

$$\frac{dT_{s1,13}}{dt} = -\frac{T_{s1,13}}{C_{131}} \left(\frac{1}{R_{132}} + \frac{1}{R_{13,cout}} \right) + \frac{T_{s2,13}}{R_{131}C_{131}} + \frac{T_{out}}{C_{131}R_{13,cout}} + \frac{\dot{Q}_{13}}{C_{131}} \quad (5.3)$$

$$\frac{dT_{s2,13}}{dt} = \frac{T_{s1,13}}{R_{131}C_{132}} - \frac{T_{s2,13}}{C_{132}} \left(\frac{1}{R_{132}} + \frac{1}{R_{13,cin}} \right) + \frac{T_z}{C_{132}R_{13,cin}} \quad (5.4)$$

$$\frac{dT_{s1,14}}{dt} = -\frac{T_{s1,14}}{C_{141}} \left(\frac{1}{R_{142}} + \frac{1}{R_{14,cout}} \right) + \frac{T_{s2,14}}{R_{141}C_{141}} + \frac{T_{room}}{C_{141}R_{14,cout}} \quad (5.5)$$

$$\frac{dT_{s2,14}}{dt} = \frac{T_{s1,14}}{R_{141}C_{142}} - \frac{T_{s2,14}}{C_{142}} \left(\frac{1}{R_{142}} + \frac{1}{R_{14,cin}} \right) + \frac{T_z}{C_{142}R_{14,cin}} \quad (5.6)$$

$$\frac{dT_{s1,15}}{dt} = -\frac{T_{s1,15}}{C_{151}} \left(\frac{1}{R_{152}} + \frac{1}{R_{15,cout}} \right) + \frac{T_{s2,15}}{R_{151}C_{151}} + \frac{T_{out}}{C_{151}R_{15,cout}} + \frac{\dot{Q}_{15}}{C_{151}} \quad (5.7)$$

$$\frac{dT_{s2,15}}{dt} = \frac{T_{s1,15}}{R_{151}C_{152}} - \frac{T_{s2,15}}{C_{152}} \left(\frac{1}{R_{152}} + \frac{1}{R_{15,cin}} \right) + \frac{T_z}{C_{152}R_{15,cin}} \quad (5.8)$$

$$\frac{dT_{s1,16}}{dt} = -\frac{T_{s1,16}}{C_{161}} \left(\frac{1}{R_{162}} + \frac{1}{R_{16,cout}} \right) + \frac{T_{s2,16}}{R_{161}C_{161}} + \frac{T_{room-top}}{C_{161}R_{16,cout}} \quad (5.9)$$

$$\frac{dT_{s2,16}}{dt} = \frac{T_{s1,16}}{R_{161}C_{162}} - \frac{T_{s2,16}}{C_{162}} \left(\frac{1}{R_{162}} + \frac{1}{R_{16,cin}} \right) + \frac{T_z}{C_{162}R_{16,cin}} \quad (5.10)$$

$$\frac{dT_{s1,17}}{dt} = -\frac{T_{s1,17}}{C_{171}} \left(\frac{1}{R_{172}} + \frac{1}{R_{17,cout}} \right) + \frac{T_{s2,17}}{R_{171}C_{171}} + \frac{T_{out}}{C_{171}R_{17,cout}} \quad (5.11)$$

$$\frac{dT_{s2,17}}{dt} = \frac{T_{s1,17}}{R_{171}C_{172}} - \frac{T_{s2,17}}{C_{172}} \left(\frac{1}{R_{172}} + \frac{1}{R_{17,cin}} \right) + \frac{T_z}{C_{172}R_{17,cin}} \quad (5.12)$$

$$C_z \frac{dT_z}{dt} = \sum_{j=2}^7 \frac{T_{s2,1j} - T_z}{R_{1j,cin}} + \frac{T_{out} - T_z}{R_{window}} + \dot{Q}_{in} + \dot{Q}_{s,wi} + \dot{Q}_{heat} \quad (5.13)$$

where, C_z - the zone air capacitance,

C_{1j2} - the wall capacitance indoor side,

C_{1j1} - capacitance at outdoor side of the wall,

T_{out} - ambient temperature,

$\dot{Q}_{heat,pump}$ - heating or cooling energy supplied from heat pump,

\dot{Q}_{vent} - heating or cooling energy supplied from ventilation system,

\dot{Q}_{in} - heat gains from occupants and electrical appliances,

$\dot{Q}_{s,wi}$ - solar gains through windows,

\dot{Q}_{1j} - solar gains from the building external walls,

\dot{Q}_{heat} - total supplied energy from $\dot{Q}_{heat,pump}$ and \dot{Q}_{vent} ,

$T_{sj,12}$ - surface temperatures for north facing wall,

$T_{sj,13}$ - surface temperatures for south facing wall,

$T_{sj,14}$ - surface temperatures for west facing wall,

$T_{sj,15}$ - surface temperatures for east facing wall,

$T_{sj,16}$ - surface temperatures for roof,

$T_{sj,17}$ - surface temperatures for floor,

$R_{1j,cin} = R_{1j3} + R_{convection,in}$ and

$R_{1j,cout} = R_{1j1} + R_{convection,out}$.

The equation 5.13 represents the zone temperature, which interacts with the inside surface temperature of the walls, heat gain from the occupants, heat systems, and direct solar gains through windows. The resistor and capacitor values of these equations are determined by using optimization technique presented in the previous chapters. These values are determined only once and they are time and temperature independent, this helps in increasing the computational efficiency.

The system equations from 5.1 to 5.13 have various inputs to the system. These inputs are outdoor dry bulb temperature T_{out} , solar heat gains from the surface of the walls and through windows \dot{Q}_{1j} and $\dot{Q}_{s,wi}$, respectively, heat gains from the occupants and electrical appliances \dot{Q}_{in} , and heat gains from the heating system \dot{Q}_{heat} . The model consists of overall 13 nodes: two nodes for each envelope wall, floor, roof and a zone node. The installed lighting appliances in the room is low energy consumption hi-tech light systems, thus the gains from these light systems are neglected. However, heat gains from student's laptop is considered during the simulation.

The formulation of the thermal network model of the building in state-space representation is given as follows.

$$\begin{aligned} X(k+1) &= AX(k) + Bu(k) + B_1d(k) \\ y(k) &= CX(k) + Du(k) + D_1d(k) \end{aligned} \quad (5.14)$$

where, state-vector X is :

$$X = \begin{bmatrix} T_{s1,12} \\ T_{s2,12} \\ T_{s1,13} \\ T_{s2,13} \\ T_{s1,14} \\ T_{s2,14} \\ T_{s1,15} \\ T_{s2,15} \\ T_{s1,16} \\ T_{s2,16} \\ T_{s1,17} \\ T_{s2,17} \\ T_z \end{bmatrix} \quad (5.15)$$

Input vector u represents only the controllable inputs, in our case-study building only ventilation system is controllable :

$$u = \begin{bmatrix} \dot{Q}_{vent} \end{bmatrix} \quad (5.16)$$

The ventilation system \dot{Q}_{vent} is equal to:

$$\dot{Q}_{vent} = \dot{m}c_p(T_{set} - T_z) \quad (5.17)$$

The vector d represents the uncontrollable inputs (or disturbances) of the system :

$$d = \begin{bmatrix} T_{out} \\ \dot{Q}_{12} \\ \dot{Q}_{13} \\ \dot{Q}_{15} \\ T_{room} \\ T_{room,top} \\ \dot{Q}_{in} \\ \dot{Q}_{heatpump,vrf} \\ \dot{Q}_{s,wi} \end{bmatrix} \quad (5.18)$$

5.2.1 Model Inputs

The data of model inputs of both controllable and uncontrollable are collected from the case-study building using the sensors. However, some of the measurable but uncontrollable inputs are easily measurable (directly) or readily available concerning to the building location such as: ambient temperature. However, other inputs such as solar irradiation are not readily available or measured as global horizontal irradiance. Hence, a detailed analysis on the solar irradiation incident on the building envelope is essential. To calculate the total irradiation energy on the building envelope, it is needed to obtain radiation energy on each surface. These total irradiation thus can be used to estimate the total solar gains on the walls and through the windows using equation 5.19.

$$\dot{Q}_{s,w} = \alpha_w A_w q_{rad}'' \quad (5.19)$$

where, \dot{Q}_{wall} = solar radiation on walls,

α_w = solar absorptance of the surface (between 0 and 1),

A_w = surface area of the wall, and

q_{rad}'' = total irradiation incident on the wall.

The total irradiation incident on the wall is essential in estimating the zone temperature and heating/cooling loads. In our study, we compared different

models to have better estimation of the solar irradiation. We found solar irradiation model proposed by Hay–Davies–Klucher–Reindl (HDKR) has near accurate estimation than other models.

Solar Heat Gains Model

In the literature, many studies were conducted to calculate the solar irradiation incident on the tilted surface by taking account of the isotropic diffuse sky model. In isotropic diffuse sky model, three components of radiations are considered: isotropic diffuse, diffused radiation reflected from the ground, and beam radiation [164]. The isotropic model is straightforward and calculation of radiation on tilted surfaces becomes simple. However, it fails to take account of circumsolar diffuse and/or horizon brightening components on a inclined surface, this results in the underestimation of solar radiation (around 10 to 15%). More advanced approaches like Hay–Davies–Klucher–Reindl (HDKR) uses anisotropic sky models that consist three components: isotropic, circumsolar diffuse and horizon brightening [165–167]. Figure 5.2 shows the distribution of all parts of solar radiation on a tilted surface.

Considering an anisotropic sky model, the incident solar radiation on a tilted surface based on HDKR model, is calculated by [166]:

$$I_{Total} = (I_b + I_d A_i) R_b + I_d (1 - A_i) \left(\frac{1 + \cos \beta}{2} \right) \times \left[1 + f \sin^3 \left(\frac{\beta}{2} \right) \right] + I_{gh} \rho_g \left(\frac{1 - \cos \beta}{2} \right) \quad (5.20)$$

where I_b = beam radiation,

I_d = diffuse radiation,

R_b = geometric factor,

θ = angle of incidence,

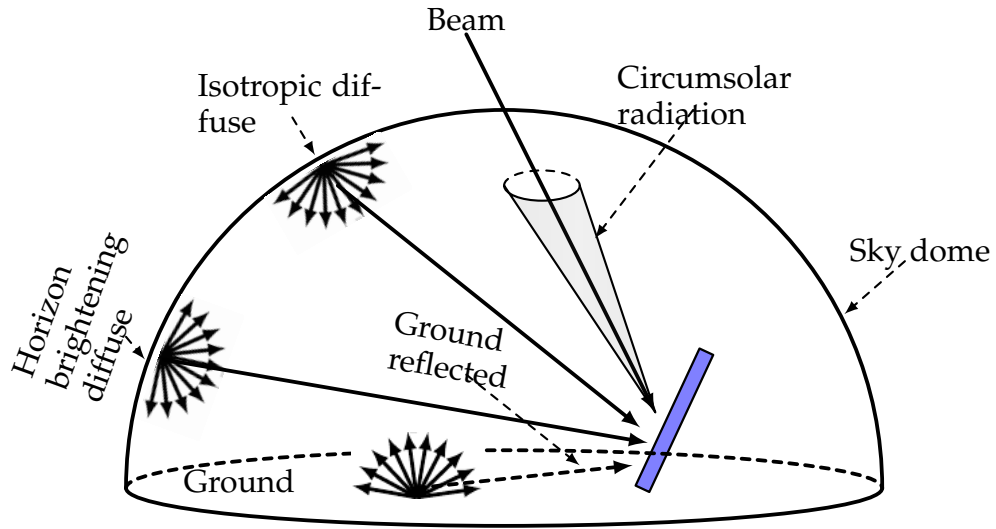
γ = surface azimuth angle,

β = angle between tilted surface and the horizontal plane,

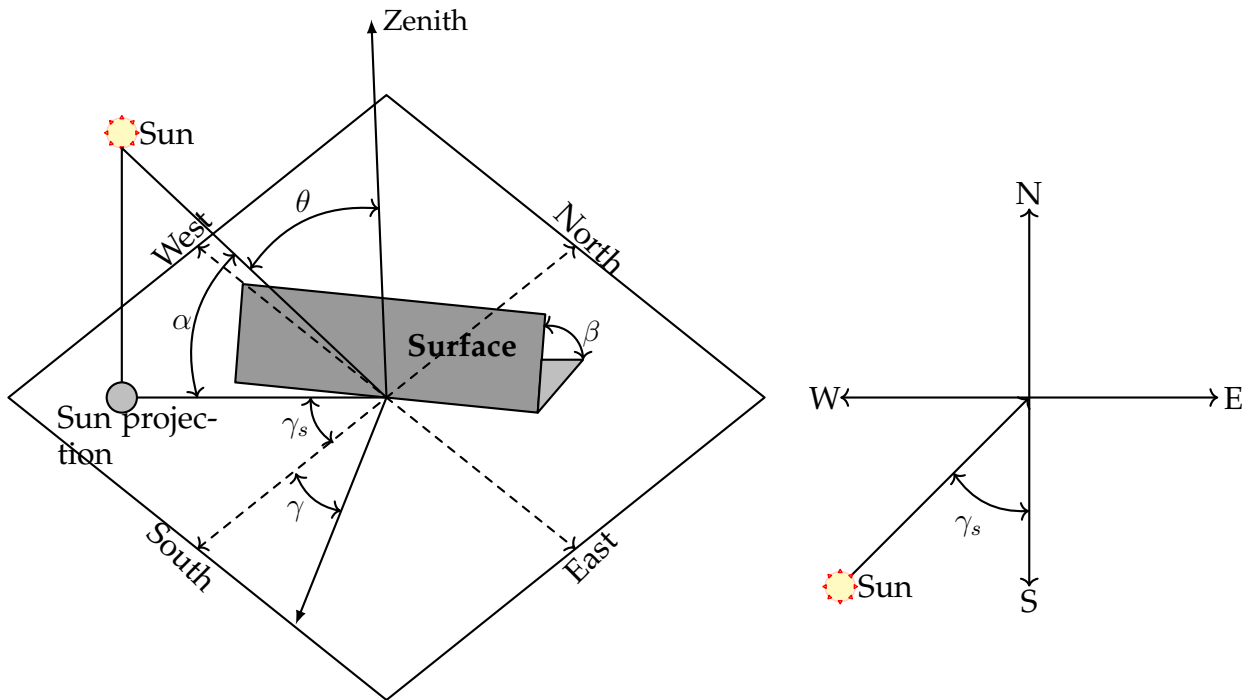
I_{gh} = total radiation on horizontal surface,

ρ_g = ground albedo (0.3).

The angles under consideration and other solar angles are illustrated by Figure 5.2b.



(A) Isotropic and anisotropic diffuse solar radiation model.



(B) Zenith angle, slope, surface azimuth angle, and solar azimuth angle for a tilted surface.

FIGURE 5.2: Solar sky models and solar angles diagram.

Anisotropy index (A_i) in Equation (5.20), is a function of the transmittance of the atmosphere for beam radiation. It is the ratio of beam radiation on a horizontal ground surface to extraterrestrial radiation (I_o).

$$A_i = \frac{I_b}{I_o} \tag{5.21}$$

The modulating factor f in the correction factor is to account for cloudiness.

$$f = \sqrt{\frac{I_b}{I}} \quad (5.22)$$

The angle θ is the incidence angle of the beam radiation on tilted surface, and the angle θ_T is the incidence angle of the beam radiation on the inclined surface. These angles are calculated by:

$$R_b = \frac{\cos \theta}{\cos \theta_z} \quad (5.23)$$

$$\begin{aligned} \cos \theta = & \sin \delta \sin \phi \cos \beta - \sin \delta \cos \phi \sin \beta \cos \gamma + \cos \delta \cos \phi \cos \beta \cos \omega \\ & + \cos \delta \sin \phi \sin \beta \cos \gamma \cos \omega + \cos \delta \sin \beta \sin \gamma \sin \omega \end{aligned} \quad (5.24)$$

$$\cos \theta_z = \sin \phi \sin \delta + \cos \delta \cos \phi \cos \omega \quad (5.25)$$

Since, building envelope walls are perpendicular to the horizontal plane, the β angle between the plane of the surface and the horizontal is 90°. The (5.25), then becomes:

$$\cos \theta = -\sin \delta \cos \phi \cos \gamma + \cos \delta \sin \phi \cos \gamma \cos \omega + \cos \delta \sin \gamma \sin \omega \quad (5.26)$$

the total solar radiation on a surface is given by:

$$I_{Total} = (I_b + I_d A_i) R_b + I_d (1 - A_i) (1 + 0.3535 f) / 2 + I_{gh} \rho_g / 2 \quad (5.27)$$

The total solar radiation for complete building envelope is calculated as follows:

$$\dot{Q}_{sol} = \sum_{j=1}^4 I_{Tj} S_j \alpha_j \quad (5.28)$$

The sums of hourly solar radiation incident on a south facing wall for 5 days in May in Nanterre, France are shown in Figure 5.3. The solar radiation calculated for isotropic and anisotropic sky models. These two calculated sums of the radiations are compared with the data procured from the weather station on horizontal surface. The ground albedo is considered as 0.2.

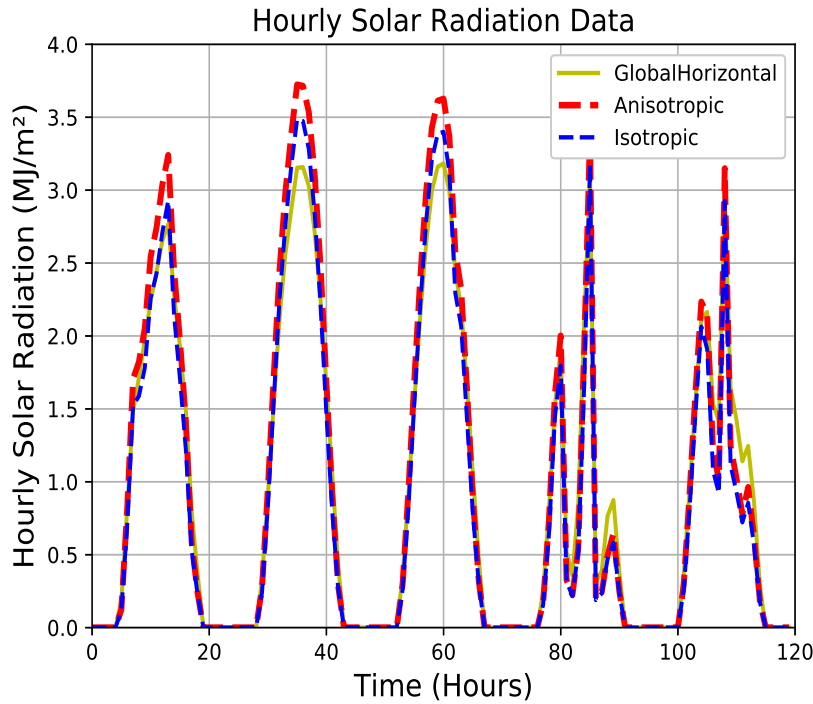


FIGURE 5.3: Hourly solar irradiation sums on south facade of the building.

Internal Heat Gains

The internal heat gain \dot{Q}_{in} is the sum of all internal gains (inhabitants and electrical equipment) and \dot{Q}_{heat} is the sum of energy supplied from heating equipment (heat pump and ventilation system). Internal gains from the occupants can be exploited to heat the zone. The heat gains from the occupants is dynamic and it depends on many parameters such as: occupants activity, physical dimension, clothing, building type, season, etc. Since, the chosen room is a classroom, the students (adults) will be mostly sitting and reading. We have considered body surface area to be 1.2 m^2 , Table 5.1 represents average body surface area for occupants in different types of building.

Based on the body surface area and the activity we have assumed the heat gains from one adult student is equal to 116 W in summer and 114 W in winter (Table 5.2 and 5.3) [23, 168].

Similarly, for the heat gains from electrical appliances, the assumed heat gains from one laptop equaled 30 W [23], and there are no other electrical systems installed in the classroom. Furthermore, the selected controllable input and measurable disturbances are: outside air temperature, internal free gains and solar gains. Heating system is the only controllable input in the model.

TABLE 5.1: Standard data of average body surface area of occupants in different types of building [168].

Building type	Body surface area (m^2)
Detached house	1.80
Apartment building	1.80
Office building	1.80
Department store	1.80
Hotel	1.80
Restaurant	1.80
Sport, terminal, theatre	1.80
School	1.68
Daycare center (2–4 yr)	0.66
Kinder garden (5–6 yr)	0.77
Hospital	1.80

TABLE 5.2: Heat loss from the occupants during summer [168].

Building type	Metabolic rate (met)	$Q_{convection}$ (W)	$Q_{radiation}$ (W)	Q_{vapor} (W)	Q_{sweat} (W)
Detached house	1.2	44.1	38.7	25.9	9.7
Apartment building	1.2	44.1	38.7	25.9	9.7
Office building	1.2	44.1	38.7	25.9	9.7
Department store	1.6	41.7	36.0	27.8	52.4
Hotel	1.2	44.1	38.7	25.9	9.7
Restaurant	1.2	44.1	38.7	25.9	9.7
Sport, terminal, theatre	1.6	41.7	36.0	27.8	52.4
School	1.2	39.6	32.7	25.2	19.4
Daycare center (2–4 yr)	1.0	16.1	13.4	9.5	0.0
Kinder garden (5–6 yr)	1.39	17.6	14.4	11.9	18.1
Hospital	1.2	44.1	38.7	25.9	9.7

TABLE 5.3: Heat loss from the occupants during winter [168].

Building type	Metabolic rate (met)	$Q_{convection}$ (W)	$Q_{radiation}$ (W)	Q_{vapor} (W)	Q_{sweat} (W)
Detached house	1.2	38.3	39.5	33.4	7.1
Apartment building	1.2	38.3	39.5	33.4	7.1
Office building	1.2	38.3	39.5	33.4	7.1
Department store	1.6	36.9	37.3	35.9	47.6
Hotel	1.2	38.3	39.5	33.4	7.1
Restaurant	1.2	38.3	39.5	33.4	7.1
Sport, terminal, theatre	1.6	36.9	37.3	35.9	47.6
School	1.2	37.8	38.9	32.9	7.2
Daycare center (2–4 yr)	1.0	15.1	15.8	12.5	0.0
Kinder garden (5–6 yr)	1.39	17.1	17.4	15.7	11.9
Hospital	1.2	38.3	39.5	33.4	7.1

This thermal network model can be used for real-time HVAC control applications. For example, model predictive controller is applied for comfort and energy optimization based on the simplified thermal network model [19].

5.3 Simulation Results - Whole Building Model

The simplified thermal network model of the zone is validated against the measured data from case-study classroom of the CESI smart building. The data was collected from the building for almost 8 months. However, there were some discrepancies in the collected data due to malfunction of the system for few days in 8 months. These discrepancies treated while data-preprocessing stage. We studied the model performance analysis for the two seasons: summer and winter. The duration of the simulation is considered two months in each season.

The developed model is simulated for two months in different seasons, winter (see Figure 5.4) and summer (see Figure 5.5). The model dynamics follow the trajectory of the measured temperature dynamics of the real building. The model was trained for seven days before the simulating for two months in summer and winter. Furthermore, we have analyzed our model with different error methods for its validation.

From the simulation results, several key observations are noted here, during the summer the model has less variation in temperature output as compared to the response of the same in winter season. Many factors have influence on the performance, particularly the data of occupant numbers and their activities were not available precisely, and these activities have influence on the performance. Moreover, students were on holidays during the summer period thus the summer simulation is without occupants. Whereas, students were present most of the days in the classroom during the winter season. Their unpredicted indoor activities, door/windows openings, varying internal gains and air infiltration have influenced for higher variations in the response.

The occupants are students in the selected case study building. The data received from the building on occupancy that they considered maximum occupancy when that particular room was used for classes. Hence, the high variation in the temperature profile. Nevertheless, the dynamics follow the tendency of the measured data. There need to be a fine-tuning of the model in order to get more accuracy in prediction.

In the selected summer period, the building was mostly unoccupied due to the summer holidays. Therefore, there is less variation in the response and in both the model outputs, zone temperature follows the dynamics of the actual measured temperature of the zone. Furthermore, in summer (see Figure 5.5)

5.3. Simulation Results - Whole Building Model

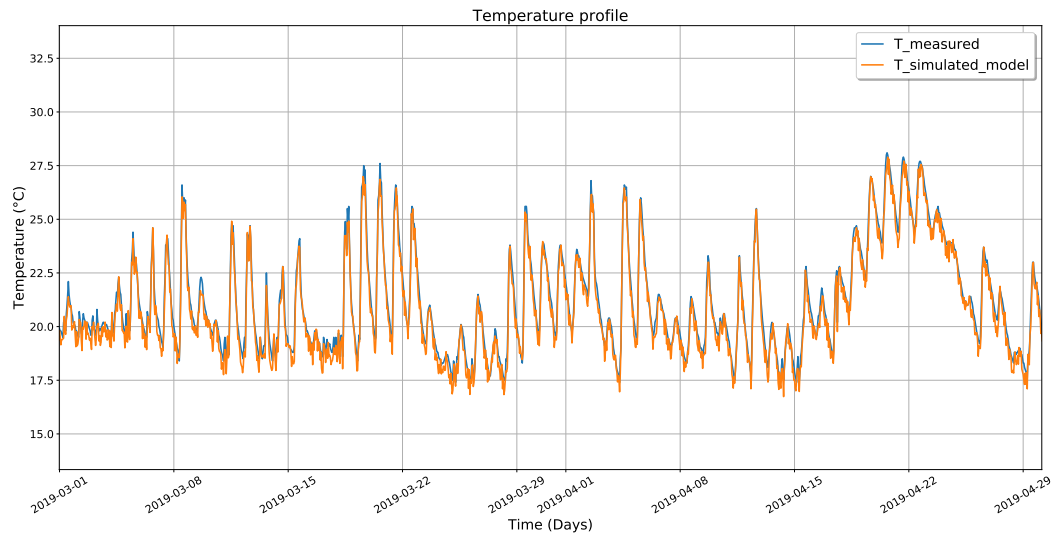


FIGURE 5.4: Validation of simplified thermal network model with measured zone temperature data (winter).

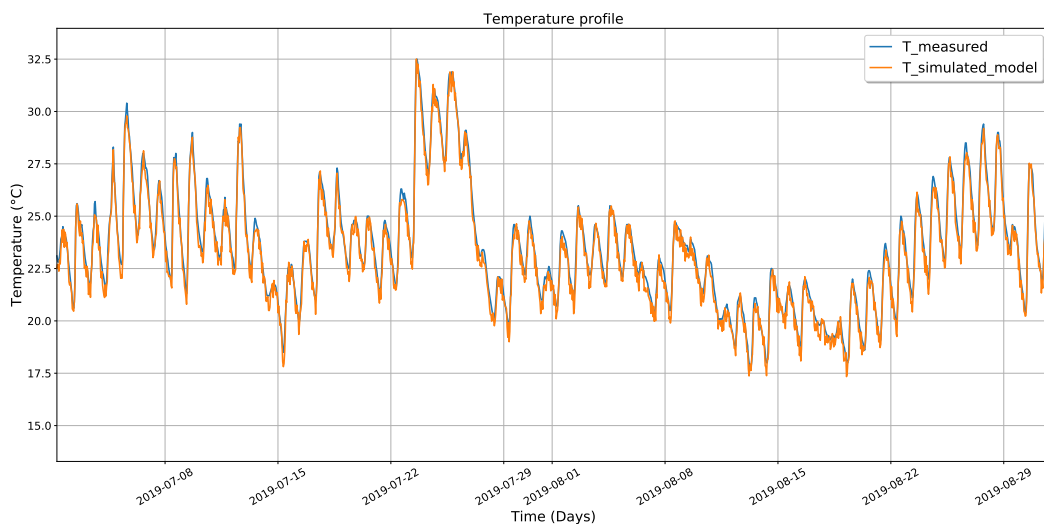


FIGURE 5.5: Validation of simplified thermal network model with measured zone temperature data (summer).

the raise in indoor temperature reaching almost 30°C is due to non-operation of the HVAC system during holidays. The HVAC systems are scheduled to operate only during the office hours. The comparison between the winter and summer model show that the occupancy activities does have high influence in the properly insulated buildings.

We observed that there is maximum of $\pm 2^{\circ}\text{C}$ difference between the predicted and the measured temperature data. However, the RMSE error for summer period is $\approx 0.6^{\circ}\text{C}$. This indicates the better fitting of our model with optimized parameter values.

Similarly, for both summer and winter simulations, we have analyzed model performance with different error methods (given in Table 5.4).

TABLE 5.4: Model performance evaluation for summer and winter simulations.

Season	MAE ($^{\circ}\text{C}$)	RMSE ($^{\circ}\text{C}$)	MAPE (%)	sMAPE (%)
Summer	0.52	0.61	4.71	5.37
Winter	0.59	0.69	6.53	5.84

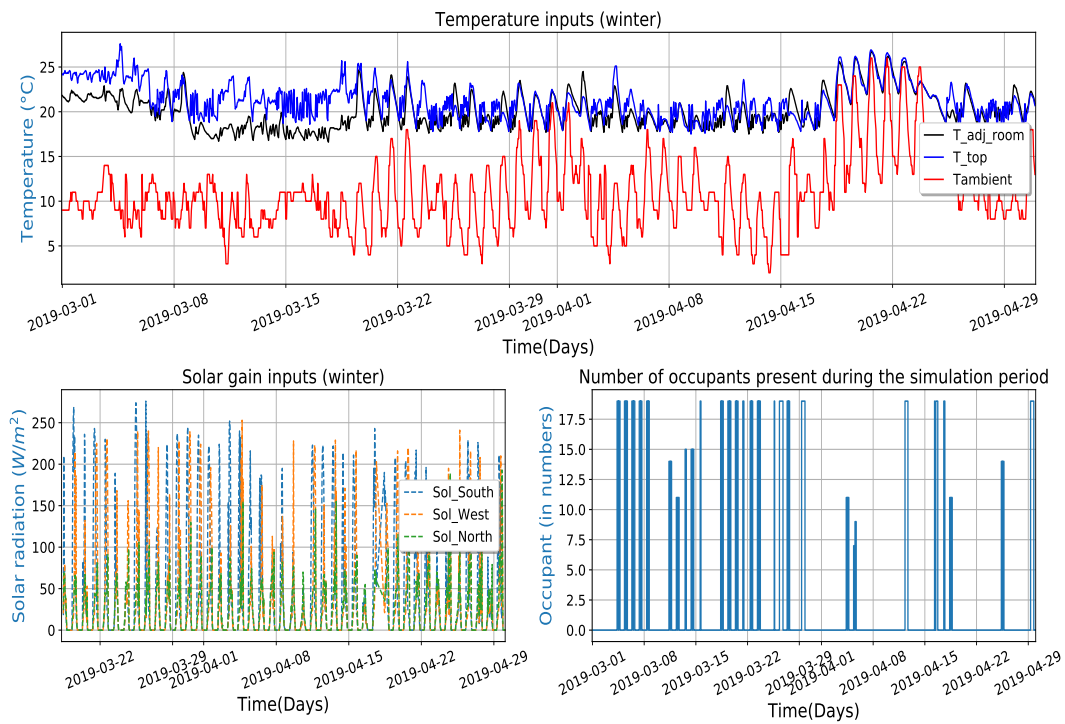


FIGURE 5.6: Measured inputs of the model: ambient and adjacent zones temperatures, solar irradiation, and occupant numbers (winter).

Measurable but uncontrollable inputs for the system: outdoor dry bulb, adjacent room, and top floor room temperatures, occupancy presence, solar irradiation (using HDKR model), internal gains, and heat from HVAC system. Figure 5.6 represents some of these inputs used for our simulation. However, in Figure 5.7 we have shown two inputs because for most of the time HVAC system was turned off and occupancy were not present at the building. Nevertheless, in both seasons the model reproduces the dynamics of zone temperature of the building efficiently. The results show that the simplified thermal network model with parameter identification is well-suited approach to model the building thermal dynamics, and the models can be used for the controller purpose.

5.4. Conclusion

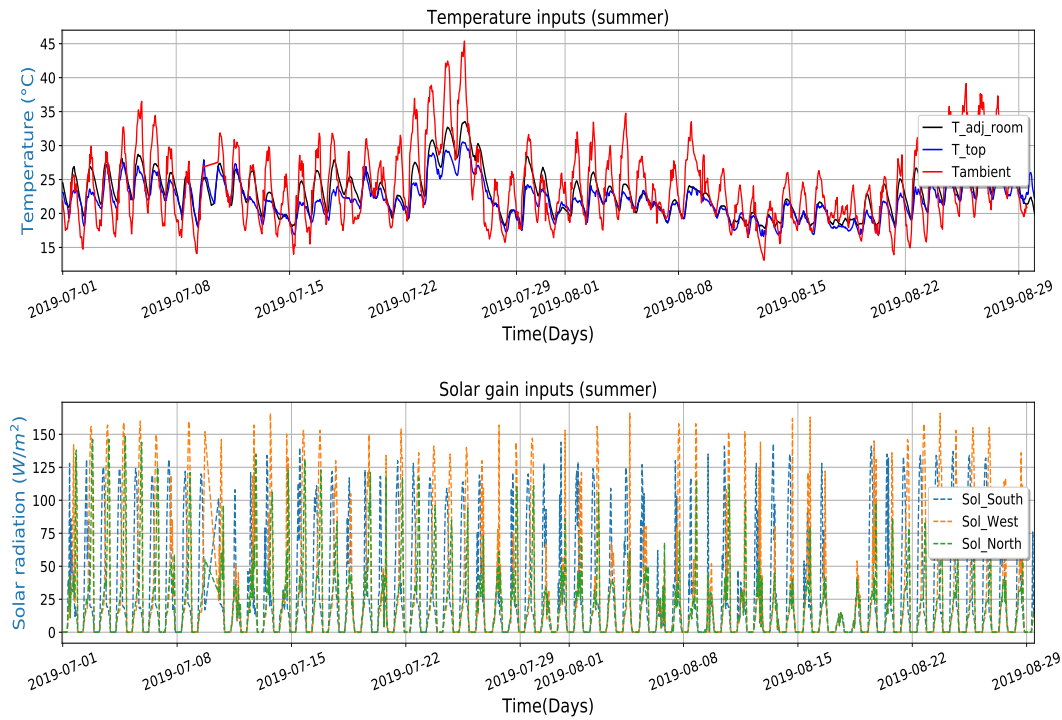


FIGURE 5.7: Measured inputs of the model: ambient and adjacent zones temperatures, and solar irradiation (summer).

5.4 Conclusion

The objective of this chapter was to present development of thermal network model for whole building. Building elements were represented using 3R2C thermal network that we have simplified and validated in the previous chapters. Model thermal parameters resistor and capacitor values are determined using the method proposed in the previous chapter using constrained PSO.

In this chapter, we have presented model development for the case-study building. We have developed the input models that are essential in increasing the model performance accuracy. The model has 13 set of first order ODE's, which are represented using the state-space representation. We have divided our inputs as controllable and uncontrollable but measurable inputs. In general, the solar irradiation measured using Pyrometer is the horizontal diffused solar radiation, we have noticed that these values are underestimation of the actual solar irradiance value. Thus, we incorporated HDKR model with complex anisotropic sky conditions to have better estimation of the solar irradiation on the vertical wall. The results show that using this method we can estimate around 10% 15% better than the isotropic sky model and measured global horizontal radiation.

We have developed the model and validated with the data of case study building. The model validation result has shown a second order thermal network model produce exact thermal behavior with a better accuracy. In this study, we observed that the presence of occupants and their activities has significant influence on the thermal performance of building. When occupants were present in the case study room, there was high variations in the predicted temperature profile, however, when the same room is simulated without occupants has shown much less variations. We evaluated our model performance using different evaluation methods. The model RMSE error is around 0.6 °C for summer and 0.7 °C for winter. Furthermore, sMAPE shows that error between predicted and measured data is around 5%, which is under the acceptable range.

The presented method is applied for model development of one zone, however the same can be applied for multi-zonal model development.

Chapter 6

Model Predictive Control (MPC)

6.1 Model Predictive Controller

Model Predictive Control (MPC) produces a sequence of controller variable input strategy by using a system model to optimize an objective function (minimizing energy consumption) of system model behavior based on a quadratic performance objective, subject to equality or inequality constraints on states, inputs, and outputs over a future time horizon.

The classical objective function for the MPC has the following quadratic formulation:

$$J(t_k) = \sum_{j=N_1}^{N_p} \delta(j) [\hat{y}(t_k + j) - y^{sp}(t_k + j)]^2 + \sum_{j=1}^{N_c} \lambda(j) [u(t_k + j) - u(t_k + j - 1)]^2 \quad (6.1)$$

s.t.

$$X_{t+k+1|t} = AX_{t+k|t} + Bu_{t+k|t} + B_1d_{t+k|t} \quad (6.2)$$

$$Mu \leq \gamma \quad (6.3)$$

where, \hat{y} and y^{sp} are the predicted output and set-point temperatures, respectively. u is the control variable. In this model the control variable is $(\dot{m}_{fa}(t_k)c_a[T_{sp}(t_k) - 1/2(T_z(t_k) + T_0(t_k))])$, the input air flow is controlled through MPC while satisfying the constraints matrix M . However, the objective function tracks only the set-point (y^{sp}) temperature, which forces the building controllers to reach single set point temperature, and curtails the optimal control strategy, leading to a poor energy optimization. Hence, adding slack variables to the set-point variables gives extra freedom of controllability in the MPC. Slack variables are useful in making the output variable to keep within a certain range by penalizing for any violation in the range [169].

The new proposed formulation is given as follows:

$$\min \sum_{j=0}^{N_p-1} \left| \dot{m}_{fa}(t_j) c_a [T_{sp}(t_j) - \frac{(T_z(t_j) + T_0(t_j))}{2}] \right| + \beta(|s_j| + |s_j|) \quad (6.4)$$

s.t.

$$X_{t+j+1|t} = AX_{t+j|t} + Bu_{t+j|t} + B_1 d_{t+j|t} \quad (6.5)$$

$$Mu \leq \gamma \quad (6.6)$$

$$T_{lb} - s_{lb,t+j|t} \leq T_{zone,t+j|t} \leq T_{ub,t+j|t} + s_{ub,t+j|t} \quad (6.7)$$

$$s_{lb,t+j|t} \& s_{ub,t+j|t} \geq 0 \quad (6.8)$$

where, β is penalty factor, s is slack variable, T_{sp} is the temperature of the supply air from the ducts to room, T_z is zone temperature, T_{lb} and T_{ub} are lower and upper values of temperature, respectively. Similarly, the inequality constraints are applied to the input and rate of change inputs.

In order to solve the objective function (10), the state-space model needs to be represented in the predictive model form [170]:

$$\hat{y} = Fx(k) + \phi_1 u + \phi_2 d \quad (6.9)$$

where,

$$F = \begin{bmatrix} CA \\ CA^2 \\ CA^3 \\ \vdots \\ \vdots \\ CA^{N_p} \end{bmatrix} \quad \phi_1 = \begin{bmatrix} CB & 0 & \dots & 0 \\ CAB & CB & \dots & 0 \\ CA^2 B & CAB & \dots & 0 \\ \vdots & \vdots & \dots & \vdots \\ \vdots & \vdots & \dots & \vdots \\ CA^{N_p-1} B & CA^{N_p-2} B & \dots & CAB \end{bmatrix}$$

$$\phi_2 = \begin{bmatrix} CB_1 & 0 & \dots & 0 \\ CAB_1 & CB_1 & \dots & 0 \\ CA^2 B_1 & CAB_1 & \dots & 0 \\ \vdots & \vdots & \dots & \vdots \\ \vdots & \vdots & \dots & \vdots \\ CA^{N_p-1} B_1 & CA^{N_p-2} B_1 & \dots & CAB_1 \end{bmatrix}$$

$$\hat{y} = \left[\hat{y}^T(k+1) \quad \hat{y}^T(k+2) \quad \dots \quad \hat{y}^T(k+N_p) \right]^T$$

$$u = \left[u^T(k+1) \quad u^T(k+2) \quad \dots \quad u^T(k+N_p-1) \right]^T$$

$$d = \left[d^T(k+1) \quad d^T(k+2) \quad \dots \quad d^T(k+N_p-1) \right]^T$$

The matrices F , ϕ_1 , and ϕ_2 are constants of the system model. Hence, these are computed only once, thus reducing the computational cost for every control time step. Therefore, the formulated objective function (10) with constraints are solved in the MPC framework. For MPC simulation, the Python programming language is used with CVXOPT [171] solvers for minimizing the cost function.

6.1.1 Linearization of Thermal Network Model

Furthermore, in the most cases the radiative heat transfer between walls is neglected or taken as constant after linearizing it to near equilibrium point [172]. The developed model induces non-linearities due to the radiative heat transfer (6) between the walls.

$$\dot{Q}_{rad} = \epsilon \sigma (T_{hot}^4 - T_{cold}^4) \quad (6.10)$$

where,

ϵ = surface emissivity of the material,

σ = Stefan-Boltzmann constant,

T = wall surface temperatures in Kelvin degrees.

Since, the temperature difference between walls is low and the temperature relationship is in absolute temperature in (6), thus the temperature difference between walls are relatively small as compared to absolute temperature value. Hence, the radiative heat transfer coefficient is considered to be a constant value by linearizing it using the Taylor's series expansion.

Furthermore, from the model dynamics in the previous chapter in equation 5.17 the control input m is multiplied by the state X_i , which makes the dynamics of the system non-linear. However, we have split our input vector into controllable and disturbance inputs, therefore the non-linear term is present only in the controllable vector. With this, we reduce the complexity of linearization process by only applying on controllable input and the state vector. There are some techniques such as feedback linearization including input/output Linearization or Input/State Linearization techniques, which

can be used to deal with the non-linearities of the system. However, these linearization techniques produce highly complicated mathematical model when applied to high order systems. This may lead to increase in the system complexity.

Furthermore, the conventional techniques like Jacobian linearization has proven to be efficient when the system has small range of variation. Jacobian linearization is method used to linearize non-linear systems at the equilibrium points. Since building has small range of temperatures, we chose to linearize our model using Jacobian technique (Appendix A.2 [173]).

To use this strategy, we must first determine the system's equilibrium points. Fixing the input, \bar{u} , and then solving for \bar{x} produces the equilibrium positions of the states. There are infinite equilibrium points in the system that may be reached by assuming various equilibrium inputs. However, in the context of buildings, we have only few equilibrium points around that the building normally operates. Setting the temperature of the room to the set-point temperature specified by the occupants (building users), and then solving for the equilibrium temperature of the walls and the equilibrium inputs, produces the equilibrium point. The equilibrium point is achieved only by setting the non-linear differential state equation equal to zero. In our case, we have considered equilibrium point near the set-point $T_{setpoint} = 25$ °C. By solving the equation we find the equilibrium points to be

$$X_{ke} = \begin{bmatrix} T_{s1,12} \\ T_{s2,12} \\ T_{s1,13} \\ T_{s2,13} \\ T_{s1,14} \\ T_{s2,14} \\ T_{s1,15} \\ T_{s2,15} \\ T_{s1,16} \\ T_{s2,16} \\ T_{s1,17} \\ T_{s2,17} \\ T_z \end{bmatrix} = \begin{bmatrix} 0.0029 \\ 1.75 \times 10^{-5} \\ 0.0083 \\ 1.16 \times 10^{-5} \\ 0.00055 \\ 7.683 \times 10^{-5} \\ 0.00055 \\ 7.683 \times 10^{-5} \\ 7.64 \times 10^{-4} \\ 2.606 \times 10^{-4} \\ 7.64 \times 10^{-4} \\ 2.606 \times 10^{-4} \\ 22.03 \end{bmatrix} \quad u_{ke} = [0.0036]$$

Now we can find the linearized system by evaluating the matrices A and B from state space equation. We have validated the linearized model with the measured values of the case-study building. The model is validated for 6 days in February as it is one of the coldest months in Nanterre.

Figure 6.1a and 6.1b shows the temperature profile of the classroom where the system non-linear model quite accurately follows the building thermal dynamics. On the other hand, the linearized model is also closely following the dynamics of the system, but slightly less accurately. It should be taken into account that the non-linear model computational cost is higher than the linearized one, while the error between the two models is low. In this case, the linearized model is considered acceptable and therefore adopted.

The interesting observation is that the first peak of disturbance load does not cause as much temperature increase in the room as opposed to the second disturbance peak. The reason is that in the morning the walls which represent the slow-dynamic masses in the system are cold due to low temperature at night. Therefore, part of the heating load, earlier in the day, goes toward warming up the slow-dynamic thermal masses in the building (e.g. walls and furniture). However, in the afternoon the slow-dynamic thermal masses absorb heat at a slower rate and therefore, cause faster increase to the temperature of the fast-dynamic thermal mass of the system, which is the air in the room.

6.1.2 Simulation Results

To demonstrate the optimal control strategy of the MPC for multi-objective control within given constraints, a comparison is performed between the MPC and conventional controller for building temperature control in the presence of measurable disturbances.

The simulations are carried out for 6 days (01/02/2019 to 07/02/2019) to calculate the energy consumption during heating season. The MPC implementations are performed with hourly time step for prediction horizon of one day. The lower and upper limits for zone temperature is set to 19°C and 23°C, respectively.

The conventional controller does not predict the future control strategies as compare to MPC controller, it works based on the current state of the system. On the contrary, MPC controller predicts the future control strategies, while satisfying the given constraints.

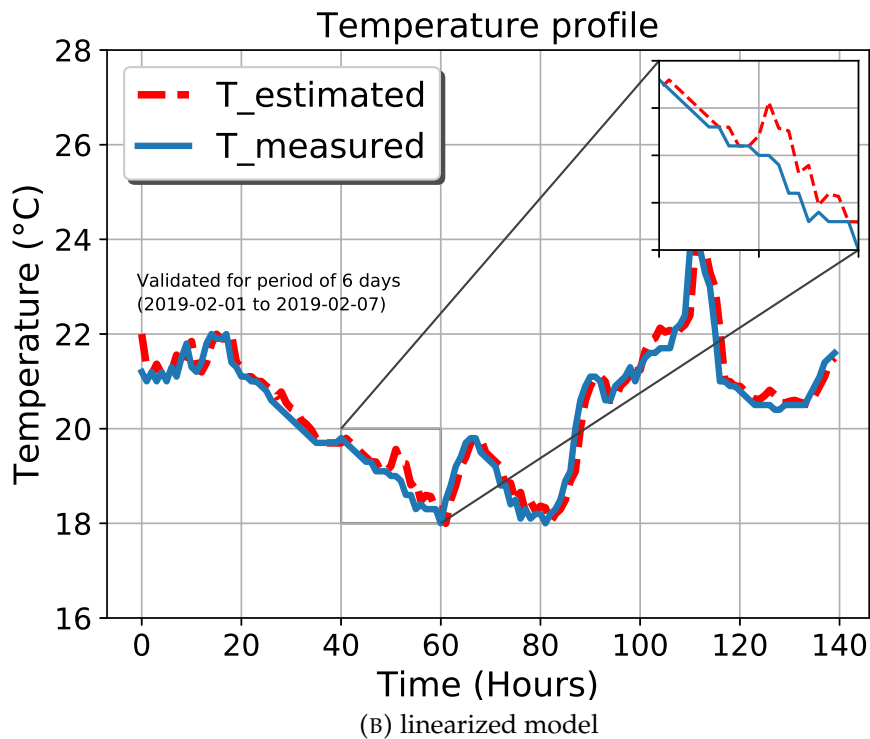
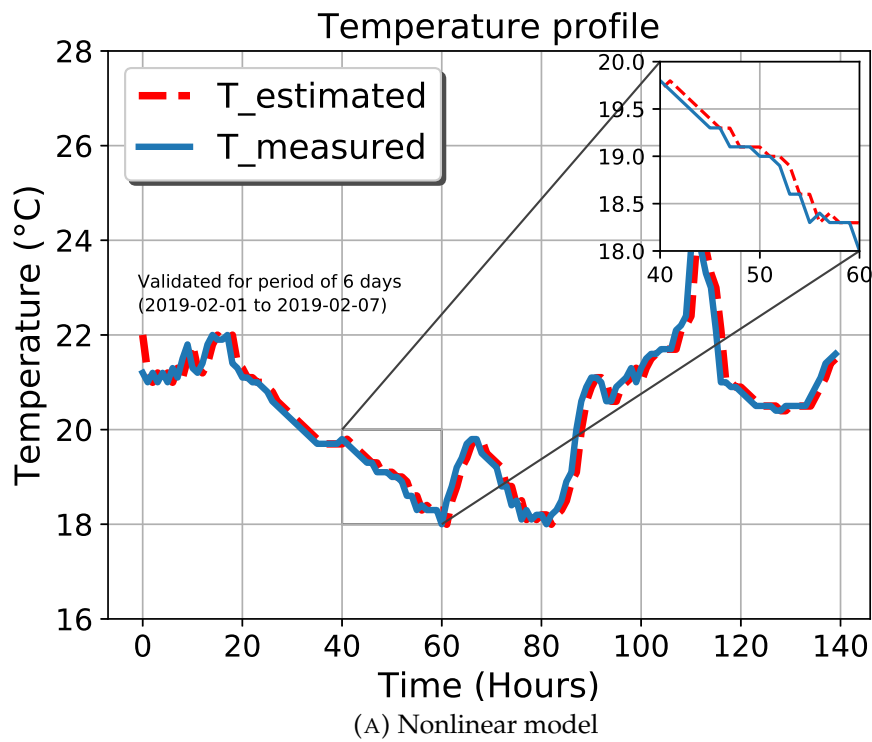


FIGURE 6.1: Validation of developed model against the measured room temperature.

The results are shown in Figure 6.2, it can be noticed that the temperature

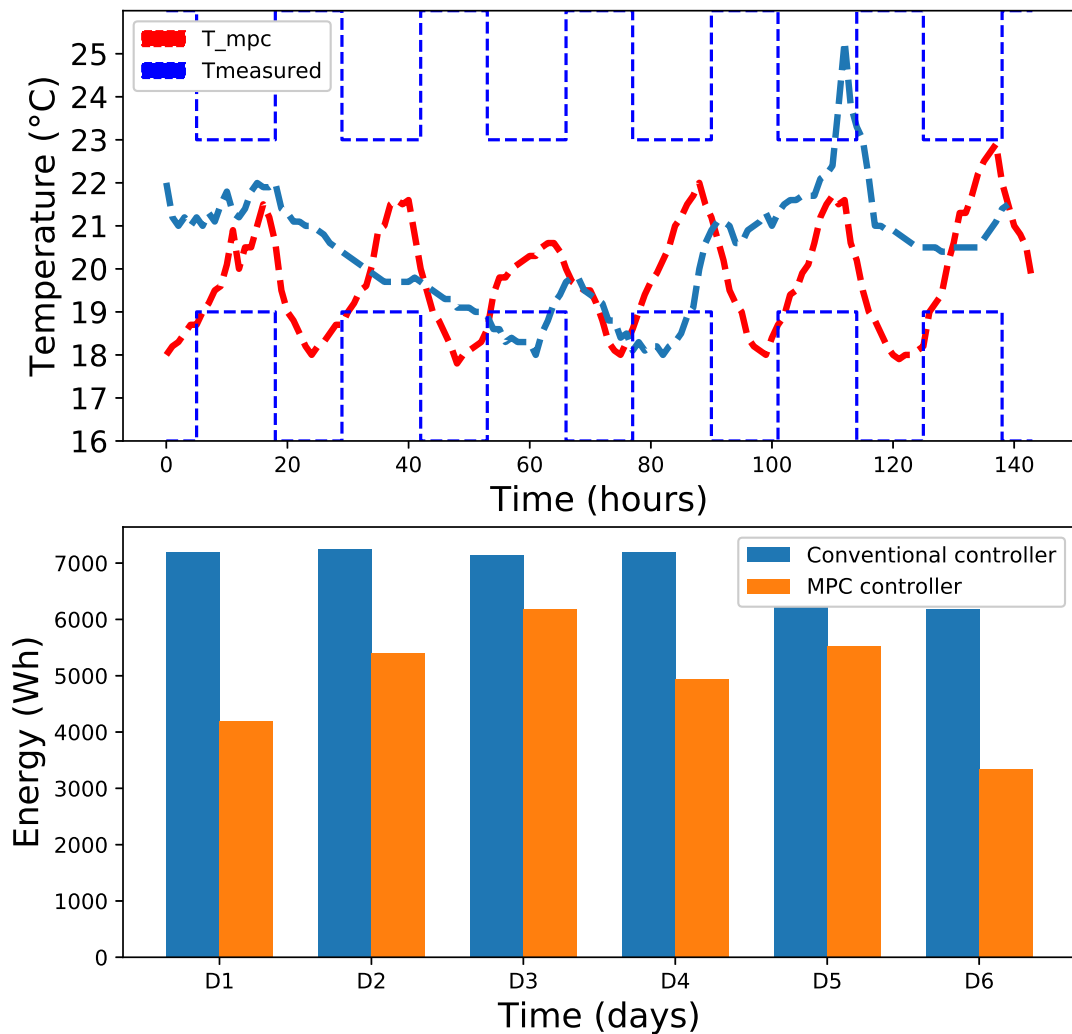


FIGURE 6.2: Comparison of results of the MPC and conventional controller.

profile of MPC controller based model clearly satisfies the objective of meeting comfort criteria, while the conventional controller violates the standard indoor temperature range. As per the characteristic of MPC it's more reactive and it can be seen in the results that temperature is forced to reach around 21°C - 22°C in order to not to violate the set temperature boundaries. The ventilation airflow is controlled optimally and efficiently. However, due to hard constraints implied on the MPC such as the system operating timings, initial stage temperature control always took more time to reach set temperature range.

6.1. Model Predictive Controller

The multi-objective control, and considerations of measurable disturbances of MPC has shown good control strategy, but the conventional controller without having consideration of disturbances, supplied heat energy even though the zone temperature reached the upper limit, it shows poor performance of the conventional controller. The measurable inputs for the system are shown in Figure 6.3. The conventional controller is a rule-based controller and it works based on the occupancy presence detection. Furthermore, the airflow is always constant irrespective of the heat load requirements.

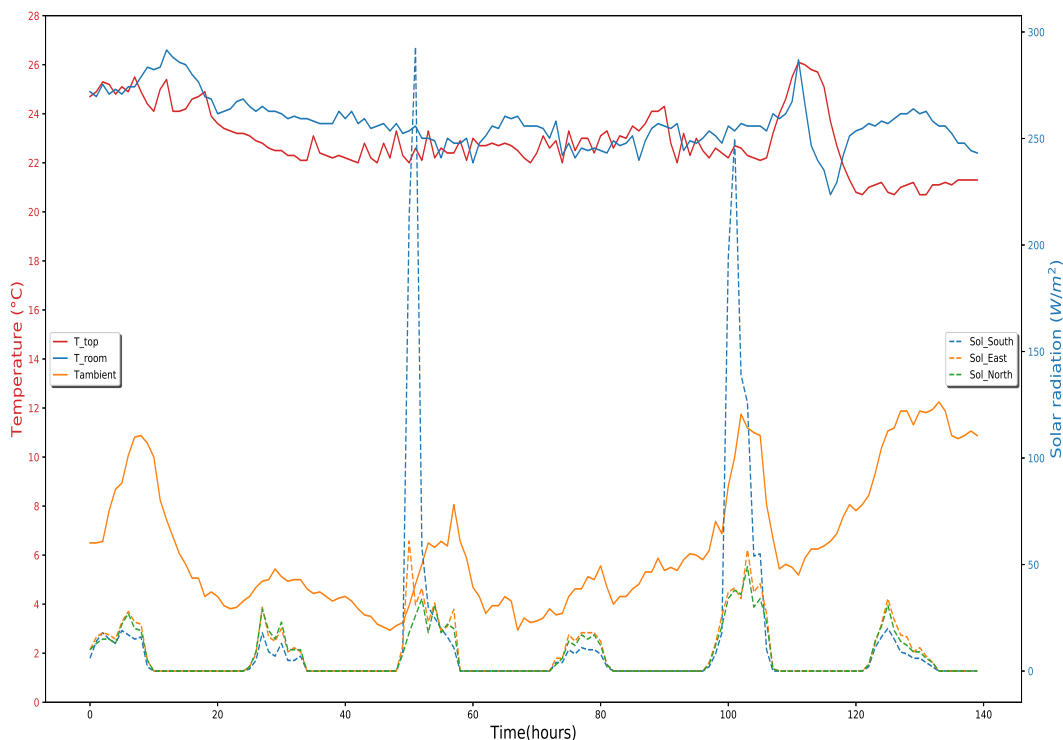


FIGURE 6.3: Measurable disturbances of the system: solar radiation, adjacent rooms temperature, and ambient temperature.

From Figure 6.2, we have analyzed that by applying MPC controller we can reduce significant amount of energy consumed by the HVAC system. The estimated energy consumption required to for maintaining thermal comfort is estimated for a 6-day period. The energy consumed by the conventional controller is almost equal all days due to the operating schedule and not integrating dynamic operation. Whereas, HVAC controlled from MPC has consumed more energy when the outside temperature is low. The first and fifth day outside temperatures were high in those six days. This influenced in the room peak temperature of first and fifth day. The conventional controlled has not considered this effect while MPC has considered this influence thus reducing the energy consumption in both the days. The cumulative energy

for the conventional controller control is 42.23 kWh, while it is 29.55 kWh for the MPC one, resulting in almost 31% reduction in energy consumption.

6.2 Conclusion

In this chapter, we have presented the MPC general formulation, controller developments, and system model linearization. A building model that developed in the previous chapter had a non-linearity for controlling ventilation airflow. We have linearized it using Jacobian linearization approach. The linearized model is then validated against the measured data, the results of linearized model is within the acceptable range of accuracy, and thus it was used to implement a controller.

A simple MPC model is implemented for indoor thermal comfort control. The MPC has shown the ability to multi-objective control under given constraints, the average indoor temperature is always maintained within the lower and upper limits.

The energy consumption of the HVAC system for thermal comfort management during the 6 days was performed. The results indicate that the MPC system produces optimal control strategy, and offering reduced energy consumption in comparison, while the conventional controller is seen to be wasting energy and performing poorly. The presented MPC application has shown almost 31% of energy saving compared to the conventional controller. Indeed, it has reduced system states number, it is computationally efficient, and can be adapted to any type of buildings.

Chapter 7

Conclusions and perspectives

Conclusions

The aim this dissertation was to investigate the different modeling techniques for developing a model-based controller and to analyze the models that can be used for retrofitting buildings in the case of lack of availability of data. This work presented various modeling methods for building dynamic modeling, factors that influence the performance of buildings. It was observed from the simulations results that the occupants' number and activities has high influence in well-insulated buildings.

The energy consumption from the buildings is very high and the occupants spend almost 90% of their life in closed environment, such as residential building, commercial buildings, and industrial buildings. Hence, management of indoor comfort has huge impact on the occupant's health and productivity. These two objectives are to be achieved through implementing intelligent controllers. The controllers, which are implemented, should be able to handle multi-objectives. We have properly reviewed different techniques that are used for modeling and controlling purposes. Mainly three techniques are reviewed critically and have been compared for their suitability, adaptability, and for various application scenarios. This give the insights on the controllers and modeling methods.

Most of the well-established intelligent controller's performance efficiency depends on accuracy and computational efficiency of the building model. The building model should replicate dynamics of the heat transfer in building, able to predict zone heat loads/air temperatures as a function of controllable (HVAC systems) and uncontrollable measurable inputs (weather, internal heat gains, solar gains, etc.), and simplified enough to connect to optimization techniques.

The well-established software tools are not suitable for quick reactive controller applications and another method data-driven models need handful amount of data to train the model, hence gray box models are well suited for controller applications where there is lack of availability of data. The gray box model lumped parameter thermal network models have proven to be feasible for dynamic thermal response simulation of buildings. These models produce acceptable accuracy results with superior computational efficiency over other models. Accordingly, this work greatly focused on the building thermal dynamic modeling, which are the essential part of above mentioned controller application.

In the chapter 2, we presented simplified thermal modeling technique particularly for retrofitting buildings. We compared different thermal network configurations and from results we noticed that 3R2C models have high accuracy and are computationally efficient. It was observed that the parameter values have most significant impact on efficiency of 2nd order 3R2C thermal network model. The method proposed in this work successfully considers constraints and searches for global optimal solution for identifying the parameters value. The constrained PSO is better than conventional optimization techniques because of its diverse search space and convergence rate to solution.

The proposed method was applied on various types of building envelope types and validated the model against the reference model. This method provides a significant approximation of the parameters when compared to the reference model whilst allowing low-order model to achieve 40% to 50% computational efficiency than the reference one. In the chapter 3, the proposed method was validated with the measured data. Furthermore, we have proposed a well-established but complex solar model for modeling solar gains. The conventional isotropic model is straightforward and calculation of radiation on tilted surfaces becomes simple. However, it fails to take account of circumsolar diffuse and/or horizon brightening components on an inclined surface, this results in the underestimation of solar radiation (around 10 to 15%). Furthermore, we made an attempt to model ASHP-VRF systems, we simulated our model for two rooms and compared it with the measured values of the real building. The model has shown good fitting with the measured values, however authors believe that there needs to be further research on the modeling.

In general, proposed method is simple, accurate, and adaptable to all type building modeling. The developed model can be well implement for the MPC controller applications, we have presented a simple MPC that is applied for thermal comfort optimization based on the developed model for the case study building. MPC model implemented in the building for one week has shown promising results of almost 31% energy savings as compared to the conventional control system installed in the building. The developed 3R2C network model is well suited for model-based controller application. Indeed, it has reduced system states number, it is computationally efficient, and can be adapted to any type of buildings.

Future Perspectives

This work presents an alternative approach for simplified model development for building design. Despite the models have been validated for various types of construction elements, there is still need more concrete verification and the methods needs to be examined before directly applying to the other buildings.

The simplified model is applied for only single zone with the different building envelope materials for each side. The modeling approach proposed in this paper will be further extended to model multi-zone buildings, considering inter-zonal heat transfer. Furthermore, it will be used to predict other comfort parameters such as humidity.

The HVAC systems of the building to be modeled to predict the energy behavior with inclusion of electrical appliances and radiators model as well. This will be interesting for residential and commercial buildings. Authors strongly believe that there is a need of further research on ASHP-VRF model to validate it with more indoor units and for longer duration.

Integrating occupancy model to the controller model to efficiently manage comfort condition. Analysis of their behavior and study on prediction model of number of occupants present in the building. A more advanced MPC controlled to be applied for building for longer simulation period.

Finally, consideration of integrating BIM and building model. The data from BIM model used for building performance simulation, analysis of their interoperability, limitations, and operational benefits.

References

- [1] *Communication from the commission to the European parliament, the council, the European economic and social committee and the committee of the regions.* The European Commission, 2011.
- [2] "The European Energy Efficiency Commission," 2018.
- [3] "Final Energy Consumption in households - EU27 - 2018 -Environment and energy," 2018.
- [4] "Building energy performance metrics, supporting energy efficiency progress in major economies," tech. rep., 2015.
- [5] "IEA energy technology perspectives," tech. rep., 2015.
- [6] F. M. Vieira, P. S. Moura, and A. T. de Almeida, "Energy storage system for self-consumption of photovoltaic energy in residential zero energy buildings," *Renewable Energy*, vol. 103, pp. 308–320, Apr. 2017.
- [7] D. Minoli, K. Sohraby, and B. Occhiogrosso, "IoT Considerations, Requirements, and Architectures for Smart Buildings – Energy Optimization and Next Generation Building Management Systems," *IEEE Internet of Things Journal*, pp. 1–1, 2017.
- [8] B. Todorovic, "Towards zero energy buildings: New and retrofitted existing buildings," in *2011 IEEE 3rd International Symposium on Exploitation of Renewable Energy Sources (EXPRES)*, pp. 7–14, IEEE, 2011.
- [9] M. Manic, D. Wijayasekara, K. Amarasinghe, and J. J. Rodriguez-Andina, "Building energy management systems: The age of intelligent and adaptive buildings," *IEEE Industrial Electronics Magazine*, vol. 10, no. 1, pp. 25–39, 2016.
- [10] T. H. Pedersen, R. E. Hedegaard, and S. Petersen, "Space heating demand response potential of retrofitted residential apartment blocks," *Energy and Buildings*, vol. 141, pp. 158–166, 2017.
- [11] Y. Ma, F. Borrelli, B. Hancey, B. Coffey, S. Benghea, and P. Haves, "Model predictive control for the operation of building cooling systems," *IEEE Transactions on control systems technology*, vol. 20, no. 3, pp. 796–803, 2011.
- [12] G. Mantovani and L. Ferrarini, "Temperature control of a commercial building with model predictive control techniques," *IEEE Transactions on Industrial Electronics*, vol. 62, no. 4, pp. 2651–2660, 2014.
- [13] R. Missaoui, H. Joumaa, S. Ploix, and S. Bacha, "Managing energy smart homes according to energy prices: analysis of a building energy management system," *Energy and Buildings*, vol. 71, pp. 155–167, 2014.
- [14] D. Sant'Anna, P. Dos Santos, N. Vianna, and M. Romero, "Indoor environmental quality perception and users' satisfaction of conventional

- and green buildings in Brazil," *Sustainable Cities and Society*, vol. 43, pp. 95–110, Nov. 2018.
- [15] Caniato and Gasparella, "Discriminating People's Attitude towards Building Physical Features in Sustainable and Conventional Buildings," *Energies*, vol. 12, p. 1429, Apr. 2019.
- [16] A. Leaman and B. Bordass, "Are users more tolerant of 'green' buildings?," *Building Research & Information*, vol. 35, pp. 662–673, Nov. 2007.
- [17] R. V. Andersen, J. Toftum, K. K. Andersen, and B. W. Olesen, "Survey of occupant behaviour and control of indoor environment in Danish dwellings," *Energy and Buildings*, vol. 41, pp. 11–16, Jan. 2009.
- [18] O. Masoso and L. Grobler, "The dark side of occupants' behaviour on building energy use," *Energy and Buildings*, vol. 42, pp. 173–177, Feb. 2010.
- [19] A. Boodi, K. Beddiar, Y. Amirat, and M. Benbouzid, "Model Predictive Control-based Thermal Comfort and Energy Optimization," in *IECON 2019-45th Annual Conference of the IEEE Industrial Electronics Society*, vol. 1, pp. 5801–5806, IEEE, 2019.
- [20] M. Killian and M. Kozek, "Ten questions concerning model predictive control for energy efficient buildings," *Building and Environment*, vol. 105, pp. 403–412, 2016.
- [21] A. Boodi, K. Beddiar, M. Benamour, Y. Amirat, and M. Benbouzid, "Intelligent systems for building energy and occupant comfort optimization: A state of the art review and recommendations," *Energies*, vol. 11, no. 10, p. 2604, 2018.
- [22] Y. Yao and Y. Yu, *Modeling and Control in Air-Conditioning Systems*. Springer, 2017.
- [23] A. F. Handbook, "American society of heating, refrigerating and air-conditioning engineers," *Inc.: Atlanta, GA, USA*, 2017.
- [24] P. Bacher and H. Madsen, "Identifying suitable models for the heat dynamics of buildings," *Energy and Buildings*, vol. 43, pp. 1511–1522, July 2011.
- [25] Z. Yu, B. C. Fung, F. Haghghat, H. Yoshino, and E. Morofsky, "A systematic procedure to study the influence of occupant behavior on building energy consumption," *Energy and Buildings*, vol. 43, pp. 1409–1417, June 2011.
- [26] P. Rocha, A. Siddiqui, and M. Stadler, "Improving energy efficiency via smart building energy management systems: A comparison with policy measures," *Energy and Buildings*, vol. 88, pp. 203–213, Feb. 2015.
- [27] M. S. Gul and S. Patidar, "Understanding the energy consumption and occupancy of a multi-purpose academic building," *Energy and Buildings*, vol. 87, pp. 155–165, Jan. 2015.
- [28] P. H. Shaikh, N. M. Nor, P. Nallagownden, I. Elamvazuthi, and T. Ibrahim, "Robust stochastic control model for energy and comfort management of buildings," *Australian Journal of Basic and Applied Sciences*, vol. 7, no. 10, pp. 137–144, 2013.

- [29] S. Carlucci, G. Cattarin, F. Causone, and L. Pagliano, "Multi-objective optimization of a nearly zero-energy building based on thermal and visual discomfort minimization using a non-dominated sorting genetic algorithm (NSGA-II)," *Energy and Buildings*, vol. 104, pp. 378–394, Oct. 2015.
- [30] D. L. Ha, F. F. de Lamotte, and Q. H. Huynh, "Real-time dynamic multilevel optimization for demand-side load management," in *2007 IEEE international conference on industrial engineering and engineering management*, pp. 945–949, IEEE, 2007.
- [31] H. Asan and Y. Sancaktar, "Effects of wall's thermophysical properties on time lag and decrement factor," *energy and buildings*, vol. 28, no. 2, pp. 159–166, 1998.
- [32] K. J. Moss, *Heat and mass transfer in buildings*. Routledge, 2015.
- [33] C. Underwood and F. Yik, *Modelling methods for energy in buildings*. John Wiley & Sons, 2008.
- [34] X. Berisha and B. Dragusha, "The influence of the outside temperature during the design of a heating system," in *International Conference & Workshop REMOO-2015, Budva*, 2015.
- [35] P. W. O'Callaghan and S. D. Probert, "Sol-air temperature," *Applied Energy*, vol. 3, no. 4, pp. 307–311, 1977.
- [36] K. A. Al-Saud, "Measured versus calculated roof peak sol-air temperature in hot-arid regions," *Red*, vol. 29, p. 95, 2009.
- [37] H. Zhang, *Building Materials in Civil Engineering*. Elsevier, 2011.
- [38] M. S. Al-Homoud, "Computer-aided building energy analysis techniques," *Building and Environment*, vol. 36, no. 4, pp. 421–433, 2001.
- [39] F. Amara, K. Agbossou, A. Cardenas, Y. Dubé, S. Kelouwani, *et al.*, "Comparison and simulation of building thermal models for effective energy management," *Smart Grid and renewable energy*, vol. 6, no. 04, p. 95, 2015.
- [40] Y. Kwak, J.-H. Huh, and C. Jang, "Development of a model predictive control framework through real-time building energy management system data," *Applied Energy*, vol. 155, pp. 1–13, Oct. 2015.
- [41] M. Maasoumy, C. Rosenberg, A. Sangiovanni-Vincentelli, and D. S. Callaway, "Model predictive control approach to online computation of demand-side flexibility of commercial buildings HVAC systems for Supply Following," (Portland, OR, USA), pp. 1082–1089, IEEE, June 2014.
- [42] "EnergyPlus Documentation," tech. rep.
- [43] S. A. Klein, "TRNSYS-A transient system simulation program," *University of Wisconsin-Madison, Engineering Experiment Station Report*, pp. 38–12, 1988.
- [44] J. J. Hirsch, "eQuest, the QUick energy simulation tool," *DOE2 Com, epub*, <http://www.doe2.com/equest>, 2006.

- [45] M. Farrokhifar, F. Momayyezi, N. Sadoogi, and A. Safari, "Real-time based approach for intelligent building energy management using dynamic price policies," *Sustainable Cities and Society*, vol. 37, pp. 85–92, Feb. 2018.
- [46] W. Kim, Y. Jeon, and Y. Kim, "Simulation-based optimization of an integrated daylighting and HVAC system using the design of experiments method," *Applied Energy*, vol. 162, pp. 666–674, Jan. 2016.
- [47] J. Liu, W. Zhang, X. Chu, and Y. Liu, "Fuzzy logic controller for energy savings in a smart LED lighting system considering lighting comfort and daylight," *Energy and Buildings*, vol. 127, pp. 95–104, Sept. 2016.
- [48] N. Delgarm, B. Sajadi, F. Kowsary, and S. Delgarm, "Multi-objective optimization of the building energy performance: A simulation-based approach by means of particle swarm optimization (PSO)," *Applied Energy*, vol. 170, pp. 293–303, May 2016.
- [49] F. Ascione, N. Bianco, C. De Stasio, G. M. Mauro, and G. P. Vanoli, "Artificial neural networks to predict energy performance and retrofit scenarios for any member of a building category: A novel approach," *Energy*, vol. 118, pp. 999–1017, Jan. 2017.
- [50] K. Li, C. Hu, G. Liu, and W. Xue, "Building's electricity consumption prediction using optimized artificial neural networks and principal component analysis," *Energy and Buildings*, vol. 108, pp. 106–113, Dec. 2015.
- [51] R. Platon, V. R. Dehkordi, and J. Martel, "Hourly prediction of a building's electricity consumption using case-based reasoning, artificial neural networks and principal component analysis," *Energy and Buildings*, vol. 92, pp. 10–18, Apr. 2015.
- [52] J. von Grabe, "Potential of artificial neural networks to predict thermal sensation votes," *Applied Energy*, vol. 161, pp. 412–424, Jan. 2016.
- [53] M. Macarulla, M. Casals, N. Forcada, and M. Gangolells, "Implementation of predictive control in a commercial building energy management system using neural networks," *Energy and Buildings*, vol. 151, pp. 511–519, Sept. 2017.
- [54] J. W. Moon and S. K. Jung, "Development of a thermal control algorithm using artificial neural network models for improved thermal comfort and energy efficiency in accommodation buildings," *Applied Thermal Engineering*, vol. 103, pp. 1135–1144, June 2016.
- [55] S. Naji, A. Keivani, S. Shamshirband, U. J. Alengaram, M. Z. Jumaat, Z. Mansor, and M. Lee, "Estimating building energy consumption using extreme learning machine method," *Energy*, vol. 97, pp. 506–516, Feb. 2016.
- [56] M. Macas, F. Moretti, A. Fonti, A. Giantomassi, G. Comodi, M. Annunziato, S. Pizzuti, and A. Capra, "The role of data sample size and dimensionality in neural network based forecasting of building heating related variables," *Energy and Buildings*, vol. 111, pp. 299–310, Jan. 2016.

- [57] G. Reynders, J. Diriken, and D. Saelens, "Quality of grey-box models and identified parameters as function of the accuracy of input and observation signals," *Energy and Buildings*, vol. 82, pp. 263–274, Oct. 2014.
- [58] N. Li, H. Cui, C. Zhu, X. Zhang, and L. Su, "Grey preference analysis of indoor environmental factors using sub-indexes based on Weber/Fechner's law and predicted mean vote," *Indoor and Built Environment*, vol. 25, pp. 1197–1208, Dec. 2016.
- [59] B. Paris, J. Eynard, S. Grieu, and M. Polit, "Hybrid PID-fuzzy control scheme for managing energy resources in buildings," *Applied Soft Computing*, vol. 11, pp. 5068–5080, Dec. 2011.
- [60] R. Missaoui, H. Joumaa, S. Ploix, and S. Bacha, "Managing energy Smart Homes according to energy prices: Analysis of a Building Energy Management System," *Energy and Buildings*, vol. 71, pp. 155–167, Mar. 2014.
- [61] F. Farmani, M. Parvizmosaed, H. Monsef, and A. Rahimi-Kian, "A conceptual model of a smart energy management system for a residential building equipped with CCHP system," *International Journal of Electrical Power & Energy Systems*, vol. 95, pp. 523–536, Feb. 2018.
- [62] K. Basu, L. Hawarah, N. Arghira, H. Joumaa, and S. Ploix, "A prediction system for home appliance usage," *Energy and Buildings*, vol. 67, pp. 668–679, 2013.
- [63] "Building Energy Software Tools, IBPSA-USA."
- [64] F. C. Winkelmann, B. E. Birdsall, W. F. Buhl, K. L. Ellington, A. E. Erdem, J. J. Hirsch, and S. Gates, "DOE-2 supplement: version 2.1 E," tech. rep., 1993.
- [65] P. Zhao, S. Suryanarayanan, and M. G. Simoes, "An Energy Management System for Building Structures Using a Multi-Agent Decision-Making Control Methodology," *IEEE Transactions on Industry Applications*, vol. 49, pp. 322–330, Jan. 2013.
- [66] R. Baheti and H. Gill, "Cyber-physical systems," *The impact of control technology, IEEE Control Systems Society*, vol. 12, no. 1, pp. 161–166, 2011.
- [67] S. Hussain, H. A. Gabbar, D. Bondarenko, F. Musharavati, and S. Pokharel, "Comfort-based fuzzy control optimization for energy conservation in HVAC systems," *Control Engineering Practice*, vol. 32, pp. 172–182, Nov. 2014.
- [68] P. A. Fritzson, *Principles of object-oriented modeling and simulation with Modelica 2.1*. Piscataway, N.J. : [New York]: IEEE Press ; Wiley-Interscience, 2004. OCLC: ocm52920516.
- [69] M. Wetter, "GenOpt (R), generic optimization program, User Manual, Version 2.0. 0," 2003.
- [70] Y. Kwak and J.-H. Huh, "Development of a method of real-time building energy simulation for efficient predictive control," *Energy Conversion and Management*, vol. 113, pp. 220–229, Apr. 2016.
- [71] M. Wetter, P. Haves, and B. Coffey, "Building controls virtual test bed," tech. rep., 2008.

- [72] Y. Lu, S. Wang, C. Yan, and K. Shan, "Impacts of renewable energy system design inputs on the performance robustness of net zero energy buildings," *Energy*, vol. 93, pp. 1595–1606, Dec. 2015.
- [73] J. Langevin, J. Wen, and P. L. Gurian, "Quantifying the human–building interaction: Considering the active, adaptive occupant in building performance simulation," *Energy and Buildings*, vol. 117, pp. 372–386, Apr. 2016.
- [74] A. Afram and F. Janabi-Sharifi, "Gray-box modeling and validation of residential HVAC system for control system design," *Applied Energy*, vol. 137, pp. 134–150, Jan. 2015.
- [75] A. Marvuglia, A. Messineo, and G. Nicolosi, "Coupling a neural network temperature predictor and a fuzzy logic controller to perform thermal comfort regulation in an office building," *Building and Environment*, vol. 72, pp. 287–299, Feb. 2014.
- [76] B. Yuce, H. Li, Y. Rezgüi, I. Petri, B. Jayan, and C. Yang, "Utilizing artificial neural network to predict energy consumption and thermal comfort level: An indoor swimming pool case study," *Energy and Buildings*, vol. 80, pp. 45–56, Sept. 2014.
- [77] P. Ferreira, A. Ruano, S. Silva, and E. Conceição, "Neural networks based predictive control for thermal comfort and energy savings in public buildings," *Energy and Buildings*, vol. 55, pp. 238–251, Dec. 2012.
- [78] S. D'Oca and T. Hong, "Occupancy schedules learning process through a data mining framework," *Energy and Buildings*, vol. 88, pp. 395–408, Feb. 2015.
- [79] A. Mahdavi and F. Tahmasebi, "Predicting people's presence in buildings: An empirically based model performance analysis," *Energy and Buildings*, vol. 86, pp. 349–355, Jan. 2015.
- [80] R. J. Schalkoff, *Artificial neural networks*, vol. 1. McGraw-Hill New York. original-date: 1997.
- [81] M. Hearst, S. Dumais, E. Osuna, J. Platt, and B. Scholkopf, "Support vector machines," *IEEE Intelligent Systems and their Applications*, vol. 13, pp. 18–28, July 1998.
- [82] D. Whitley, "A genetic algorithm tutorial," *Statistics and Computing*, vol. 4, June 1994.
- [83] J. R. Quinlan, "Induction of decision trees," *Machine Learning*, vol. 1, pp. 81–106, Mar. 1986.
- [84] M. Benedetti, V. Cesarotti, V. Introna, and J. Serranti, "Energy consumption control automation using Artificial Neural Networks and adaptive algorithms: Proposal of a new methodology and case study," *Applied Energy*, vol. 165, pp. 60–71, Mar. 2016.
- [85] P. H. Shaikh, N. B. M. Nor, P. Nallagownden, I. Elamvazuthi, and T. Ibrahim, "Intelligent multi-objective control and management for smart energy efficient buildings," *International Journal of Electrical Power & Energy Systems*, vol. 74, pp. 403–409, Jan. 2016.

- [86] Z. O'Neill and C. O'Neill, "Development of a probabilistic graphical model for predicting building energy performance," *Applied Energy*, vol. 164, pp. 650–658, Feb. 2016.
- [87] N. Friedman, D. Geiger, and M. Goldszmidt, "Bayesian network classifiers," *Machine learning, Springer*, vol. 29, no. 2-3, pp. 131–163, 1997.
- [88] J. van Hoof, "Forty years of Fanger's model of thermal comfort: comfort for all?," *Indoor Air*, vol. 18, pp. 182–201, June 2008.
- [89] M. J. Gacto, R. Alcalá, and F. Herrera, "A multi-objective evolutionary algorithm for an effective tuning of fuzzy logic controllers in heating, ventilating and air conditioning systems," *Applied Intelligence*, vol. 36, pp. 330–347, Mar. 2012.
- [90] F. R. d'Ambrosio Alfano, B. I. Palella, and G. Riccio, "The role of measurement accuracy on the thermal environment assessment by means of PMV index," *Building and Environment*, vol. 46, pp. 1361–1369, July 2011.
- [91] X. Chen, Q. Wang, and J. Srebric, "A data-driven state-space model of indoor thermal sensation using occupant feedback for low-energy buildings," *Energy and Buildings*, vol. 91, pp. 187–198, Mar. 2015.
- [92] X. Chen, Q. Wang, and J. Srebric, "Occupant feedback based model predictive control for thermal comfort and energy optimization: A chamber experimental evaluation," *Applied Energy*, vol. 164, pp. 341–351, Feb. 2016.
- [93] R. Ricciu, A. Galatioto, G. Desogus, and L. Besalduch, "Uncertainty in the evaluation of the Predicted Mean Vote index using Monte Carlo analysis," *Journal of Environmental Management*, vol. 223, pp. 16–22, Oct. 2018.
- [94] A. S. Ribeiro, J. Alves e Sousa, M. G. Cox, A. B. Forbes, L. C. Matias, and L. L. Martins, "Uncertainty Analysis of Thermal Comfort Parameters," *International Journal of Thermophysics*, vol. 36, pp. 2124–2149, Aug. 2015.
- [95] J. Široký, F. Oldewurtel, J. Cigler, and S. Prívvara, "Experimental analysis of model predictive control for an energy efficient building heating system," *Applied Energy*, vol. 88, pp. 3079–3087, Sept. 2011.
- [96] I. Hazyuk, C. Ghiaus, and D. Penhouet, "Optimal temperature control of intermittently heated buildings using Model Predictive Control: Part I – Building modeling," *Building and Environment*, vol. 51, pp. 379–387, May 2012.
- [97] J. Cai and J. E. Braun, "A practical and scalable inverse modeling approach for multi-zone buildings," 9th International Conference on System Simulation in Buildings, 2014.
- [98] I. Sharma, J. Dong, A. A. Malikopoulos, M. Street, J. Ostrowski, T. Kuruganti, and R. Jackson, "A modeling framework for optimal energy management of a residential building," *Energy and Buildings*, vol. 130, pp. 55–63, Oct. 2016.

- [99] H. Harb, N. Boyanov, L. Hernandez, R. Streblow, and D. Müller, "Development and validation of grey-box models for forecasting the thermal response of occupied buildings," *Energy and Buildings*, vol. 117, pp. 199–207, Apr. 2016.
- [100] D. Sturzenegger, D. Gyalistras, M. Morari, and R. S. Smith, "Model Predictive Climate Control of a Swiss Office Building: Implementation, Results, and Cost–Benefit Analysis," *IEEE Transactions on Control Systems Technology*, vol. 24, pp. 1–12, Jan. 2016.
- [101] G. Serale, M. Fiorentini, A. Capozzoli, D. Bernardini, and A. Bemporad, "Model Predictive Control (MPC) for Enhancing Building and HVAC System Energy Efficiency: Problem Formulation, Applications and Opportunities," *Energies*, vol. 11, p. 631, Mar. 2018.
- [102] J. Cigler, S. Prívará, Z. Váňa, E. Žáčková, and L. Ferkl, "Optimization of Predicted Mean Vote index within Model Predictive Control framework: Computationally tractable solution," *Energy and Buildings*, vol. 52, pp. 39–49, Sept. 2012.
- [103] Y. Ma, F. Borrelli, B. Hancey, B. Coffey, S. Bengea, and P. Haves, "Model Predictive Control for the Operation of Building Cooling Systems," *IEEE Transactions on Control Systems Technology*, vol. 20, pp. 796–803, May 2012.
- [104] J. B. Rawlings, D. Q. Mayne, and M. M. Diehl, *Model predictive control: theory, computation, and design*. Madison, Wisconsin: Nob Hill Publishing, 2nd edition ed., 2017. OCLC: 1020170256.
- [105] M. Castilla, J. D. Álvarez, M. Berenguel, F. Rodríguez, J. L. Guzmán, and M. Pérez, "A comparison of thermal comfort predictive control strategies," *Energy and Buildings*, vol. 43, pp. 2737–2746, Oct. 2011.
- [106] D. Kolokotsa, A. Pouliezios, G. Stavrakakis, and C. Lazos, "Predictive control techniques for energy and indoor environmental quality management in buildings," *Building and Environment*, vol. 44, pp. 1850–1863, Sept. 2009.
- [107] S. Prívará, J. Široký, L. Ferkl, and J. Cigler, "Model predictive control of a building heating system: The first experience," *Energy and Buildings*, vol. 43, pp. 564–572, Feb. 2011.
- [108] W. Liang, R. Quinte, X. Jia, and J.-Q. Sun, "MPC control for improving energy efficiency of a building air handler for multi-zone VAVs," *Building and Environment*, vol. 92, pp. 256–268, Oct. 2015.
- [109] R. Godina, E. M. G. Rodrigues, E. Pouresmaeil, and J. P. S. Catalão, "Optimal residential model predictive control energy management performance with PV microgeneration," *Computers & Operations Research*, vol. 96, pp. 143–156, Aug. 2018.
- [110] A. Alahmer and S. Alsaqoor, "Simulation and optimization of multi-split variable refrigerant flow systems," *Ain Shams Engineering Journal*, vol. 9, no. 4, pp. 1705–1715, 2018.
- [111] T. N. Aynur, "Variable refrigerant flow systems: A review," *Energy and Buildings*, vol. 42, no. 7, pp. 1106–1112, 2010.

- [112] W. Goetzler, "Variable refrigerant flow systems," *Ashrae Journal*, vol. 49, no. 4, pp. 24–31, 2007.
- [113] W. Grassi, *Heat pumps: fundamentals and applications*. Springer, 2017.
- [114] H. Demir, M. Mobedi, and S. Ülkü, "A review on adsorption heat pump: Problems and solutions," *Renewable and Sustainable Energy Reviews*, vol. 12, no. 9, pp. 2381–2403, 2008.
- [115] J. Braun, P. Bansal, and E. Groll, "Energy efficiency analysis of air cycle heat pump dryers," *International Journal of Refrigeration*, vol. 25, no. 7, pp. 954–965, 2002.
- [116] G. Xu, X. Zhang, and S. Deng, "A simulation study on the operating performance of a solar–air source heat pump water heater," *Applied Thermal Engineering*, vol. 26, no. 11–12, pp. 1257–1265, 2006.
- [117] J. Xia, E. Winandy, B. Georges, and J. Lebrun, "Experimental analysis of the performances of variable refrigerant flow systems," *Building Services Engineering Research and Technology*, vol. 25, no. 1, pp. 17–23, 2004.
- [118] J. Choi and Y. C. Kim, "Capacity modulation of an inverter-driven multi-air conditioner using electronic expansion valves," *Energy*, vol. 28, no. 2, pp. 141–155, 2003.
- [119] H. Harb, N. Boyanov, L. Hernandez, R. Streblow, and D. Müller, "Development and validation of grey-box models for forecasting the thermal response of occupied buildings," *Energy and Buildings*, vol. 117, pp. 199–207, 2016.
- [120] S. Mahendra, P. Stéphane, and W. Frederic, "Modeling for reactive building energy management," *Energy Procedia*, vol. 83, pp. 207–215, 2015.
- [121] K. K. Andersen, H. Madsen, and L. H. Hansen, "Modelling the heat dynamics of a building using stochastic differential equations," *Energy and Buildings*, vol. 31, no. 1, pp. 13–24, 2000.
- [122] H. Park, M. Ruellan, A. Bouvet, E. Monmasson, and R. Bennacer, "Thermal parameter identification of simplified building model with electric appliance," in *11th International Conference on Electrical Power Quality and Utilisation*, pp. 1–6, IEEE, 2011.
- [123] A. Boodi, K. Beddiar, Y. Amirat, and M. Benbouzid, "Simplified Building Thermal Model Development and Parameters Evaluation Using a Stochastic Approach," *Energies*, vol. 13, no. 11, p. 2899, 2020.
- [124] A. Boodi, K. Beddiar, Y. Amirat, and M. Benbouzid, "A Numerical Approach for Buildings Reduced Thermal Model Parameters Evaluation," p. 8, 2019.
- [125] M. M. Gouda, S. Danaher, and C. P. Underwood, "Building thermal model reduction using nonlinear constrained optimization," *Building and environment*, vol. 37, no. 12, pp. 1255–1265, 2002.
- [126] B. Bueno, L. Norford, G. Pigeon, and R. Britter, "A resistance-capacitance network model for the analysis of the interactions between

- the energy performance of buildings and the urban climate," *Building and Environment*, vol. 54, pp. 116–125, 2012.
- [127] X. Xu and S. Wang, "A simplified dynamic model for existing buildings using CTF and thermal network models," *International Journal of Thermal Sciences*, vol. 47, no. 9, pp. 1249–1262, 2008.
- [128] F. Lorenz and G. Masy, "Méthode d'évaluation de l'économie d'énergie apportée par l'intermittence de chauffage dans les bâtiments," *Traitement par différences finies d'un model a deux constantes de temps*, Report No. GM820130-01. Faculte des Sciences Appliquees, University de Liege, Liege, Belgium, 1982.
- [129] M. G. Davies, "Wall transient heat flow using time-domain analysis," *Building and Environment*, vol. 32, no. 5, pp. 427–446, 1997.
- [130] J. E. Braun and N. Chaturvedi, "An inverse gray-box model for transient building load prediction," *HVAC&R Research*, vol. 8, no. 1, pp. 73–99, 2002.
- [131] I. Hazyuk, C. Ghiaus, and D. Penhouet, "Optimal temperature control of intermittently heated buildings using Model Predictive Control: Part I – Building modeling," *Building and Environment*, vol. 51, pp. 379–387, May 2012.
- [132] X. Xu and S. Wang, "Optimal simplified thermal models of building envelope based on frequency domain regression using genetic algorithm," *Energy and Buildings*, vol. 39, no. 5, pp. 525–536, 2007.
- [133] A. P. Ramallo-González, M. E. Eames, and D. A. Coley, "Lumped parameter models for building thermal modelling: An analytic approach to simplifying complex multi-layered constructions," *Energy and Buildings*, vol. 60, pp. 174–184, May 2013.
- [134] M. G. Davies, *Building Heat Transfer*. Chichester, UK: John Wiley & Sons, Ltd, Mar. 2004.
- [135] J. A. Clarke, *Energy Simulation in Building Design*. Oxford: Butterworth-Heinemann, 2nd ed ed., 2001.
- [136] D. G. Stephenson and G. P. Mitalas, "Calculation of heat conduction transfer functions for multi-layers slabs," *Air Cond. Engrs. Trans;(United States)*, vol. 77, 1971.
- [137] S. Wang and Y. Chen, "A novel and simple building load calculation model for building and system dynamic simulation," *Applied Thermal Engineering*, vol. 21, no. 6, pp. 683–702, 2001.
- [138] M. N. Özışık, H. R. B. Orlande, M. J. Colaco, and R. M. Cotta, *Finite Difference Methods in Heat Transfer*. Boca Raton: CRC Press, Taylor & Francis Group, second edition ed., 2017.
- [139] G. D. Smith and G. D. Smith, *Numerical Solution of Partial Differential Equations: Finite Difference Methods*. Oxford university press, 1985.
- [140] W. J. Minkowycz, E. M. Sparrow, G. E. Schneider, and R. H. Pletcher, "Handbook of numerical heat transfer," *wi*, 1988.

- [141] D. R. Croft, J. A. R. Stone, and D. G. Lilley, *Heat Transfer Calculations Using Finite Difference Equations*. No. 283, Applied science publishers London., 1977.
- [142] J. Crank and P. Nicolson, "A practical method for numerical evaluation of solutions of partial differential equations of the heat-conduction type," in *Mathematical Proceedings of the Cambridge Philosophical Society*, vol. 43, pp. 50–67, Cambridge University Press, 1947.
- [143] W. T. Lee, "Tridiagonal matrices: Thomas algorithm," *MS6021, Scientific Computation, University of Limerick*, 2011.
- [144] Y. Shi and R. C. Eberhart, "Parameter selection in particle swarm optimization," in *International Conference on Evolutionary Programming*, pp. 591–600, Springer, 1998.
- [145] M. Reyes-Sierra and C. C. Coello, "Multi-objective particle swarm optimizers: A survey of the state-of-the-art," *International journal of computational intelligence research*, vol. 2, no. 3, pp. 287–308, 2006.
- [146] Y. Shi and R. C. Eberhart, "Empirical study of particle swarm optimization," in *Proceedings of the 1999 Congress on Evolutionary Computation-CEC99 (Cat. No. 99TH8406)*, vol. 3, pp. 1945–1950, IEEE, 1999.
- [147] R. C. Eberhart and Y. Shi, "Comparison between genetic algorithms and particle swarm optimization," in *International Conference on Evolutionary Programming*, pp. 611–616, Springer, 1998.
- [148] A. P. Engelbrecht, *Computational Intelligence: An Introduction*. Chichester, England ; Hoboken, NJ: John Wiley & Sons, 2nd ed ed., 2007.
- [149] A. El-Gallad, M. El-Hawary, A. Sallam, and A. Kalas, "Enhancing the particle swarm optimizer via proper parameters selection," in *IEEE CCECE2002. Canadian Conference on Electrical and Computer Engineering. Conference Proceedings (Cat. No. 02CH37373)*, vol. 2, pp. 792–797, IEEE, 2002.
- [150] Y. Shi, "Particle swarm optimization," *IEEE connections*, vol. 2, no. 1, pp. 8–13, 2004.
- [151] J. Hensen and R. Lamberts, eds., *Building Performance Simulation for Design and Operation*. London ; New York: Spon Press, 2011.
- [152] J. Herman and W. Usher, "Salib: an open-source python library for sensitivity analysis," *Journal of Open Source Software*, vol. 2, no. 9, p. 97, 2017.
- [153] "Bâtiments Basse Consommation, France," tech. rep., Guide AIT-F/EDF, 2008.
- [154] M.-E. Duprez, E. Dumont, and M. Frère, "Modelling of reciprocating and scroll compressors," *International Journal of Refrigeration*, vol. 30, no. 5, pp. 873–886, 2007.
- [155] Y. Chen, N. P. Halm, J. E. Braun, and E. A. Groll, "Mathematical modeling of scroll compressors—part ii: overall scroll compressor modeling," *International Journal of Refrigeration*, vol. 25, no. 6, pp. 751–764, 2002.

- [156] Y. Chen, N. P. Halm, E. A. Groll, and J. E. Braun, "Mathematical modeling of scroll compressors—part i: compression process modeling," *International Journal of Refrigeration*, vol. 25, no. 6, pp. 731–750, 2002.
- [157] Y. Zhu, X. Jin, Z. Du, B. Fan, and S. Fu, "Generic simulation model of multi-evaporator variable refrigerant flow air conditioning system for control analysis," *international journal of refrigeration*, vol. 36, no. 6, pp. 1602–1615, 2013.
- [158] Y. Ge and R. Cropper, "Performance evaluations of air-cooled condensers using pure and mixture refrigerants by four-section lumped modelling methods," *Applied thermal engineering*, vol. 25, no. 10, pp. 1549–1564, 2005.
- [159] G. Ding, C. Zhang, and Z. Lu, "Dynamic simulation of natural convection bypass two-circuit cycle refrigerator-freezer and its application: Part i: Component models," *Applied Thermal Engineering*, vol. 24, no. 10, pp. 1513–1524, 2004.
- [160] Z. Lu, G. Ding, and C. Zhang, "Dynamic simulation of natural convection bypass two-circuit cycle refrigerator-freezer and its application: Part ii: System simulation and application," *Applied thermal engineering*, vol. 24, no. 10, pp. 1525–1533, 2004.
- [161] I. H. Bell, J. Wronski, S. Quoilin, and V. Lemort, "Pure and pseudo-pure fluid thermophysical property evaluation and the open-source thermophysical property library coolprop," *Industrial & Engineering Chemistry Research*, vol. 53, no. 6, pp. 2498–2508, 2014.
- [162] M. Nitsche and R. O. Gbadamosi, *Heat exchanger design guide: A practical guide for planning, selecting and designing of shell and tube exchangers*. Butterworth-Heinemann, 2015.
- [163] C. Park, H. Cho, Y. Lee, and Y. Kim, "Mass flow characteristics and empirical modeling of r22 and r410a flowing through electronic expansion valves," *International Journal of Refrigeration*, vol. 30, no. 8, pp. 1401–1407, 2007.
- [164] B. Y. Liu and R. C. Jordan, "The long-term average performance of flat-plate solar-energy collectors: With design data for the US, its outlying possessions and Canada," *Solar energy*, vol. 7, no. 2, pp. 53–74, 1963.
- [165] D. A. Chwieduk, "Recommendation on modelling of solar energy incident on a building envelope," *Renewable Energy*, vol. 34, no. 3, pp. 736–741, 2009.
- [166] J. A. Duffie and W. A. Beckman, *Solar Engineering of Thermal Processes*. John Wiley & Sons, 2013.
- [167] I. Dincer, C. O. Colpan, O. Kizilkan, and M. A. Ezan, *Progress in Clean Energy, Novel Systems and Applications*, vol. 2. Springer, 2015.
- [168] K. Ahmed, J. Kurnitski, and B. W. Olesen, "Data for occupancy internal heat gain calculation in main building categories," *Data in brief*, vol. 15, pp. 1030–1034, 2017.
- [169] L. Wang, *Model Predictive Control System Design and Implementation Using MATLAB®*. Springer Science & Business Media, 2009.

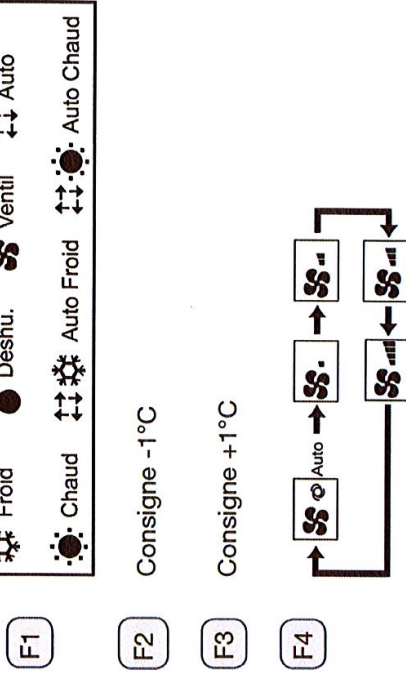
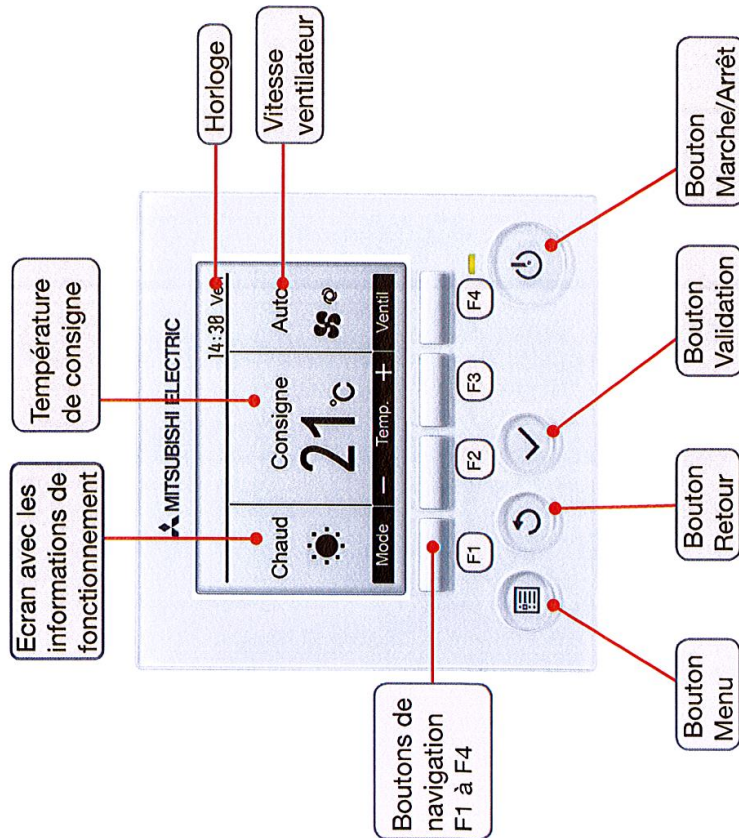
REFERENCES

- [170] J. Rossiter, *Model-Based Predictive Control: A Practical Approach*. CRC Press, 1 ed., July 2017.
- [171] M. S. Andersen, J. Dahl, and L. Vandenberghe, "CVXOPT: A Python package for convex optimization," *abel. ee. ucla. edu/cvxopt*, 2013.
- [172] Z. Liao and A. Dexter, "A simplified physical model for estimating the average air temperature in multi-zone heating systems," *Building and Environment*, vol. 39, pp. 1013–1022, Sept. 2004.
- [173] F. Haugen, "Jacobian linearization." <http://techt teach.no/fag/so303e/2007/diverse/linearization.pdf>, 2007. Accessed: 2018-02-06.

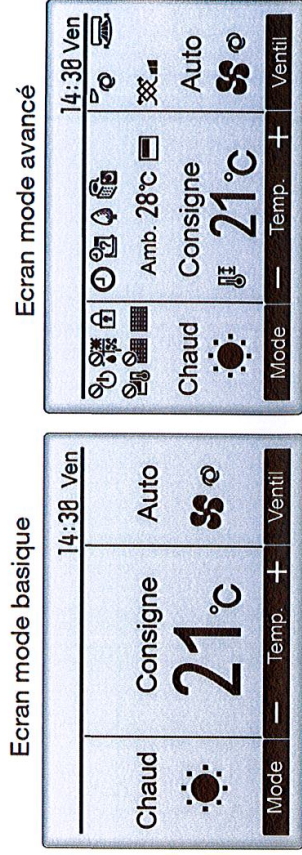
Appendices

A.1 Control System HMI

PAR31-MAA-J



Boutons de navigation F1 à F4



18

A.2 Jacobian Linearization

3.4 Linearization of nonlinear state space models

The formulas for linearizing nonlinear discrete-time state space models are presented without derivation below. They can be derived in the same way as for linearizing nonlinear continuous-time models [1]. In the formulas below it is assumed a second order system. I guess it is clear how the formulas can be generalized to higher orders.

Given the following discrete-time nonlinear state space model

$$x_1(k+1) = f_1[x_1(k), x_2(k), u_1(k), u_2(k)] \quad (3.9)$$

$$x_2(k+1) = f_2[x_1(k), x_2(k), u_1(k), u_2(k)]$$

$$y_1(k) = g_1[x_1(k), x_2(k), u_1(k), u_2(k)] \quad (3.10)$$

$$y_2(k) = g_2[x_1(k), x_2(k), u_1(k), u_2(k)]$$

where f_1 and f_2 are nonlinear functions. The corresponding linear model, which defines the system's dynamic behaviour about a specific operating point, is

$$\Delta x_1(k+1) = \left. \frac{\partial f_1}{\partial x_1} \right|_{\text{op}} \Delta x_1(k) + \left. \frac{\partial f_1}{\partial x_2} \right|_{\text{op}} \Delta x_2(k) + \left. \frac{\partial f_1}{\partial u_1} \right|_{\text{op}} \Delta u_1(k) + \left. \frac{\partial f_1}{\partial u_2} \right|_{\text{op}} \Delta u_2(k)$$

$$\Delta x_2(k+1) = \left. \frac{\partial f_2}{\partial x_1} \right|_{\text{op}} \Delta x_1(k) + \left. \frac{\partial f_2}{\partial x_2} \right|_{\text{op}} \Delta x_2(k) + \left. \frac{\partial f_2}{\partial u_1} \right|_{\text{op}} \Delta u_1(k) + \left. \frac{\partial f_2}{\partial u_2} \right|_{\text{op}} \Delta u_2(k) \quad (3.11)$$

$$\Delta y_1(k) = \left. \frac{\partial g_1}{\partial x_1} \right|_{\text{op}} \Delta x_1(k) + \left. \frac{\partial g_1}{\partial x_2} \right|_{\text{op}} \Delta x_2(k) + \left. \frac{\partial g_1}{\partial u_1} \right|_{\text{op}} \Delta u_1(k) + \left. \frac{\partial g_1}{\partial u_2} \right|_{\text{op}} \Delta u_2(k)$$

$$\Delta y_2(k) = \left. \frac{\partial g_2}{\partial x_1} \right|_{\text{op}} \Delta x_1(k) + \left. \frac{\partial g_2}{\partial x_2} \right|_{\text{op}} \Delta x_2(k) + \left. \frac{\partial g_2}{\partial u_1} \right|_{\text{op}} \Delta u_1(k) + \left. \frac{\partial g_2}{\partial u_2} \right|_{\text{op}} \Delta u_2(k) \quad (3.12)$$

or

$$\Delta x(k+1) = A\Delta x(k) + B\Delta u(k) \quad (3.13)$$

$$\Delta y(k) = C\Delta x(k) + D\Delta u(k) \quad (3.14)$$

where

$$\Delta x(k) = \begin{bmatrix} \Delta x_1(k) \\ \vdots \\ \Delta x_2(k) \end{bmatrix} \quad (3.15)$$

and similarly for $\Delta u(k)$ and $\Delta y(k)$. The system matrices are¹

$$A = \left[\begin{array}{cc} \frac{\partial f_1}{\partial x_1} & \frac{\partial f_1}{\partial x_2} \\ \frac{\partial f_2}{\partial x_1} & \frac{\partial f_2}{\partial x_2} \end{array} \right] \Big|_{\text{op}} = \frac{\partial f}{\partial x^T} \Big|_{\text{op}} \quad (3.16)$$

$$B = \left[\begin{array}{cc} \frac{\partial f_1}{\partial u_1} & \frac{\partial f_1}{\partial u_2} \\ \frac{\partial f_2}{\partial u_1} & \frac{\partial f_2}{\partial u_2} \end{array} \right] \Big|_{\text{op}} = \frac{\partial f}{\partial u^T} \Big|_{\text{op}} \quad (3.17)$$

$$C = \left[\begin{array}{cc} \frac{\partial g_1}{\partial x_1} & \frac{\partial g_1}{\partial x_2} \\ \frac{\partial g_2}{\partial x_1} & \frac{\partial g_2}{\partial x_2} \end{array} \right] \Big|_{\text{op}} = \frac{\partial g}{\partial x^T} \Big|_{\text{op}} \quad (3.18)$$

$$D = \left[\begin{array}{cc} \frac{\partial g_1}{\partial u_1} & \frac{\partial g_1}{\partial u_2} \\ \frac{\partial g_2}{\partial u_1} & \frac{\partial g_2}{\partial u_2} \end{array} \right] \Big|_{\text{op}} = \frac{\partial g}{\partial u^T} \Big|_{\text{op}} \quad (3.19)$$

In the formulas above the subindex *op* is for operating point, which is a particular set of values of the variables. Often, the operating point is assumed to be an equilibrium (or static) operating point, which means that all variables have constant values there.

Example 1 Linearization

Given the following non-linear state-space model:

$$x_1(k+1) = \underbrace{ax_1(k) + bx_1(k)x_2(k) + cx_1(k)u_1(k)}_{f_1} \quad (3.20)$$

$$x_2(k+1) = \underbrace{dx_2(k)}_{f_2} \quad (3.21)$$

$$y_1(k) = \underbrace{x_1(k)}_{g_1} \quad (3.22)$$

The system matrices of the corresponding linear model are

$$A = \left[\begin{array}{cc} \frac{\partial f_1}{\partial x_1} & \frac{\partial f_1}{\partial x_2} \\ \frac{\partial f_2}{\partial x_1} & \frac{\partial f_2}{\partial x_2} \end{array} \right] \Big|_{\text{op}} = \left[\begin{array}{cc} a + bx_2(k) + cu_1(k) & bx_1(k) \\ 0 & d \end{array} \right] \Big|_{\text{op}} \quad (3.23)$$

¹Partial derivative matrices are denoted Jacobians.

$$B = \left[\begin{array}{c} \frac{\partial f_1}{\partial u_1} \\ \frac{\partial f_2}{\partial u_1} \end{array} \right] \Big|_{\text{op}} = \left[\begin{array}{c} cx_1(k) \\ 0 \end{array} \right] \Big|_{\text{op}} \quad (3.24)$$

$$C = \left[\begin{array}{cc} \frac{\partial g_1}{\partial x_1} & \frac{\partial g_1}{\partial x_2} \end{array} \right] \Big|_{\text{op}} = [1 \quad 0] \quad (3.25)$$

$$D = \left[\frac{\partial g_1}{\partial u_1} \right] \Big|_{\text{op}} = [0] \quad (3.26)$$

[End of Example 1]

3.5 Calculating responses in discrete-time state space models

3.5.1 Calculating dynamic responses

Calculating responses in discrete-time state space models is quite easy. The reason is that the model *is* the algorithm! For example, assume that Euler's forward method has been used to get the following discrete-time state space model:

$$x(k) = x(k-1) + hf(k-1) \quad (3.27)$$

This model constitutes the algorithm for calculating the response $x(k)$.

3.5.2 Calculating static responses

The static response is the response when all input variables have constant values and all output variables have converged to constant values. Assume the following possibly nonlinear state space model:

$$x(k+1) = f_1[x(k), u(k)] \quad (3.28)$$

where f_1 is a possibly nonlinear function of x and u . Let us write x_s and u_s for static values. Under static conditions (3.28) becomes

$$x_s = f_1[x_s, u_s] \quad (3.29)$$

which is an algebraic equation from which we can try to solve for unknown variables.

If the model is linear:

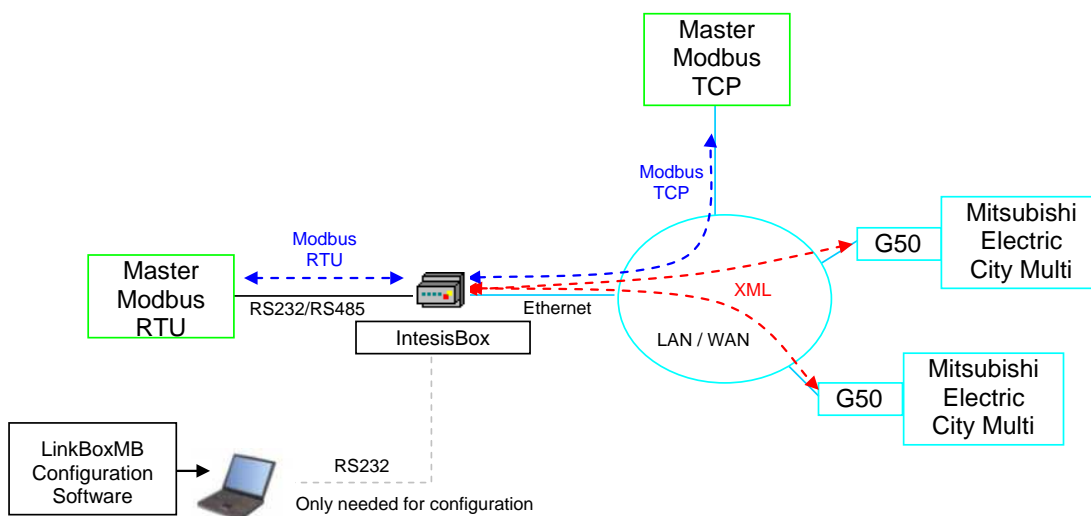
$$x(k+1) = Ax(k) + Bu(k) \quad (3.30)$$

A.3 Sensor Data Collection System



IntesisBox® Modbus Server - Mitsubishi Electric G50

Gateway for monitor and control Mitsubishi Electric City Multi Air Conditioning systems from any Modbus master device TCP or RTU (BMS, PLC, SCADA, HMI, TouchPanel...)



This integration requires the Mitsubishi Electric City Multi AC system be equipped with the Mitsubishi Electric G-50A, GB-50A o AG-150A gateway. This gateway from Mitsubishi Electric offers the signals of the City Multi AC system through XML protocol. Every G50 (G-50A, GB-50A o AG-150A) allows access to the signals of up to 50 City Multi internal units and 50 groups, no matter the number of external units installed. In the G50, the group is the control unit, every group can have from 1 to 16 associated internal units. This integration supervises and control groups, not internal units, although if only one internal unit is associated to every group then you can supervise and control internal units individually. This G50 gateway is supplied by Mitsubishi Electric. Contact your nearest Mitsubishi Electric distributor for details.

IntesisBox® can “talk” to up to 2 Mitsubishi Electric G50s using XML protocol, and offers the signals of all these City Multi groups through its Modbus slave interface, each signal in a predefined fixed Modbus address. The AG-150A can be used with Expansions Cards as explained in the section IntesisBox capacity

The Modbus interface of IntesisBox can be freely configured as RTU RS232, RTU RS485 or TCP.

The commissioning of IntesisBox® is almost plug & play, only IP parameters of the box and of G50s have to be configured using *LinkBoxMB*, a friendly software configuration tool for Windows™ supplied along with IntesisBox with no additional cost.

1. IntesisBox capacity

Element	Max.	Notes
Num. of G50	2	Number of independent G50 interfaces 2 x G-50A / GB-50A 2 x AG150 (without Expansion Controllers) 1 x AG150 (with 2 Expansion Controllers)
Number of City Multi groups: (Number of G50s X 50)	100	Maximum number of groups
Number of variables per group	19	Modbus addresses
Number of variables per G50	951	Modbus addresses
Maximum number of variables	1.902	Modbus addresses

There are 2 different models of *IntesisBox® Modbus server - Mitsubishi Electric G50* with different capacity every one of them. The table above shows the capacity for the top model (with maximum capacity).

The 2 different models allow integrating respectively: 1 or 2 G50s.

And their order codes are:

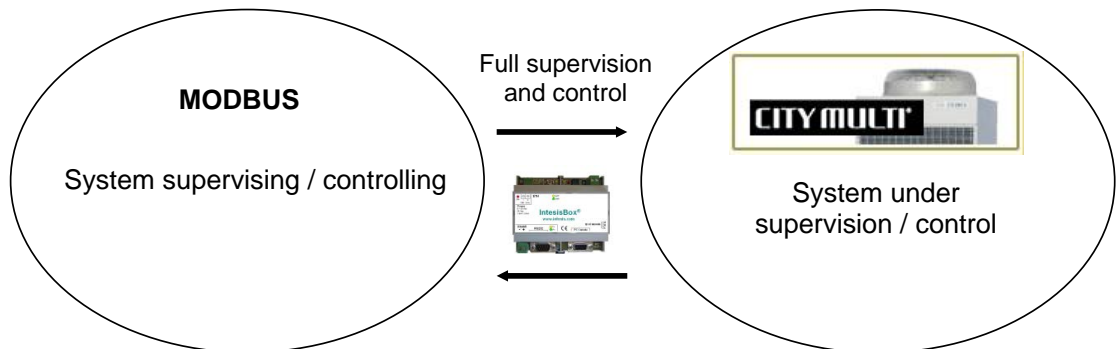
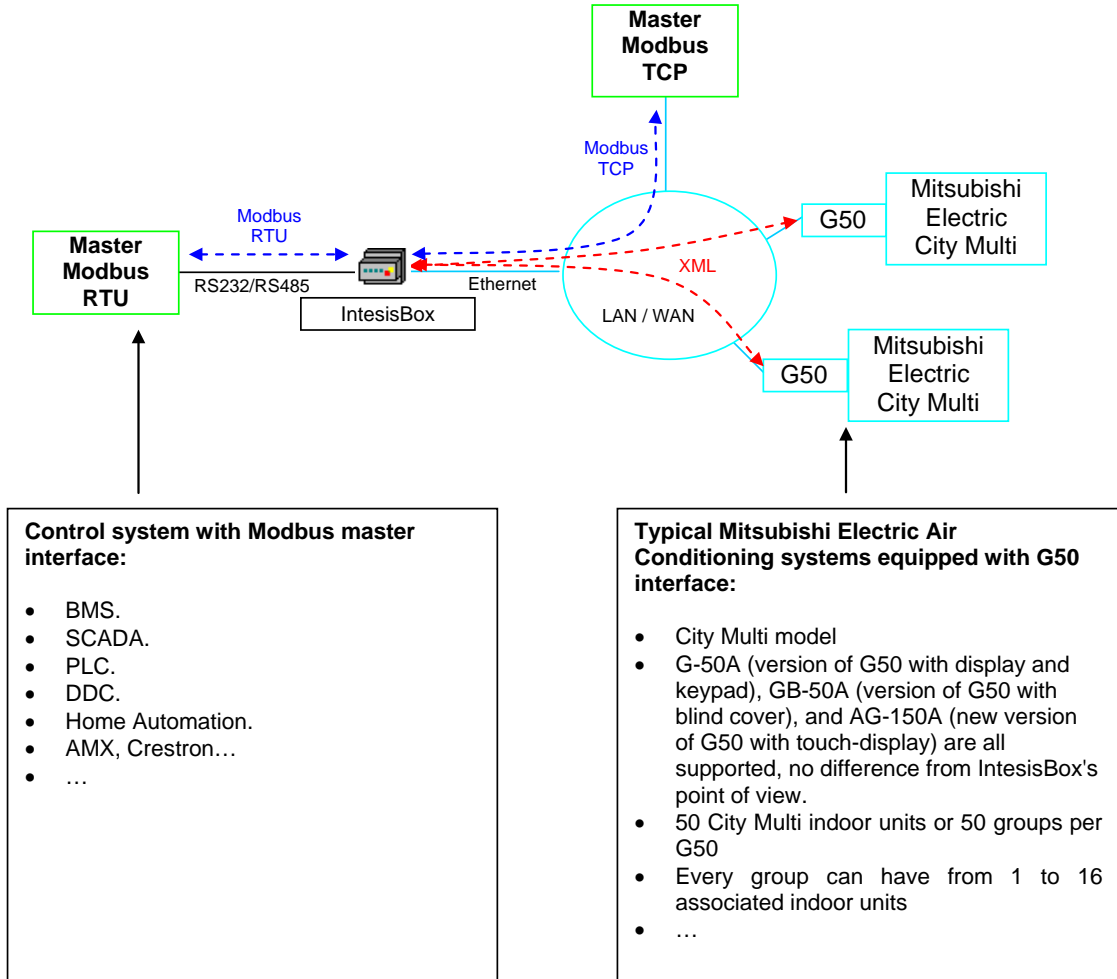
- **ME-AC-MBS-50.** Model supporting up to 1 G50 and 50 City Multi groups.
- **ME-AC-MBS-100.** Model supporting up to 2 G50s and 100 City Multi groups.



NOTE: Please, remember that Mitsubishi Electric AG-150A requires a software license, PC-Monitoring license (SW-Mon), that has to be purchased together with the AG-150A gateway.

2. Sample applications

Integration of Mitsubishi Electric City Multi Air Conditioning systems equipped with the interface G50 into Modbus control systems.



TRADEMARKS: Todas las marcas y nombres utilizados en este documento se reconocen como marcas registradas de sus respectivos propietarios.

© Intesis Software S.L. - Todos los derechos reservados
La información de este documento puede cambiar sin previo aviso.

IntesisBox® es una marca registrada de Intesis Software SL

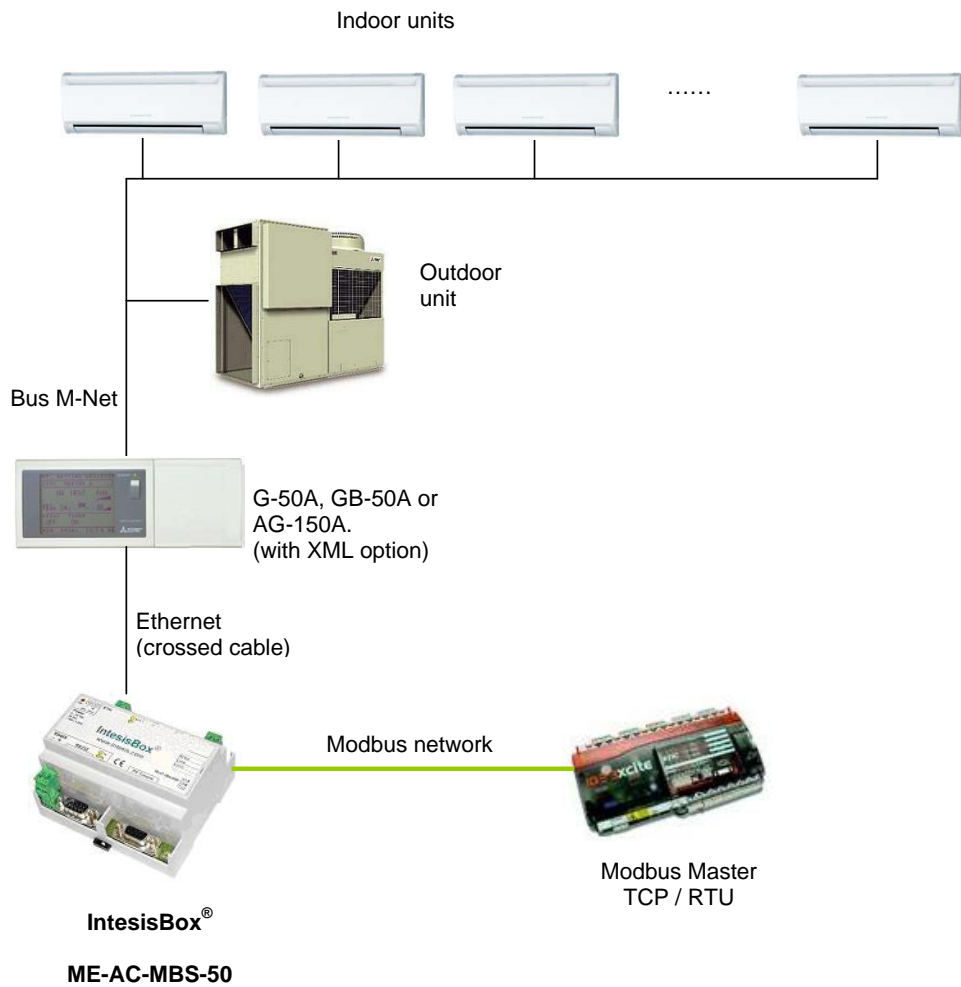


URL | <http://www.intesis.com>
email | info@intesis.com
tel | +34 938047134

3. Typical applications

Integration of Mitsubishi Electric Air Conditioning into Modbus systems.

For this application, Mitsubishi Air Conditioning system must be equipped with G-50A, GB-50A or AG-150A Gateway. For more information about these devices contact Mitsubishi Electric.



TRADEMARKS: Todas las marcas y nombres utilizados en este documento se reconocen como marcas registradas de sus respectivos propietarios.

© Intesis Software S.L. - Todos los derechos reservados
La información de este documento puede cambiar sin previo aviso.

IntesisBox® es una marca registrada de Intesis Software SL



URL | <http://www.intesis.com>
email | info@intesis.com
tel | +34 938047134

4. Modbus interface

General	
Max. Number of Mitsubishi Elec.G50s	Up to two G50s can be supported.
Virtual signals	<ul style="list-style-type: none"> • One communication error virtual signal per every G50 device defined. • One communication error virtual signal per every group into the G50 device. • One virtual signal per every group into the G50 device to enable/disable this group in the polling process. <p>All these virtual signals can be read/written from Modbus.</p>
Modbus interface	
Device type	Slave.
Modbus modes supported	TCP, RTU RS232 or RS485.
Modbus TCP configuration parameters	<ul style="list-style-type: none"> • IP address. • Subnet mask. • Default gateway address. • TCP port.
Modbus RTU configuration parameters	<ul style="list-style-type: none"> • RS232/RS485. • Baud rate. • Parity. • Slave number.
Points	
Configuration	No point configuration needs to be done, all the Mitsubishi Electric G50 signals are automatically associated to predefined fixed Modbus Addresses.
Modbus function codes supported	<p>Read functions:</p> <ul style="list-style-type: none"> • 3- Read holding registers. • 4- Read input registers. <p>Write functions:</p> <ul style="list-style-type: none"> • 6- Write single register. • 16- Write multiple registers. <p><i>If poll records are used to read/write multiple records, the range of addresses requested must contain valid addresses, if not the corresponding Modbus error code will be responded.</i></p>
Modbus data coding	All the point's values are coded in 2 bytes registers (even if their possible values are 0 and 1) and expressed in MSB..LSB.

4.1 Extract of the predefined Modbus address table

Modbus Address	G50	Group	Property
1	1		0 Error Com. G50
101	1	1	1 Drive
102	1	1	2 Mode
103	1	1	3 SetTemp
104	1	1	4 AirDirection
105	1	1	5 FanSpeed
106	1	1	6 RemoCon
107	1	1	7 Driveltem
108	1	1	8 Modeltem
109	1	1	9 SetTempltem
110	1	1	10 FilterItem
111	1	1	11 Ventilation
112	1	1	12 FilterSign
113	1	1	13 ErrorSign
114	1	1	14 InletTemp
115	1	1	15 FilterSignReset
116	1	1	16 ErrorSignReset
117	1	1	17 Error Com. Group
118	1	1	18 Polling Active

Modbus Address	G50	Group	Property
2	2		0 Error Com. G50
5101	2	1	1 Drive
5102	2	1	2 Mode
5103	2	1	3 SetTemp
5104	2	1	4 AirDirection
5105	2	1	5 FanSpeed
5106	2	1	6 RemoCon
5107	2	1	7 Driveltem
5108	2	1	8 Modeltem
5109	2	1	9 SetTempltem
5110	2	1	10 FilterItem
5111	2	1	11 Ventilation
5112	2	1	12 FilterSign
5113	2	1	13 ErrorSign
5114	2	1	14 InletTemp
5115	2	1	15 FilterSignReset
5116	2	1	16 ErrorSignReset
5117	2	1	17 Error Com. Group
5118	2	1	18 Polling Active

Modbus Address	G50	Group	Property
5001	1	50	1 Drive
5002	1	50	2 Mode
5003	1	50	3 SetTemp
5004	1	50	4 AirDirection
5005	1	50	5 FanSpeed
5006	1	50	6 RemoCon
5007	1	50	7 Driveltem
5008	1	50	8 Modeltem
5009	1	50	9 SetTempltem
5010	1	50	10 FilterItem
5011	1	50	11 Ventilation
5012	1	50	12 FilterSign
5013	1	50	13 ErrorSign
5014	1	50	14 InletTemp
5015	1	50	15 FilterSignReset
5016	1	50	16 ErrorSignReset
5017	1	50	17 Error Com. Group
5018	1	50	18 Polling Active

Modbus Address	G50	Group	Property
10001	2	50	1 Drive
10002	2	50	2 Mode
10003	2	50	3 SetTemp
10004	2	50	4 AirDirection
10005	2	50	5 FanSpeed
10006	2	50	6 RemoCon
10007	2	50	7 Driveltem
10008	2	50	8 Modeltem
10009	2	50	9 SetTempltem
10010	2	50	10 FilterItem
10011	2	50	11 Ventilation
10012	2	50	12 FilterSign
10013	2	50	13 ErrorSign
10014	2	50	14 InletTemp
10015	2	50	15 FilterSignReset
10016	2	50	16 ErrorSignReset
10017	2	50	17 Error Com. Group
10018	2	50	18 Polling Active

There are also a series of signals that indicate an Alarm Code in any of the devices present in the M-Net Mitsubishi network. To obtain the Modbus address, you must apply following formula:

$$\text{ADDRESS MODBUS} = (20000 + (\text{Numb.G50} \times 1000)) + \text{M-Net Add}$$

where *M-Net Add* is 0 for the G50 device, 1 to 50 for Indoor Units, 51 to 100 for Outdoor Unit, 101 to 200 for Remote Controllers and 200 to 250 for System Controllers.

For more information contact Mitsubishi Electric

TRADEMARKS: Todas las marcas y nombres utilizados en este documento se reconocen como marcas registradas de sus respectivos propietarios.

© Intesis Software S.L. - Todos los derechos reservados
La información de este documento puede cambiar sin previo aviso.

IntesisBox® es una marca registrada de Intesis Software SL



URL | <http://www.intesis.com>
email | info@intesis.com
tel | +34 938047134

5. Mitsubishi Electric G50 interface

Mitsubishi Electric G50 interface	
Device type	Client.
Configuration Parameters	Polling interval (1..600 seconds). Per every G50 defined: <ul style="list-style-type: none">• Descriptive name.• IP address.• TCP port.

5.1 Signals available per every Mitsubishi Electric City Multi AC indoor unit or group of indoor units

Property	Description / Status
Drive	Start/Stop Read/Write: ON, OFF
Mode ¹	AC Mode Read/Write: COOL, DRY, FUN, HEAT, AUTO, HEAT RECOVERY, LC_AUTO, BYPASS Read: AUTO HEAT, AUTO COOL
SetTemp ¹	Temperature Set Point (only integer numbers allowed) Read/Write: For COOL or DRY mode:19..30 °C, for HEAT mode: 17..28 °C, for AUTO mode:19..28 °C)
AirDirection	Air output direction Read/Write: HORIZONTAL, MID1, MID2, VERTICAL, SWING
FanSpeed	AC fan speed or LOSSNAY Read/Write: HIGH, MIDH, MIDL, LOW
RemoCon	Prohibition for General control from the local panel Read/Write: PROHIBIT, PERMIT
Driveltem	Prohibition for ON/OFF control from the local panel Read/Write: CHK_ON, CHK_OFF
Modeltem	Prohibition for Mode control from the local panel Read/Write: CHK_ON, CHK_OFF
SetTempltem	Prohibition for Set Point control from the local panel Read/Write: CHK_ON, CHK_OFF
FilterItem	Prohibition for Filter Reset control from the local panel Read/Write: CHK_ON, CHK_OFF
Ventilation	Operational status for LOSSNAY or OA Read/Write: HIGH, LOW, OFF
FilterSign	Status for Filter Dirty Read: ON, OFF Write: RESET
ErrorSign	Error status Read: ON, OFF Write: RESET
InletTemp	Ambient Temperature Read: 0.0 to 99.9
G50 Communication Error	Communication error with G50 Virtual signal generated by IntesisBox to indicate the status of the communication with the G50.
Group Communication Error	Group communication error Virtual signal generated by IntesisBox to indicate that the group is not configured into the G50.
Polling Active	Polling active Virtual signal to indicate or set if the Group is active or not active during the polling process.
Alarm Code	Group Alarm Code This signal provides a value. Each value has an associated alarm that has occurred in the group (0 means no alarm).

¹ PWFY units have a different mode and setTemp map explained in the signals column in LinkBoxEIB (section 3.4 in the User Manual)

TRADEMARKS: Todas las marcas y nombres utilizados en este documento se reconocen como marcas registradas de sus respectivos propietarios.

© Intesis Software S.L. - Todos los derechos reservados
La información de este documento puede cambiar sin previo aviso.

IntesisBox® es una marca registrada de Intesis Software SL



URL | <http://www.intesis.com>
email | info@intesis.com
tel | +34 938047134

6. Configuration tool

LinkBoxMB	<ul style="list-style-type: none"> Visual engineering tool, easy of use, for gateway's configuration and supervision compatible with Microsoft Windows operating systems, supplied with the gateway free of charge. Multi-window tool allowing to supervise simultaneously the communication activity with both protocols (systems), real time values for all the signals allowing to modify any value (very useful for test purposes), console window showing debug and working status messages, and configuration windows to configure all the gateway's parameters and signals. Signals configuration in plain text files (tab separated) for easy and quick configuration using Microsoft Excel (very useful in projects with a lot of points). Allows configuring the gateway's parameters and signals while in off-line (not connected to the gateway). Connection to the gateway for download the configuration and supervision by using serial COM port of the PC (serial cable supplied with the gateway). Allows configuring all the external protocols available for IntesisBox® Modbus Server series. Upgrades for this software tool available free of charge whenever a new protocol is added to the IntesisBox® Modbus Server series. Multi-project tool allowing having in the engineer's PC the configuration for all the sites with different IntesisBox® Modbus Server series gateways. Multi-language tool, all the language-dependent strings are in a plain text file (tab separated) for easy modification or addition of new languages. A list of system commands is available to send to the gateway for debugging and adjust purposes (Reset, Date/time consultation/adjust, Firmware version request...).
-----------	--

#	Signal	RW	Point	Value	Value
1	Communication Error G50	R	1	0	0-OK, 1-ERROR
2	Start/Stop	RW	101	0	0-OFF, 1-ON
3	Functioning mode	RW	102	0	0-COOL, 1-DRY, 2-FAN, 3-HEAT, 4-AUTO, 5-AUTO HEAT, 6-AUTO COOL, 7-HEAT RECOVERY, 8-LC_AUTO, 9-BYPASS
4	Temperature set point	RW	103	0	Ambient Temperatura (°C x10)
5	Direction of the air outlet	RW	104	0	0-HORIZONTAL, 1-MID1, 2-MID2, 3-VERTICAL, 4-SWING
6	Fan speed of the AC or LOSSNAY	RW	105	0	0-LOW, 1-MIDL, 2-MIDH, 3-HIGH
7	General prohibition of the control from the local panel	RW	106	0	0-PERMIT, 1-PROHIBIT
8	Prohibition of the DN/OFF control from the local panel	RW	107	0	0-CHK_ON, 1-CHK_OFF
9	Prohibition of the Mode control from the local panel	RW	108	0	0-CHK_ON, 1-CHK_OFF
10	Prohibition of the Setpoint control from the local panel	RW	109	0	0-CHK_ON, 1-CHK_OFF
11	Prohibition of the Filter Reset control from the local panel	RW	110	0	0-CHK_ON, 1-CHK_OFF
12	Operational status of the LOSSNAY or DA	RW	111	0	0-OFF, 1-LOW, 2-HIGH
13	Filter Dirty status (read)	R	112	0	0-OK, 1-DIRTY
14	Error status (read)	R	113	0	0-OK, 1-ERROR
15	Ambient Temperatura (°C x10)	R	114	0	0.0..99.9
16	Reset of the Filter Dirty indication	WR	115	0	Writing 1 resets the Filter indication
17	Reset of the Error indication	WR	116	0	Writing 1 resets the Error indication
18	Communication Error Group	R	117	1	0-OK, 1-ERROR
19	Polling Activated (Active in G50)	RW	118	0	0-NOT G50 CONFIGURED & NO POLL, 1-OK & POLL

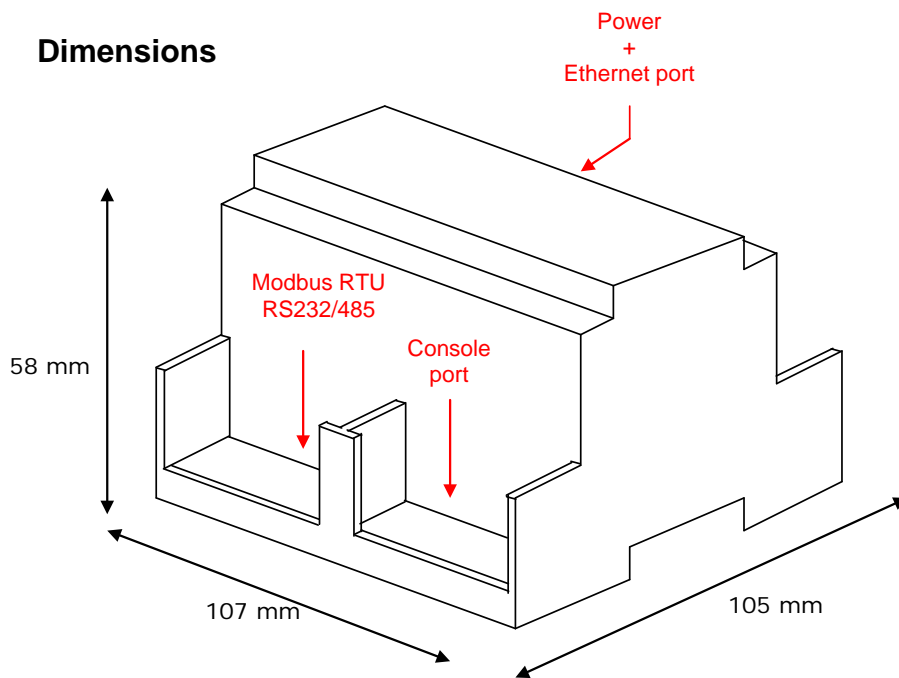
Mechanical & Electrical characteristics



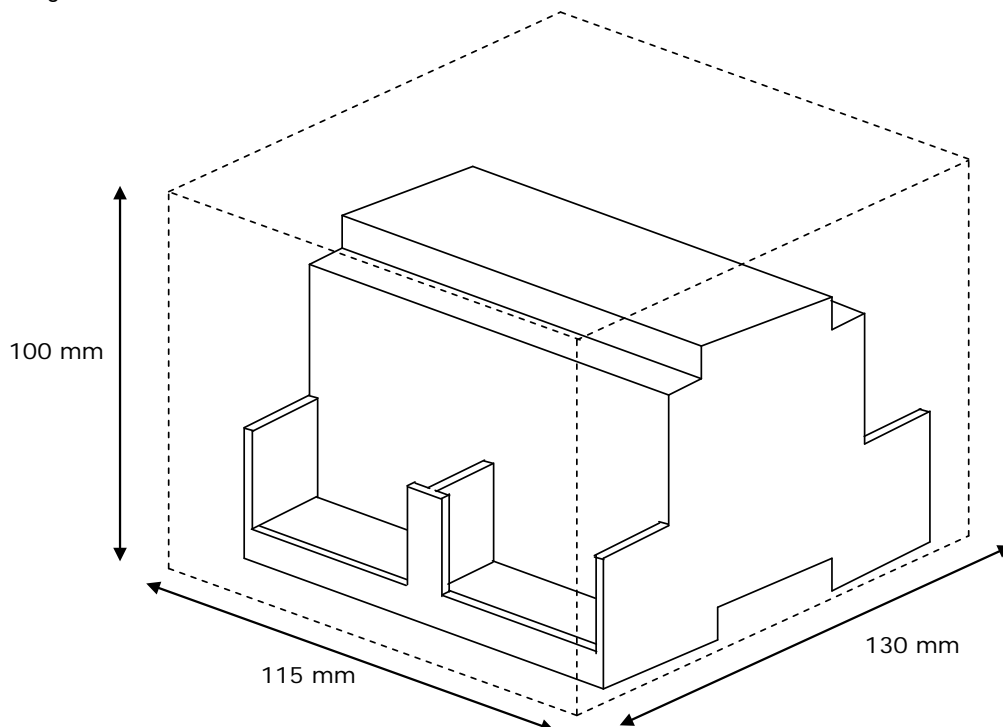
Envelope	Plastic type PC (UL 94 V-0). Size: 107mm x 105mm x 58mm.
Color	Grey. RAL 7035.
Power	9 to 30VDC +/-10% 1.4W. 24VAC +/-10% 1.4VA. Power connector is a 2 pole plug-in screw terminal bloc.
Mounting options	Wall DIN rail EN60715 TH35.
Modbus RTU ports	1 x Serial RS232 (DB9 male DTE). 1 x Serial RS485 (Plug-in screw terminal block 2 poles).
Modbus TCP & Mitsubishi Elec.G50 port	1 x Ethernet 10BT RJ45 connector.
LED indicators	1 x Power. 2 x Ethernet port link and activity (LNK, ACT). 2 x Modbus RTU port activity (Tx, Rx).
Console port	RS232. DB9 female connector (DCE).
Configuration	Via console port. ¹
Firmware	Allows upgrades via console port.
Operational temperature range	0°C to +70°C
Operational humidity range	5% to 95%, non condensing
Protection	IP20 (IEC60529).
RoHS conformity	Compliant with RoHS directive (2002/95/CE).
Certifications	CE

¹ Along with the device it is also supplied a standard DB9 male - DB9 female 1.8 m. cable for configuring and monitoring the device using a PC via serial COM port. The configuration software, compatible with MS Windows® operating systems, is also supplied.

8. Dimensions



Recommended available space for its installation into a cabinet (wall or DIN rail mounting), with space enough for external connections:



TRADEMARKS: Todas las marcas y nombres utilizados en este documento se reconocen como marcas registradas de sus respectivos propietarios.

© Intesis Software S.L. - Todos los derechos reservados
La información de este documento puede cambiar sin previo aviso.

IntesisBox® es una marca registrada de Intesis Software SL



URL | <http://www.intesis.com>
email | info@intesis.com
tel | +34 938047134

A.4 Heat Pump Outdoor Unit

Air Conditioning

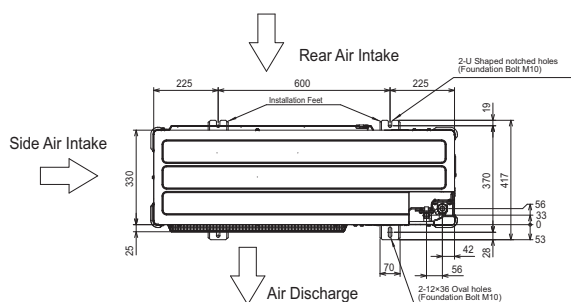
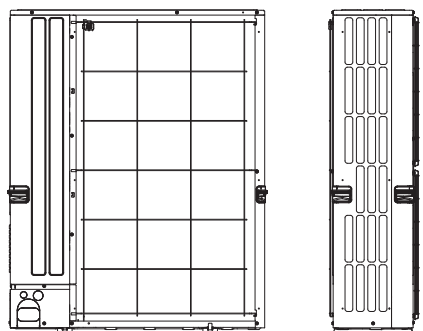
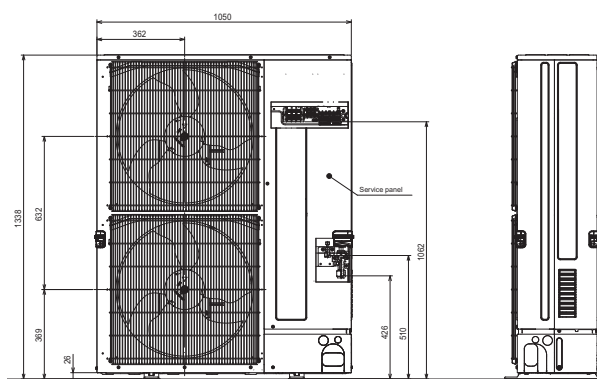
Product Information

PUMY-P140YKM2
Heat Pump Outdoor Unit

Making a
World of
Difference

PUMY - OUTDOOR UNIT		PUMY-P140YKM2
CAPACITY (kW)	Heating (nominal)	18.0
	Cooling (nominal)	15.5
	Heating (UK)	14.9
	Cooling (UK)	14.3
POWER INPUT (kW)	Heating (nominal)	4.47
	Cooling (nominal)	4.52
	Heating (UK)	3.98
	Cooling (UK)	3.03
COP / EER (nominal)		4.03 / 3.43
SCOP / SEER (system)		3.61 / 5.60
Max no. OF CONNECTABLE INDOOR UNITS		12
MAX CONNECTABLE CAPACITY		50-130% OU Capacity
AIRFLOW (m³/min)		110
PIPE SIZE mm (in)	Gas	15.88 (5/8")
	Liquid	9.52 (3/8")
SOUND PRESSURE LEVEL (dBA)		51
WEIGHT (kg)		125
DIMENSIONS (mm)	Width	1050
	Depth	330+30
	Height	1338
ELECTRICAL SUPPLY		380-415v, 50Hz
PHASE		Three
STARTING CURRENT (A)		5
NOMINAL SYSTEM RUNNING CURRENT (A)*		6.79 / 6.87 [13.0]
Heating / Cooling [MAX]		
GUARANTEED OPERATING RANGE (°C) Heating / Cooling		-20~15 / -5~46
FUSE RATING (BS88) - HRC (A)		1 x 16
MAINS CABLE No. Cores		4 + earth

DIMENSIONS



Telephone: 01707 282880

email: air.conditioning@meuk.mee.com web: www.airconditioning.mitsubishielectric.co.uk

UNITED KINGDOM Mitsubishi Electric Europe Living Environmental Systems Division
Travellers Lane, Hatfield, Hertfordshire, AL10 8XB, England General Enquiries Telephone: 01707 282880 Fax: 01707 278881
IRELAND Mitsubishi Electric Europe Westgate Business Park, Ballymount, Dublin 24, Ireland
Telephone: Dublin (01) 419 8800 Fax: Dublin (01) 419 8890 International code: (003531)

Country of origin: United Kingdom - Japan - Thailand - Malaysia. ©Mitsubishi Electric Europe 2015. Mitsubishi and Mitsubishi Electric are trademarks of Mitsubishi Electric Europe B.V. The company reserves the right to make any variation in technical specification to the equipment described, or to withdraw or replace products without prior notification or public announcement. Mitsubishi Electric is constantly developing and improving its products. All descriptions, illustrations, drawings and specifications in this publication present only general particulars and shall not form part of any contract. All goods are supplied subject to the Company's General Conditions of Sale, a copy of which is available on request. Third-party product and brand names may be trademarks or registered trademarks of their respective owners.



Note: The fuse rating is for guidance only. Please refer to the relevant databook for detailed specification. It is the responsibility of a qualified electrician/engineer to select the correct cable size and fuse rating based on current regulation and site specific conditions. Mitsubishi Electric's air conditioning and heat pump systems contain fluorinated greenhouse gases R410A, R407C and R134a.



www.greengateway.mitsubishielectric.co.uk
Mitsubishi Electric UK's commitment
to the environment

Follow us @meuk_Jes
Follow us @green_gateway

Mitsubishi Electric
Living Environmental Systems UK

mitsubishielectric2

Effective as of April 2015

A.5 Heat Exchanger Indoor Unit

UNITÉS INTÉRIEURES DRV



PFFY-P VLRMM-E

R410A

Compatible
R407C
R22

Garantie
3 ans
pièces

Seulement
27dB(A)

Haut
639 mm

Pression
statique
20 à
60 Pa

Selon modalités
des CGV

Selon modèle

Hall d'accueil, bureaux décorés, restaurants, résidentiel...

Console non carrossée avec pression

PFFY-P VLRMM-E

Les + installateurs

- Dimensions compactes pour une discrétion maximum
- Traitement efficace en périmétrie des locaux recevant du public
- 3 vitesses de ventilation
- Pression statique disponible jusqu'à 60 Pa

Les + utilisateurs

- Intégration adaptée aux intérieurs décorés



PFFY-P(...) VLRMM-E		20	25	32	40	50	63		
❄️	Puissance nominale froid	kW	2.2	2.8	3.6	4.5	5.6	7.1	
	Puissance absorbée totale nominale ⁽¹⁾	W	40	40	40	50	50	70	
☀️	Puissance nominale chaud	kW	2.5	3.2	4.0	5.0	6.3	8.0	
	Puissance absorbée totale nominale ⁽¹⁾	W	40	40	40	50	50	70	
Caractéristiques techniques									
Unités extérieures compatibles		-	PUMY-P-V/YKM(2) PURY-(E)P-Y(S)LM PQHY/PQRY-P-Y(S)LM		PUHY-P-Y(S)KB PUHY/PURY-RP-Y(S)JM	PUHY-EP-Y(S)LM PUHY/PURY-RP-Y(S)JM	PUHY-HP-Y(S)HM PUCY-P-Y(S)KA		
Unités intérieures	Débit d'air en Froid	PV	270	270	390	480	600	660	
		MV	m³/h	330	330	450	570	720	780
		GV	390	390	540	660	840	930	
	Pression statique disponible [réglage usine]		[20]	[20]	[20]	[20]	[20]	[20]	
		Pa	40	40	40	40	40	40	
			60	60	60	60	60	60	
			-	-	-	-	-	-	
	Pression acoustique en Froid à 1,5 m ⁽²⁾	PV	31	31	27	30	32	35	
		MV	dB(A)	36	36	32	36	37	40
		GV	[20] Pa	40	40	37	40	41	44
Dimensions	Hauteur	mm	639	639	639	639	639	639	
	Largeur	886	886	1006	1006	1246	1246		
	Profondeur	220	220	220	220	220	220		
Poids net	kg	18,5	18,5	20	21	25	27		
Diamètres des condensats	mm	26	26	26	26	26	26		
Frigo	Diamètre liquide flare	pouce	1/4 "	1/4 "	1/4 "	1/4 "	1/4 "	3/8 "	
	Diamètre gaz flare	pouce	1/2 "	1/2 "	1/2 "	1/2 "	1/2 "	5/8 "	
Elec	Alimentation électrique	V-Hz	230V - 1 P + N + T						
	Intensité maxi	A	0.59	0.59	0.69	0.78	0.80	0.93	

Conditions nominales : Mode FROID : intérieur : 27°C TS / 19°C TH - extérieur : 35°C TS / 24°C TH - Mode CHAUD : intérieur : 20°C TS / 15°C TH - extérieur : 7°C TS/6°C TH - Longueur tubes : 7.5 m
⁽¹⁾ MV = Petite Vitesse - MV = Moyenne Vitesse - GV = Grande Vitesse - ⁽²⁾ Donnée en Grande Vitesse - ⁽²⁾ Pression acoustique mesurée en chambre anéchoïque

Titre : Bâtiments Eco-Energétiques : Modélisation Dynamique Hybride pour l'Analyse et le Contrôle

Mots clés : Modèle de bâtiment, simulation dynamique de bâtiment, modèle de réseau thermique, identification des paramètres, optimisation par essaim de particules, commande prédictive (MPC), gestion de l'énergie du bâtiment, confort thermique.

Résumé : Ces travaux de thèse proposent une approche alternative pour une modélisation simplifiée du modèle de réseau thermique des bâtiments. Ces travaux sont motivés par la nécessité de réduire la complexité de la modélisation des bâtiments et d'améliorer ainsi les performances tout en réduisant le coût calculatoire. Les différentes techniques de modélisation pour le développement d'un contrôleur basé sur un modèle ont été étudiées et analysées pour déterminer les modèles qui peuvent être utilisés pour la modernisation des bâtiments en cas de manque de données. Nous avons ainsi présenté différentes méthodes pour la modélisation dynamique des bâtiments y compris les facteurs influençant les performances d'un bâtiment. La mise en œuvre de contrôleurs intelligents permet de gérer correctement la consommation d'énergie et le confort dans les bâtiments. Ces contrôleurs doivent être réactifs pour envoyer les signaux de contrôle nécessaires. Dans ce contexte, le contrôleur a besoin d'un modèle de faible ordre, efficace sur le plan calculatoire et précis pour tendre vers de meilleures performances. Des systèmes d'ordre inférieur simplifiés sont développés en utilisant des modèles de réseau thermique d'ordre 2 avec une valeur optimale des résistances thermiques et des condensateurs. Afin de déterminer les valeurs de ces paramètres, une approche spécifique est proposée en utilisant une optimisation stochastique des essais de particules.

Cette méthode fournit une approximation significative des paramètres par rapport au modèle de référence tout en permettant au modèle d'ordre inférieur d'atteindre une efficacité calculatoire de 40 à 50% par rapport au modèle de référence. En outre, un nombre considérable de simulations sont réalisées pour évaluer les performances du modèle simplifié proposé par rapport à un modèle complexe plus avancé de gains solaires. Le modèle simplifié développé est ensuite validé avec des données mesurées dans un bâtiment réel (notre cas d'étude) où les résultats obtenus montrent clairement un haut degré de précision par rapport aux données réelles. Enfin, un contrôleur MPC (commande prédictive) est appliqué pour le bâtiment cas d'étude pour l'optimisation du confort thermique. Les résultats de simulations obtenus démontrent l'importance du contrôleur MPC dans la gestion des contraintes, le contrôle multi-objectifs et la génération d'une stratégie de contrôle optimale. Les résultats de l'optimisation énergétique montrent une réduction de 31% de la consommation d'énergie par rapport à un contrôleur conventionnel.

Title : On Energy-Efficient Buildings : Hybrid Dynamic Modeling for Analysis and Control

Keywords : Building model, dynamic building simulation, thermal network model, parameters identification, particle swarm optimization, Model Predictive Control (MPC), building energy management, thermal comfort.

Abstract : Low cost smart sensors, intelligent controllers, and IoT systems constitute key components to develop smart buildings. These smart systems produce optimal control strategies by continuous analysis of building performance. Two major parameters are controlled in the building: occupants' comfort and heating or cooling load consumption optimization. For such intelligent controllers applications, it is essential to have building model with high performance accuracy and computational efficiency. The existing building models range from complete analytical to fully data-driven and hybrid models. The analytical model is extremely complex to model and computationally inefficient, whereas the data-driven models require a large amount of data. However, in the case of data unavailability, application of data-driven models become impossible. This work presents, hybrid modeling for heat transfer dynamics of the building using lumped parameter thermal network modeling technique. An efficient building model is developed by having proper structural knowledge of low-order model and identifying its parameter values. Simplified low-order systems are developed using 2nd order thermal network models with optimal thermal resistors and capacitors value.

In order to determine the low-order model parameter values, a specific approach is proposed using a stochastic particle swarm optimization. This method provides a significant approximation of the parameters when compared to the reference model whilst allowing low-order model to achieve 40% to 50% computational efficiency than the reference analytical model. Furthermore, extensive simulations are carried out to evaluate the proposed simplified model with a more advanced complex solar gains model and identified parameters value. The developed simplified model is afterward validated with measured data from a case study building where the achieved results clearly show a high degree of accuracy compared to the actual data. Finally, an MPC controller is applied for the same case study building for thermal comfort optimization. Simulation results demonstrate the significance of the MPC controller in handling the constraints, multi-objective control, and producing optimal control strategy. The energy optimization results of the MPC have shown 31% of energy consumption reduction compared to a conventional controller.